Multi-scale analysis and bioinspired approach towards the reconstruction of the myotendinous junction

Megane Beldjilali-Labro

Par **Megane BELDJILALI-LABRO**

Multi-scale analysis and bioinspired approach towards the reconstruction of the myotendinous junction

Thèse présentée
pour l'obtention du grade
de Docteur de l'UTC

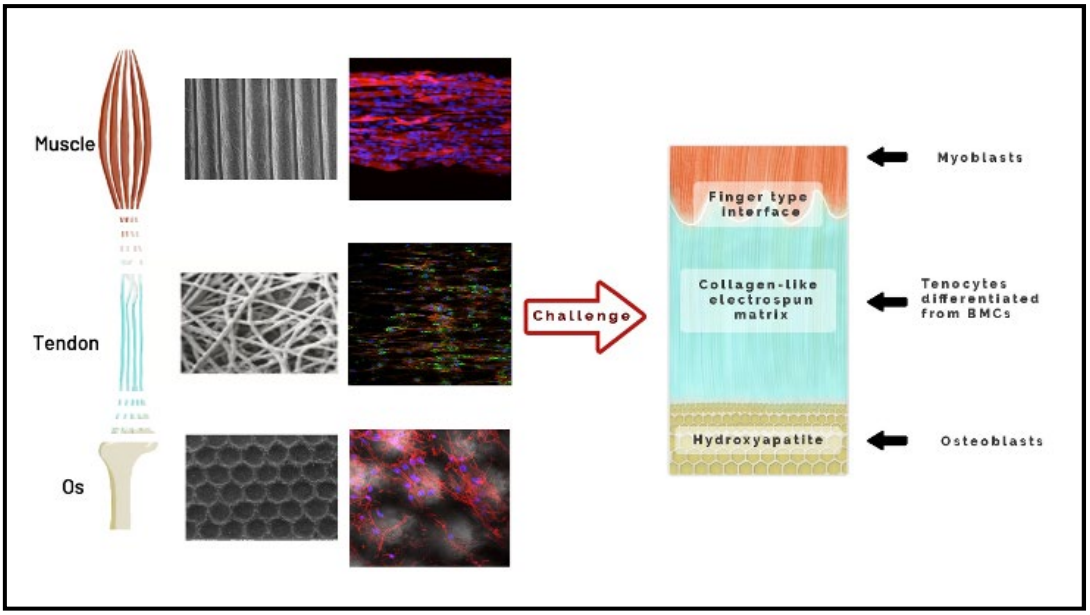

Soutenue le 28 septembre 2020
Spécialité : Biomatériaux et Bio-ingénierie : Unité de Recherche Biomécanique et Bio-ingénierie (UMR-7338)
D2565

THÈSE DE DOCTORAT

École doctorale 71 : Sciences pour l'ingénieur
Spécialité de doctorat : Biomatériaux et Bio-ingénierie

Multi-scale analysis and bioinspired approach towards the reconstruction of the myotendinous junction

---

Presented and defended by
Megane BELDJILALI LABRO
On a september 28th 2020

To obtain the doctorat degree
UNIVERSITÉ DE TECHNOLOGIE DE COMPIÈGNE

PhD Supervisors: Dr. Cécile LEGALLAIS, Dr. Grosset JEAN-FRANCOIS

Laboratoire de BioMécanique et BioIngénierie (BMBI)
Equipe Cellules Biomatériaux Bioréacteurs (CBB)
CNRS UMR 7338

Jury :

Emmanuel Pauthe	Professor, Université de Cergy-Pontoise	President of the jury
Gladys Pearson	DR, CMSSM, Manchester Metropolitan University	Referee
Delphine Duprez	DR CNRS, CNRS-SU UMR 7622, INSERM ERL U115	Examiner
Christophe Egles	Professor, BMBI-CNRS UMR7338, UTC	Examiner
Guy Schlatter	Professor, CNRS, ICPEES UMR 7515, Université de Strasbourg	Examiner
Jean François Grosset	Professor	PhD Supervisor
Cécile Legallais	Directrice de recherche, UMR CNRS 7338	PhD Supervisor
Muriel Dufresne	PRAG,	Supervisor

Contents

Acknowledgements

Je tiens tout d'abord à remercier les membres de mon jury qui ont accepté d'évaluer mes travaux de thèse: Gladys Pearson et Emmanuel Pauthe pour leurs rapports, leurs remarques et pour l'intérêt porté à mes travaux, ainsi que Delphine Duprez , Guy Schlatter et Christophe Egles pour les échanges sur leurs domaines d'expertise respectif.

Je remercie également mes directeurs de thèse, Cécile Legallais et Jean Francois Grosset, de m'avoir donné l'opportunité de réaliser cette thèse.

Un grand merci à Cécile pour sa grande confiance, sa disponibilité, son aide ainsi que l'autonomie accordée tout au long de ses 4 années, mais aussi pour sa patience pour la relecture de ce manuscrit.

Merci à Jean Francois pour ses remarques constructives et sa disponibilité et à Murielle pour avoir suivi mes travaux de thèse de bout en bout.

Merci à Guy Schlatter et Christophe Egles d'avoir fait partie de mon comité de suivi scientifique. J'ai apprécié échanger avec vous et voir votre optimisme motivait chaque année.

J'aimerais également remercier toutes les personnes avec qui j'ai pu travailler pendant ces 4 années.

Le SAPC, Frédéric Nadaud pour le temps passé ensemble à observer les échantillons au microscope électronique à balayage sans savoir vraiment à quoi s'attendre et Caroline Lefebvre pour sa formation au microscope confocal, microscope qui deviendra mon bureau annexe pour ses 4 ans.

Merci également à Milena qui m'a aidé sur différents element du projet et que j'ai eu le plaisir d'encadrer pendant son stage.

Merci à tout le laboratoire BMBI et en particulier l'équipe CBB qui m'a accompagnée pendant ce doctorat. Rachid, Ulysse, Pascale, un grand merci pour vos conseils, votre disponibilité et votre écoute. Vous avez toujours su prendre le temps pour m'aider et me remonter le moral.

Vanessa, Muriel, Patrick, merci pour les moments partagés et la bonne humeur que vous apportez au laboratoire.

Je remercie tout particulièrement les doctorants,

Alex, mon binôme, toujours partant pour des experimentations périlleuses que ce soit à l'electrospining ou avec les cellules.

Mattia et toute ses péripéties que l'on ne nommera pas, merci de m'avoir fait vivre l'experience Friends avec la Favela. tu restera à jamais mon Joe Triviani.

Augustin, merci pour tout, je ne serais pas par ou commencer, tu as toujours répondu présent, que ce soit pour des appels à l'aide pour une araignées rentrée dans ma cuisine ou m'aider sur cette thèse jusqu'au petit matin.

Lilandra, mon acolyte, merci de m'avoir supporter, suivie et épaulé pendant c'est 4 ans que ce soit au laboratoire; à verifier mes calcules où dans la vie de tout les jours avec nos rendez vous périlleux chez le coiffeurs.

Delphine, cette experience aurait été différente sans toi, nos expeditions à Action, et nos aventures rocambolesque au Japon «Zamami».

Félix, CBB de coeur, tu resteras l'une de mes plus belles rencontres.

Antoine, Manon, cela a été un honneur de partager ce bureau avec vous.

Claire, Sabrina, Mathilde, Amal, Doriane, Baptiste. Merci pour tous les moments que nous avons passés ensemble, au laboratoire et à l'extérieur, qui m'ont beaucoup apporté et qui ont pleinement contribué à mon épanouissement pendant ce doctorat.

Je tiens également à remercier ma famille et mes amis qui ont été présents quelque soit l'heure, qui m'ont toujours supportée et qui se sont toujours intéressés à mon sujet de recherche même s'ils ne comprenaient pas toujours tout.

Une thèse est faite de plein de rebondissements et celle-ci en a eu un peu plus que prévu: contaminations des cultures cellulaires, coupures électriques, travaux d'agrandissement, canicule, confinement... Malgré cela j'ai toujours essayé d'avancer et je suis fière de vous présenter les résultats de ce projet de recherche dans ce manuscrit et vous en souhaite bonne lecture.

Abstract

The complexity of the musculoskeletal system lies in the individuality of each tissues function. It has been demonstrated that a deficiency in one of these tissues can have negative effects on the whole system.

Therefore, the need to build an in vitro relevant model of the musculoskeletal system, allowing the study of each of these tissues in their surrounding environment is a key challenge today.

This thesis work is on a 2.5D tissue engineered skeletal muscle and a co-culture platform to study the establishment of the myotendinous junction.

The work focuses on the development of a material for muscle tissue regeneration. The idea was to use a combination of an PCL electrospun sheet reinforced by PEG hydrogel micropatterning to create an environment that supports myoblast proliferation and fusion.

The potential effect of cyclic stretching or electrical stimulation on the cells construct was investigated. Both stimulations enhance significantly cell differentiation and maturation.

To investigate the development of the myotendinous junctions, a co-culture of C2C12 and BMSCs was set up. The results have led to 2 scientific articles and 1 review.

Résumé

La complexité du système musculo-squelettique réside dans les fonctions de chaque tissu.

Il a été démontré que lorsque l'un de ces tissus est déficient cela peut avoir des effets néfastes sur l'ensemble du système.

Par conséquent, il est nécessaire de mettre au point un modèle in vitro du système musculo-squelettique, pour étudier chacun de ces tissus ainsi que leur environnement.

Ce travail de thèse se porte sur le developement d'un muscle squelettique par ingenierie tissulaire et de la mise au point d'un modele de co-culture pour étudier la formation de la jonction myotendineuse.

Le travail s'est focalisé sur le développement d'un matériau pour la régénération musculaire. Le but est de combiner le feuillet de PCL obtenu par electrofilage avec une topographie de surface que peut aporter l'hydrogel en PEG. Ceci pour créer un environnement qui favorise la prolifération et la fusion des myoblastes (C2C12).

Par la suite, nous avons voulu determiner si l'ajout de stimulation éléctrique ou mécanique sur nos biomatériaux avait un effet synergique sur les cellules. Les deux stimulations améliorent significativement la différenciation et la maturation des cellules.

Pour étudier le développement de la jonction myotendineuse, une co-culture de C2C12 et de BMSC a été mis en place. Les résultats de cette thèse ont donné lieu à 2 articles scientifiques et 1 revue.

List of publications and communications

Published papers

Beldjilali-Labro M.*, Garcia Garcia A.*, Farhat F.*, Bedoui F., Grosset J-F., Dufresne M., Legallais C., Biomaterials in Tendon and Skeletal Muscle Tissue Engineering: Current Trends and Challenges. Materials 2018, 11(7), 1116 - 1165; https://doi.org/10.3390/ma11071116.
Garcia, A.G., **Beldjilali-Labro M.**, Farhat, F., Perot, J.-B., Dermigny, Q., Dufresne M.,

Grosset, J.-F., Bedoui, F., Legallais, C. Multi-scale approach to reconstruct a bioartificial system of system: The example of the bone-tendon-muscle continuum. 13th System of Systems Engineering Conference, SoSE 2018, art. no. 8428779, pp. 408-410. 10.1109/SYSOSE.2018.8428779. Alejandro Garcia Garcia, Jean-Baptiste Perot, **Megane**

Beldjilali-Labro, Quentin Dermigny, MarieNaudot, et al.. Monitoring mechanical stimulation for optimal tendon tissue engineering: a mechanicaland biological multiscale study. 2020. hal-03029652

Submitted papers

Beldjilali Labro M., Jellali R., Brown A., Garcia Garcia A., Lerebours A., Dufresne D., Guenin E., Bedoui F., Claire Stewart., Grosset JF., Legallais C. Multiscale-engineered muscle constructs: PEG hydrogel micro-patterning on electrospun PCL mat functionalized with gold nanoparticles. ACS Biomaterials Science & Engineering

In preparation

Beldjilali Labro M., Jellali R., Farhat F., Lerebours A., Brown A., StewartC., Dufresne M., Grosset JF., Legallais C. Effect of mechanical or electrical stimulation applied to multiscale cell-seeded electrospun construct for skeletal muscle tissue engineering

Oral communication

Beldjilali-Labro M., Farhat F., Garcia-Garcia A., Bedoui F., Jellali R., Dufresne M., Grosset J-F., and Legallais C. Electrically Conductive Multi Dimensional Scaffolds With Controllable Architecture For Skeletal Muscle Engineering. 5th TERMIS World Congress, Kyoto, Japan sept 2018, Oral presentation. Farhat F., **Beldjilali Labro M.**, Garcia-Garcia

A., Dufresne M., Grosset JF and Legallais C. In vitro effect of electrical stimulation on mesenchymal stem cells for tenogenic differentiation. 8th World Congress of Biomechanics. Dublin July 2018, Poster. **Beldjilali-Labro M.**, Garcia Garcia A., Fahrat F., Dermigny Q.,

Jellali R., Bedoui F., Dufresne M., Legallais C., Grosset JF. Electrospun materials for tendon and muscle engineering: towards the reconstruction of the myotendinous junction. XLVI ESAO Congress, Hannover, 3-7 Sept 2019, Oral presentation.

Teaching activities

- **BL01: Biological sciences for engineers.** Histology and Cadmium toxicity in vitro: Analysis of histology sections by microscopy and MTT test on cell culture (270h of Lab's practice).

- **BL20: Cell Physiology and Metabolism.** The program identifies key issues in structural organization of the cell's membranes and the implications in terms of intra and extracellular exchanges (8h of supervised work).

- **BT03: Tissue engineering and Immunotechnology.** Overview of techniques for the study of animal tissues and the manipulation of human tissues for experimental and biomedical purposes (4h of Lecture).

Supervising Activities

- **2020 (6 months)**: Co-supervision of a final internship. Development of a core shell hydrogel through microfluidic device for C2C12 and BMSC co-culture.

- **2019 (3 months)**: Co-supervision of a student project. Differentiation of mesenchymal stem cells for tendon tissue engineering.

- **2019 (1 month)**: Co-supervision of a student project (3 students). Assessment of culture media for stem cells and C2C12 cells line for direct co culture.

- **2018 (3 months)**: Co-supervision of a final internship. Development of polyethylene glycol micro pattern on electrospinning scaffold for muscle tissue engineering.

- **2017 (1 month)**: Co-supervision of a student project. Cytotoxicity of polycaprolactone scaffolds used in tissue engineering.

List of Figures

General Introduction

Tissue engineering holds the promise to improve the quality of human life. It either I) favors in situ tissue regeneration, II) builds functional tissue substitutes that could be implanted to replace injured/pathological ones, III) proposes innovative and relevant in vitro models to study physiology, physiopathology or even development of a given tissue. The goal is the comprehensive monitoring of the development and repairing processes, as well as improvement of all human biologic systems. Moreover, tissue engineering is of interest to evaluate in vitro the effect of molecules on growing or repairing processes of a given tissue or continuum of tissues. Tissue engineering is complex and requires an in-depth understanding of all components of both in vivo and in vitro environments. This emerging science gathers interdisciplinary skills at different scales including engineering sciences such as biomechanics, materials science, instrumentation, biology, physics and chemistry, clinical sciences, among others. In almost all cases, tissue engineering is about integrating cells into scaffolds where they can adhere, proliferate or differentiate to ultimately acquire functions and properties of the native tissue. In addition, the use of bioreactor may be requested to perform 3D culture and mimic the cells' in vivo niche and environment, while ensuring a better control of cell culture condition and possibly induce cell response to mechanical stimuli. The previous achievements in the Research group Cells, Biomaterials, Bioreactors (CBB) , as well as the physiological knowledge on the musculo-skeletal system in the research group C2MUST, both in the laboratory of Biomechanics & Bioengineering (BMBI – UMR CNRS 7338) at UTC, consist of designing and validating "challenge" in 2015: to target a biohybrid reconstruction of the muscle-tendon-bone continuum. This challenge is named "Interfaces" and was funded by Labex MS2T (Maitrise de Systèmes de Systèmes Technologiques).

The overall methodology consists to design and validate a bioartificial system representing the continuum muscle-tendon-bone (Figure 1), itself composed of biohybrid systems at different scales to understand and predict the mechanical and biological behavior of the muscle-tendon- bone continuum. This reconstruction is a complex bioinspired system of systems in which the different systems are continuously changing and interacting. The goal was then to monitor these interactions through multi-scale structure modification of the scaffold and electrical/mechanical stimulation to promote cells differentiation into the desired type of tissue (bone, tendon or muscle) and to tailor the mechanical properties of the whole system (biomaterial and cell types).

To achieve the reconstruction of the continuum bone-tendon-muscle by using smart tissue engineering approaches, major challenges need to be tackled on:

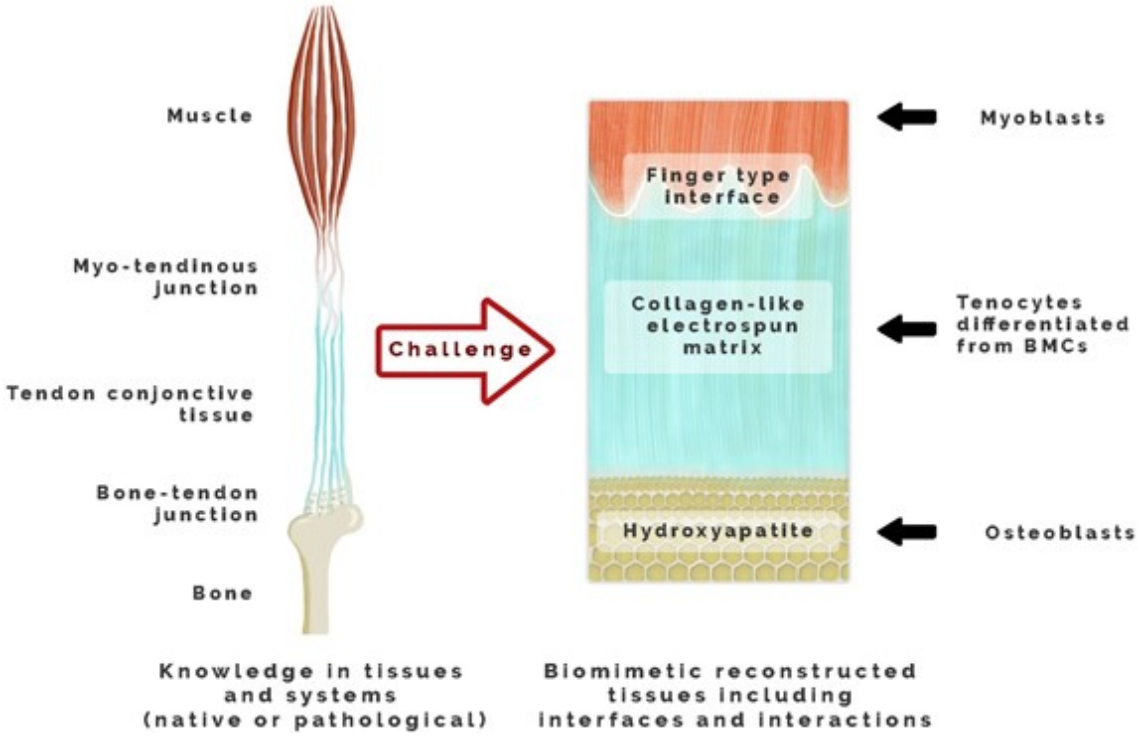

FIGURE 1: Schematic representation of the Challenge "Interface".

- the understanding of the native tissue architecture and composition at different scales,
- the design of electrospun materials mimicking the structure,
- the use of relevant cell types,
- the culture of the biohybrid constructs under dynamic conditions in bioreactors to exploit mechanical stimulation (as in a body), and/or well as electrical stimulation for enhanced tissue maturation.

Among the techniques to manufacture bio scaffolds, electrospinning has been chosen due to its versatility. Indeed, the electrospun mat can be composed of fibers aligned or randomly organized, of different sizes and compositions, and even shaped in 3D with specific collectors. We postulate that the surface properties (nano-/micro- topography, protein coating, functionalization) and physical cues guide cell adhesion, proliferation and most importantly differentiation into bone, tendon or muscle lineage.

The overall plan was to work first on the definition of optimal condition for each of these tissues, and then to assemble and investigate the osteo-tendinous junction on one hand, and the myotendinous junction on the other hand. In this 5-year project, two PhDs and two post-doctoral fellows have joined their efforts to progress towards the final goal. In the framework of this PhD, the goal is first to achieve the differentiation of myocytes into functional myotubes, and then to focus on the musculo-tendinous junction, integrating gradually the work performed in parallel by the other stakeholders.

This Ph.D. thesis is divided in five chapters. The introduction is composed of two chapters. I propose the state of the art of our bioinspired vision for the reconstruction of the tendon/muscle continuum. I therefore start from the knowledge of biological tissues,

considering both adult and embryonic stages (chapter 1). Current tissue engineering strategies are then analyzed (chapter 2). This chapter is adapted from a review article (Beldjilali-Labro et al., 2018*a*) entitled "Biomaterials in Tendon and Skeletal Muscle Tissue Engineering: Current Trends and Challenges". The first results are presented in chapter 3 through a scientific article entitled " Multiscale- engineered muscle constructs: PEG hydrogel micro-patterning on electrospun PCL mat functionalized with gold nanoparticles". This work deals with the choice of electrospun based scaffolds to guide cell differentiation. It particularly focusses with the interaction between C2C12 cells culture on PCL based scaffolds with different surface topography. The next chapter (chapter 4) is also presented through a scientific article. It is entitled "Effect of mechanical or electrical stimulation applied to multiscale cell-seeded electrospun construct for skeletal muscle tissue engineering". This work deals with the effect of physical stimulation on cell differentiation within the chosen scaffolds and is presented as a scientific paper.

In both chapters 3 and 4, qualitative and quantitative analyses are performed, RT PCR analysis has been performed in collaboration with the team of Pr Claire Stewart at Liverpool John Moores University (UK). The last chapter (chapter 5) proposes preliminary evaluation of several approaches to reconstruct the musculo-tendinous junction and will guide the future works as exposed in Conclusion and Perspective.

Chapter 1

Research Context

Musculo-tendinous system refers to the intimate interface between muscular and tendinous tissues and their interaction at the myotendinous junction (MTJ). MTJ appears early during the development and is characterized by the entanglement of muscular and tendinous fibers. MTJs are strong tissues that support movement by transmitting mechanical forces exerted by the muscle to the bones through the tendon. However, MTJ can brake due to overload or genetic condition. To study traumatic injuries or MTJ diseases, few tissues engineered approaches are currently in progress either for understanding cellular mechanism underlying MTJ weaknesses or building reconstruction models.

In this chapter, the purpose is to give an overview of the musculo-tendinous system, to understand the functions and structure at different scale for each of its components (muscle, tendon, myotendinous junction). Elements regarding biology development are provided to understand these steps in view of reaching mature engineered tissues in the framework of this PhD. Then, I analyze the state of the art in the tissue engineering approaches for the reconstruction of these components.

1.1 Myotendinous System

1.1.1 Muscle

Skeletal muscle is the most dynamic and abundant tissue in the human body, representing approximately 40% of its mass (Janssen et al., 2000) and 50-75% of its protein content. From a mechanical point of view, the main functions of skeletal muscle are to convert chemical energy into mechanical energy applied to bone via the tendinous tissue, maintain posture and support soft tissue. This soft and elastic tissue presents Young moduli around 11.10 ± 4.10 kPa depending of the muscle, age or stretching impose (Lima et al., 2018). It also plays a role in general metabolism with various functions, including locomotion, breathing, protecting internal organs, and coordinating global energy expenditure through the storage of substrates such as amino acids and carbohydrates (Trovato et al., 2016). Skeletal muscles' activation is performed under voluntary or reflex control of the central nervous system and peripheral nerves, in contrast to smooth and cardiac muscles, which are subject to involuntary control by the vegetative nervous system (Figure 1.1).

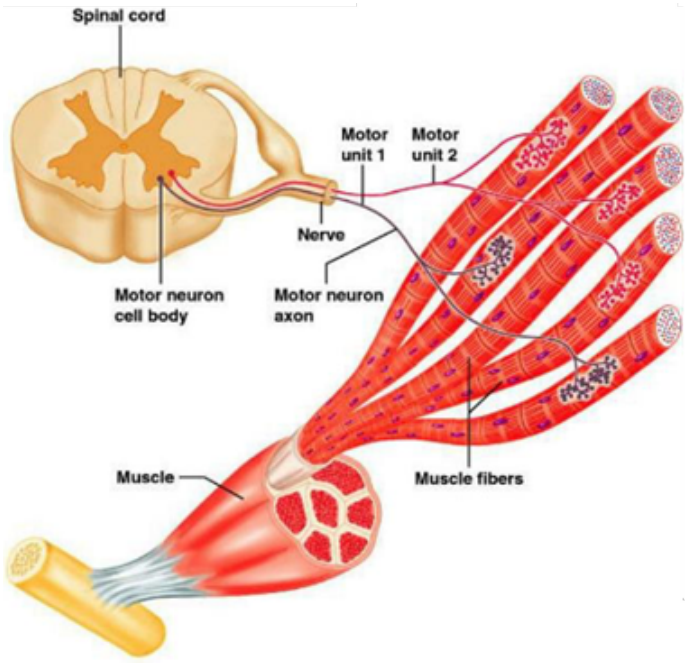

FIGURE 1.1: Schematic representation of neuromuscular junction of one motor neuron with one muscle fiber. In a motor unit the motor neuron branches to form neuromuscular junctions with several muscle fibers. ©Benjamin Cummings 2001.

Moreover, skeletal muscle is a very physiologically active tissue, but present a low turnover. Indeed, (Collins and Partridge, 2005), have demonstrated through retrospective birth dating of DNA of 14C content, that skeletal muscle nuclei from 37- and 38-year-old individuals have a renewal of average of 15 years. Nevertheless, skeletal muscle maintains a remarkable capacity to regenerate itself following injury. This capacity for regeneration is made possible through the activation of resident multipotent cells, the satellite cells (Heinemeier et al., 2013; Relaix and Zammit, 2012). They are a quiescent population of resident muscle progenitor stem cells, which, in response to injury, are activated and through asymmetric divisions and migrate to the defect site. They expand and undergo myogenic differentiation or self-renewing of the satellite cell pool (Kuang et al., 2008, 2007)(Figure 1.2).

Moreover, Rantanen et al. (1995) showed that though proliferation does not begin until about 24 hours after injury, some muscle progenitor cells (MPC) upregulate expression of the differentiation marker myogenin within 8 hours.

1.1.2 From macroscopic organization to ultrastructure

The macroscopic architecture of skeletal muscle is characterized by a highly ordered arrangement of muscle fibers known as myofibers associated with connective tissue (Frontera and Ochala, 2015) (Figure 1.3).

Myofibers are highly elongated cells with a very elastic, with a Young's modulus of 4.2 $\pm$ 1.1 kPa for a single fiber and surrounded by a resistant plasma membrane called the sarcolemma (Puttini et al., 2009). The differentiation of skeletal muscle cells is stimulated

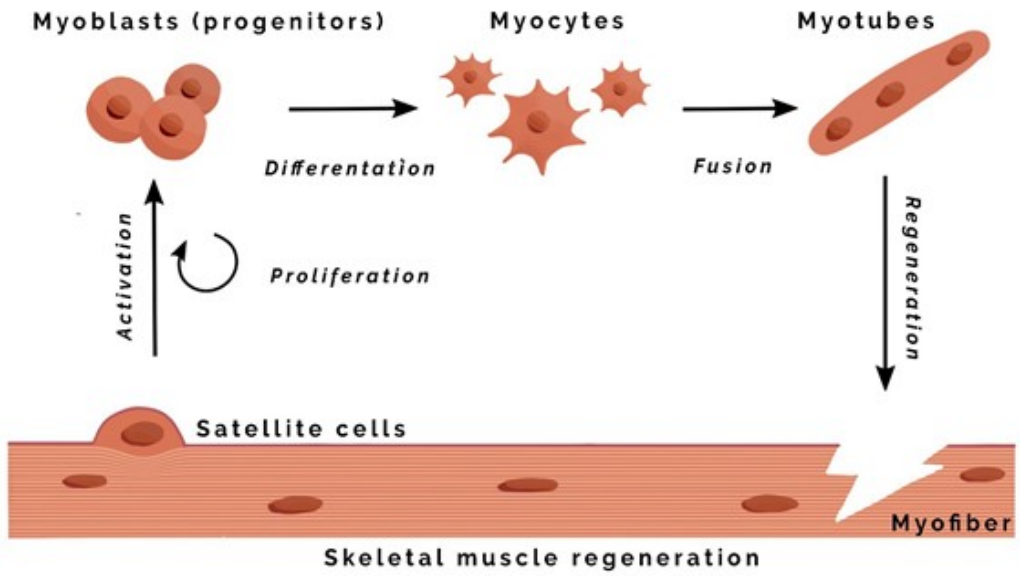

FIGURE 1.2: Skeletal muscle regeneration through satellite cells. When muscle fibers sustain damage, signals trigger dormant satellite cells to go into action. They replicate, forming one new dormant cell and one that proliferates. The proliferating satellite cells can either form a new fiber or patch the original.

by a contact- dependent process. Myofibers are thus formed when undifferentiated muscle cells i.e. myoblasts fuse together to form elongated, multinucleated myotubes, gathering nuclei in a central position. As the myotubes mature to form myofibers, the nuclei adopt positions near the plasma membrane at the cell periphery and have approximately a range from 20 to 100 µm in diameter (Roman and Gomes, 2018). They are arranged in parallel, with lengths from a couple of cm to several tens of cm in humans (Huard et al., 2002).

Myofibers are wrapped by a fibrous extracellular matrix (ECM), composed of types I and III collagen and proteoglycans, mostly from the family of small leucine-rich proteoglycans (SLRPs). This so-called endomysium bundles the myofibers into fascicles. A layer of matrix, the perimysium, in turn surrounds these fascicles providing pathways for blood vessels and nerves. Finally, a third and dense connective tissue, the epimysium, delimits the different muscles, facilitates their sliding along each other, and supports the structural and functional continuity of the muscle-tendon junction.

At the ultrastructural level, the major components of myofibers are the myofibrils. Myofibrils are divided into contractile units, or sarcomeres, that are delimited by Z lines. Hundreds of sarcomeres in series give the typical striated appearance of the muscle fiber. The main components of the sarcomeres are thick myosin and thin actin myofilaments, which represent approximatively 70% of the total protein content of a single fiber (Figure 1.4). They are responsible for muscle contraction (Greising et al., 2012). Thin myofilaments consist mainly of F-actin and other associated proteins (troponin, tropomyosin) and are anchored in the Z line, which is rich in α-actin. Other proteins are also found in the Z line, such as desmin, which helps maintaining the structural and mechanical integrity of the cell, connecting the sarcomere to the sarcolemma and other subcellular structures. Each thick myofilament is formed by several myosin molecules, each of which consists of two heavy chains in turn associated with two light chains. The myosin filaments are anchored

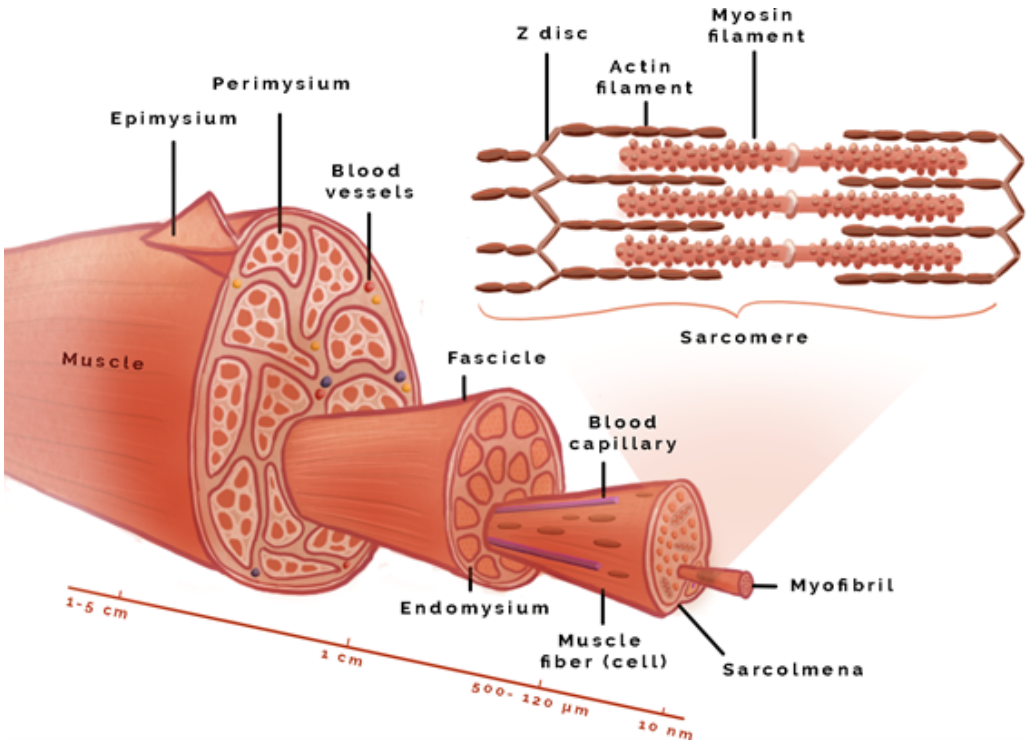

FIGURE 1.3: Organization of skeletal muscle. An entire skeletal muscle is enclosed within a dense connective tissue layer called the epimysium continuous with the tendon, binding it to bone. Each fascicle of muscle fibers is wrapped in another connective tissue layer called the perimysium. Individual muscle fibers (elongated multinuclear cells) are surrounded by a very delicate layer called the endomysium, which includes an external lamina produced by the muscle fiber (and enclosing the satellite cells) and ECM produced by fibroblasts. Each muscle fiber contains several parallel bundles called myofibrils. Each myofibril consists of a long series of sarcomeres which contain α-actinin, and myosin.

in the center of the sarcomere at the M line. The central zone of the sarcomere (the A band), where the myosin is situated, is darker (electron-dense) in transmission electron microscopy. By contrast, the area which contains only actin (the I band), presents a clearer appearance. The H band is the area at the center of the A band where there is only myosin. In the rest of the A band the actin and myosin filaments are intertwined. In this zone, the movement of the myosin heads slides actin filaments towards the center of the sarcomere, thereby shortening the sarcomere and the muscle fiber to generate force.

Depending on their speed of contraction, biochemistry and ultrastructure, two basic types of skeletal muscle fiber can be delineated: slow twitch fibers (type I) and fast twitch fibers (type II) (Figure 1.5). Moreover, type II fibers can be subdivided into subtypes such as IIA, IIB andintermediates, depending on their content in myosin heavy chain isoforms. Type I fibers use oxidative phosphorylation as a source of energy and therefore have more mitochondria. Muscles with type I fibers contract more slowly and are more resistant to fatigue. Slow-twitch fibers are also more vascularized and store more lipids and myoglobin in the sarcoplasm. By contrast, Type II fibers use in general, anaerobic metabolism to generate ATP. Muscles are composed of a mixture of fiber types, being a mosaic of both type I and type II fibers. The percentage of type I and II fibers in the

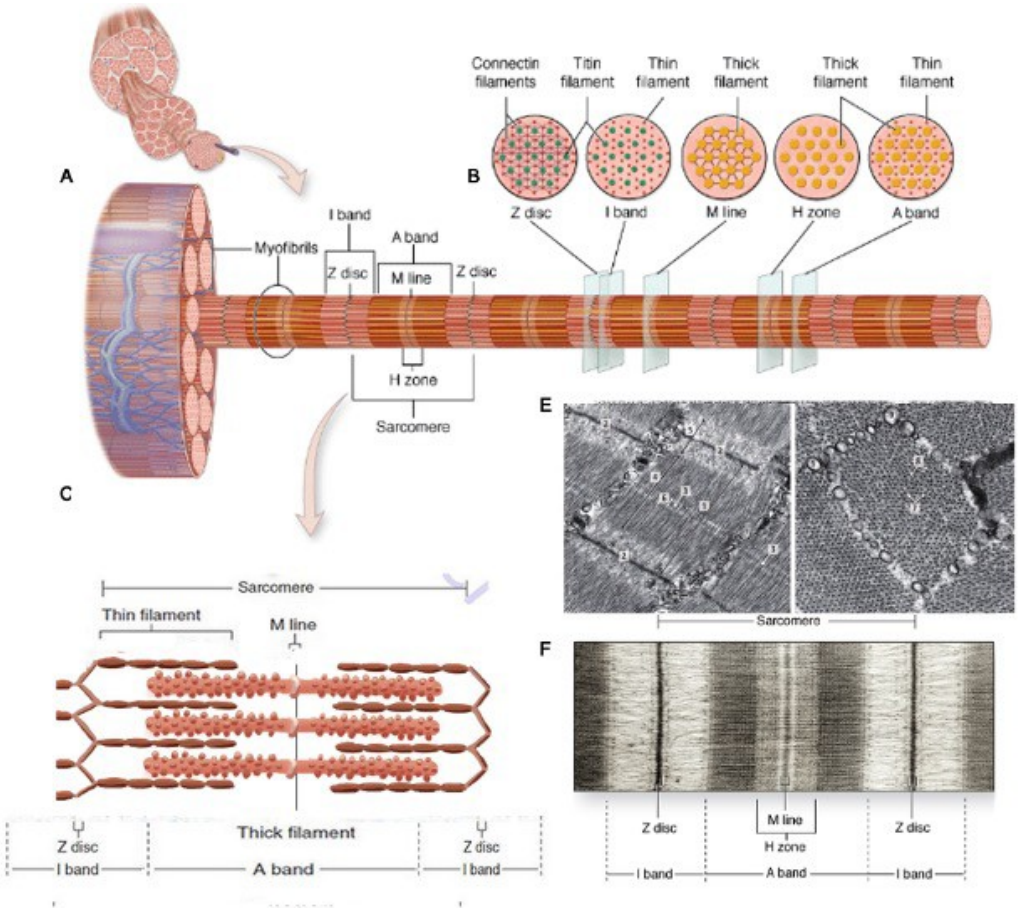

FIGURE 1.4: Sarcomere organization in a myofibril. Adapted from Mesher AL: Junquiera's Basic Histology: Text and Atlas 12th Edition. (A) Diagram indicates that each muscle fiber contains several parallel bundles called myofibrils. (B) Each myofibril consists of a long series of sarcomeres which contain thick and thin filaments and are separated from one another by Zdiscs. (C) Thin filaments are actin filaments with one end bound to α-actinin, the major protein of the Z disc. Thick filaments are bundles of myosin, which span the entire A band and are bound to proteins of the M line and to the Z disc across the I bands (by a very large protein called titin, which has spring-like domains). (E) Myofibril structure. TEM (50.000 x). Longitudinal section and Transverse section through A-band. 1. Sarcomere; 2. Z line, 3: M line; 4: A band; 5: I band; 6: H band; 7: Myosin myofilaments (thick filaments); 8. Actin filaments (thin filaments); 9. Sarcoplasmic reticulum. (F) The molecular organization of the sarcomeres has bands of greater and lesser protein density, resulting in staining differences that produce the dark and light-staining bands seen by light microscopy and TEM.

same muscle may vary over time, changing from slow to fast, depending on the degree of exercise. It appears that hybrid fibers may play a central role in many fiber-type transitions (Bottinelli and Reggiani, 2000; Medler, 2019).

In vertebrae, the skeletal system composed of the bone, cartilage, tendon, ligament and muscle derives from the mesoderm. The latter is divided into three sections: the paraxial, intermediate, and lateral mesoderm. Studies on development reveal that, excluding the craniofacial area, all components of the musculoskeletal system originate from the lateral plate mesoderm somite's (Brent and Tabin, 2002; Chal and Pourquié, 2017; Bentzinger et al., 2012). Once formed, under the inductive effect of neighboring tissues, the somites

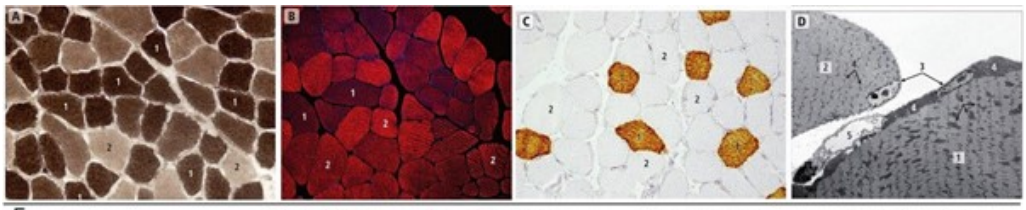

E	Type I fibers	Type IIA fibers	Type IIB fibers	Type IIX fibers
Contraction time	Slow	Moderately fast	Very fast	Fast
Resistance to fatigue	High	Fairly high	Low	Intermediate
Activity used for	Aerobic	Long-term anaerobic	Short-term anaerobic	Short-term anaerobic
Maximum duration of use	Hours	<30 minutes	<5 minutes	<1 minutes
Power produced	Low	Medium	Very high	High
Mitochondrial density	High	High	Low	Medium
Capillary density	High	Intermediate	Low	Low
Oxidative capacity	High	High	Low	Intermediate
Glycolic capaicty	Low	High	High	High
Major storage fuel	Triglycerides	Creatine phosphate, glycogen	Creatine Phosphate, glycogen	Creatine phosphate, glycogen
Myosin heavy chain Human genes	MYH7	MYH2	MYH4	MYH1

FIGURE 1.5: Characteristics of the Three Muscle Fiber Types. (A-D) Type I and type II muscle fibers. (A) Myosin APpase activity (400X). (B) immunodectection of fast myosin (Red). Confocale laser microscopy image. Nuclei counterstained with TO-PRO 3 (blue) (400X). (C) Immunodection of slow myosin (red) with DAB (brown) (400X). (D) Transmission electron microscopy image (3,000X). (E) Characteristics of the type I, type II (A, B, X) fibers in fast-twitch / slow-twitch fatigue-resistance, and fast-twitch fatigability in term of physical, anatomical and metabolic properties. Table Adapted from Bachmann (2016).

are rapidly subdivided into different compartments including the sclerotomes (bones) and the dermatomyotomes that subsequently give rise to various cell lineages. Myotome later forms muscles, whereas syndetome is the origin of tendons (Figure 1.6).

Myogenesis is characterized by successive and overlapping period of precursor cell proliferation, followed by the expression of muscle-specific genes, and finally, fusion of the differentiating myoblasts into mature myotubes (Zuk et al., 2004) (Figure 1.6B). In vertebrates, muscle formation is regulated by four basic helix–loop–helix (bHLH) transcription factors called Myogenic Regulatory Factors (MRFs); Myf5, Mrf4(Myf6), MyoD and Myogenin) (Sher et al., 2012). More precisely, at the molecular level, proteins Wnt and Sonic Hedgehog (Shh) are the main regulators of myogenesis (Bentzinger et al., 2012). Wnt and Shh are involved in lineage specification of muscle progenitors in the somite and the subsequent formation of dermomyotome and myotome by playing a critical role in upregulation of myogenic specific marker genes. The expression of Wnt proteins induces the expression of both Pax3 and Pax7, the first molecular markers of myogenic precursors in the dermomyotome while it inhibits the expression of sclerotome marker Pax1 (Capdevila et al., 1998). Wnt and Shh signaling also promotes the expression of myotome-specific markers including MyoD, Myf5, and myosin heavy chain. The expression of Pax3 gradually declines with the initiation of myogenesis, whereas the expression of basic helix-loop-helix (bHLH) transcription factors MRFs increases (Yusuf and Brand-Saberi, 2006). Pax-3 and Myf-5, work through separate pathways to activate MyoD and cause cells of dermomyotome to become committed to forming muscle. With increased levels of MyoD, the mononuclear cells, called myoblasts, begin to fuse into

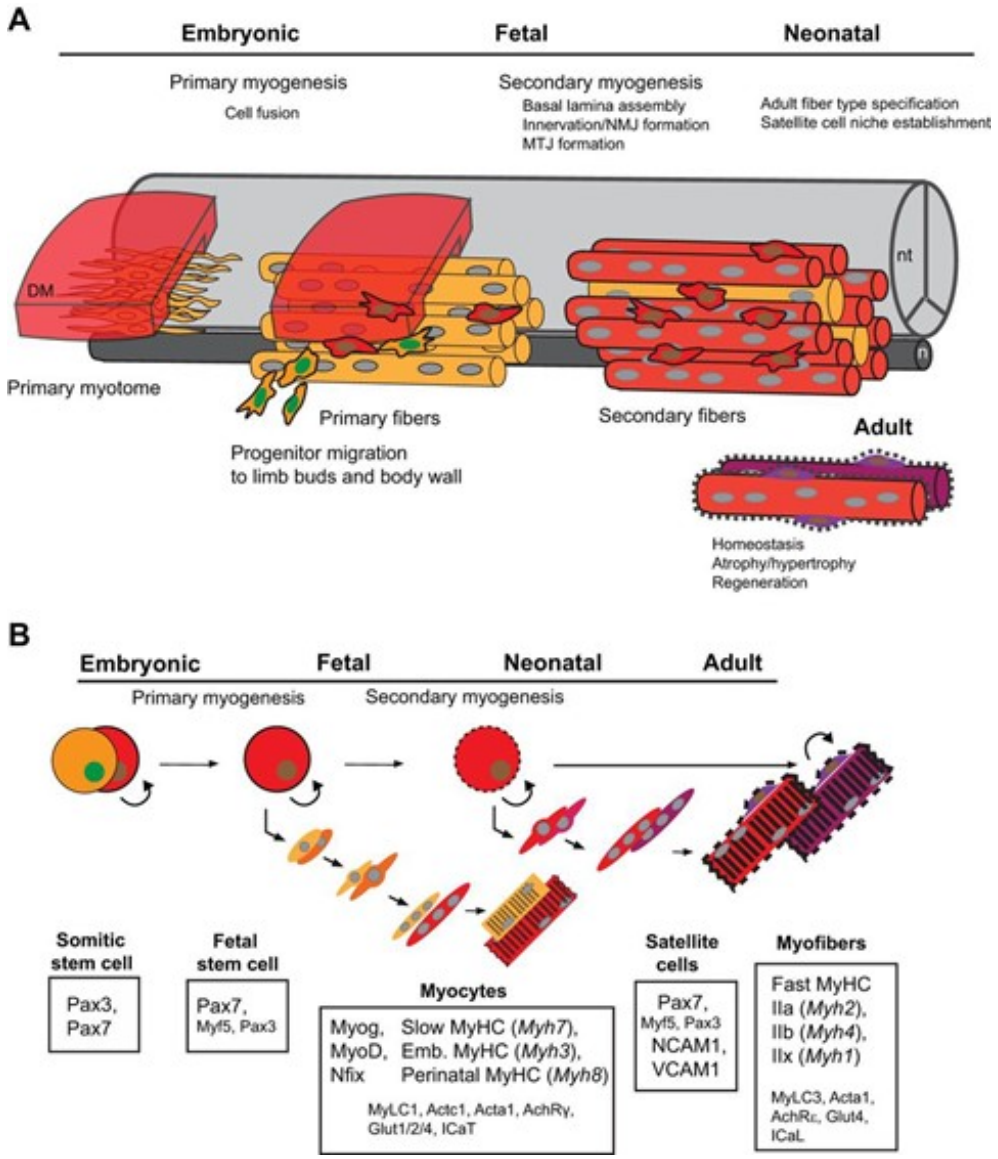

FIGURE 1.6: Stages of skeletal myogenesis from the embryo to the adult. (A) Developmental sequence of muscle formation from the dermomyotome. The early myotome (left, yellow) is composed of primary myocytes, which are aligned along the anteroposterior axis and span each somatic compartment. During primary myogenesis (middle), Pax3+ progenitors (yellow cytoplasm, green nuclei) delimitate from the dorsal side of the dermomyotome and contribute to the formation of large primary myofibers (yellow). Some Pax3+ progenitors also migrate from the ventral lip to populate the body wall and limb buds (hypaxial domain). During secondary myogenesis (right), Pax7+ myogenic progenitors (red cytoplasm, brown nuclei) contribute to secondary (red) fiber formation, using the primary fibers as a scaffold and contributing to the growth of fetal muscles. During this phase, satellite cell precursors (purple cytoplasm, brown nuclei) localize under the basal lamina (dotted line) of the fibers where they can be found in adult muscles. Key processes associated with each stage are listed above. nt, neural tube; n, notochord; DM, dermomyotome; MTJ, myotendinous junction; NMJ, neuromuscular junction. (B) Differentiation of somitic progenitors toward skeletal muscles and adult satellite cells. Myogenic stem cells contribute to fetal myogenesis while maintaining a pool of progenitors, which eventually become located on mature myofibers in the satellite cell niche. For each step, markers for the intermediates and differentiated skeletal myofibers are shown. Additional markers are also shown in smaller font. Differentiation stages along the myogenic lineages are color-coded according to A. 'Myocytes' encompasses also myotubes and myofibers. Emb., embryonic. From Chal and Pourquié (2017).

myotubes. At this stage, myogenin is expressed. Finally, Myf-6 (formerly called MRF-4) is expressed in maturing myotubes. Concurrently Pax7-positive progenitor cells at the later stages of development move from the central dermomyotome into the underlying myotome and produce a reservoir of muscle stem cells called satellite cells (Lepper and Fan, 2010). As explained in §1.1, in the adult skeletal muscle system, satellite cells are quiescent under normal conditions, whereas they become activated to proliferate and repair the damaged tissue upon injury (Yokoyama and Asahara, 2011).

Moreover, during embryogenesis, the musculoskeletal system develops while containing within itself a force generator in the form of the musculature. This generator becomes functional relatively early in development, exerting an increasing mechanical load on neighboring tissues (tendon and skeleton) as development proceeds (Felsenthal and Zelzer, 2017). Nonetheless, some recent studies have shown that, similar to the development of other musculoskeletal tissues, the initial specification of myoblasts is independent of mechanical cues reviewed by Lemke and Schnorrer (2017), whereas during subsequent stages of development mechanical signals originating from the developing muscle units are needed for proper muscle formation. During myofiber formation, the early attachment of myotubes to a tendon results in passive tension. This tension is needed for the proper assembly and alignment of myotubes during their formation. It is suggested to be maintained through titin, a protein that resembles a spring extending half the length of the sarcomere (Gautel and Djinović-Carugo, 2016; Valdivia et al., 2017). It has been shown that, in Drosophila, mechanical tension and spontaneous muscle twitching precede the formation of immature muscle fibers (Weitkunat et al., 2014, 2017). Subsequently, mechanical signals are needed for muscle morphogenesis and mechanical adaptation. In the absence of muscle contraction, muscles are smaller and display a delay in splitting, whereas exercised muscles become larger (Lima et al., 2018). The evolution of stiffness (Young Modulus) is also a good indicator of this differentiation as demonstrated by Collinsworth et al. (2002). They established that skeletal muscle cells exhibit viscoelastic behavior that change during differentiation: the apparent elastic modulus increase from 11.5 $\pm$1.3 kPa for undifferentiated myoblasts to 45.3 $\pm$ 4.0 kPa after eight days of differentiation (Collinsworth et al., 2002; Heinemeier et al., 2013).

1.2 Tendon

Tendons are specialized fibrous tissues that join skeletal muscle to bone and allow body motion through the forces generated by the skeletal muscles and transmitted to bone tissues (Kirkendall and Garrett, 2007). However, the tendon is a passive actor, unable to induce movement on its own. It acts as a highly adapted elastic spring that stretches and stores energy, which returns to the system through elastic recoil, improving locomotory efficiency. Its structure, function and physiology reflect the intense and repeated mechanical stresses that it must withstand.

The in vivo evaluation of human tendon mechanical properties depends on the investigation method (ultrasound, magnetic resonance imaging) and stretching protocols used. Young modulus ranging from 500 to 1850 MPa have been reported in the literature in Human (Maganaris and Paul, 1999; LaCroix et al., 2013; Bojsen-Møller and Magnusson, 2019).

1.2.1 From macroscopic organization to ultrastructure

Tendon's composition and structure are closely related to its function. Tendon is a dense connective tissue with limited cell content, vascularization and innervation (Hart et al., 1999). The major component of tendon is water (60 to 80 % in weight) (Birch, 2007), while its extracellular matrix is mainly constituted of type I collagen fibers (95% to 99% dry weight) and proteoglycans (<1% dry weight) such as decorin, versican, and aggrecan (Yoon and Halper, 2005)(Derwin et al. 2001; Yoon and Halper 2005). Type I collagen fibers are responsible of the fibrous structure (Kannus, 2000) and the tensile strength of the tendon whereas proteoglycans are responsible for the viscoelastic nature of the tendon.

Tendon cells are scarce but are key players in tendon growth, maintenance, adaptation to changes in homeostasis and remodeling in case of minor or more severe disturbances to tissue. Cells are responsible for the synthesis and turnover of tendon extracellular matrix (ECM) components and its related structure. Mature tendon contains predominantly tenocytes/tenoblasts (Pankaj Sharma and Maffulli 2005), which account for around 90-95% of the cellular population. The other 5-10% include the chondrocyctes, synovial cells and the vascular cells. Tenocytes are terminally differentiated cells typically anchored to the collagen and located throughout the tendon tissue. Tenoblasts are immature tendon cells that give rise to tenocytes. Recently, a new cell type has been characterized in tendon tissue: the resident tendon stem/progenitor cells (TSPC). They only represent 1-4 % of tendon resident cells and exhibit the same characteristics as adult mesenchymal stem cell (MSC) (Bi et al. 2007).

Focusing on the structure, type I collagen molecules aggregate to form collagen fibrils, the basic nano structural tendon unit. Bundles of fibrils form fibers, fibers group into fiber bundles or fascicles; and fascicles bundle together within connective tissue sheaths (endotenon) to form larger bundles that are surrounded by another connective tissue sheath (epitenon) (Silver et al., 2003) (figure 8). Collagen fibers display a wave pattern, which as a crimp (Rigby et al., 1959). Other types of collagen are present in the tendon

in smaller proportions, including type III, V, VI, XII and XIV (Mienaltowski and Birk, 2014). Types III, V and VI belong to the Fibrils-Forming family of collagens involved in fibril assembly regulation, while types XII and XIV belong to the class of Fibril-Associated Collagen with Interrupted Triple Helix (FACIT).

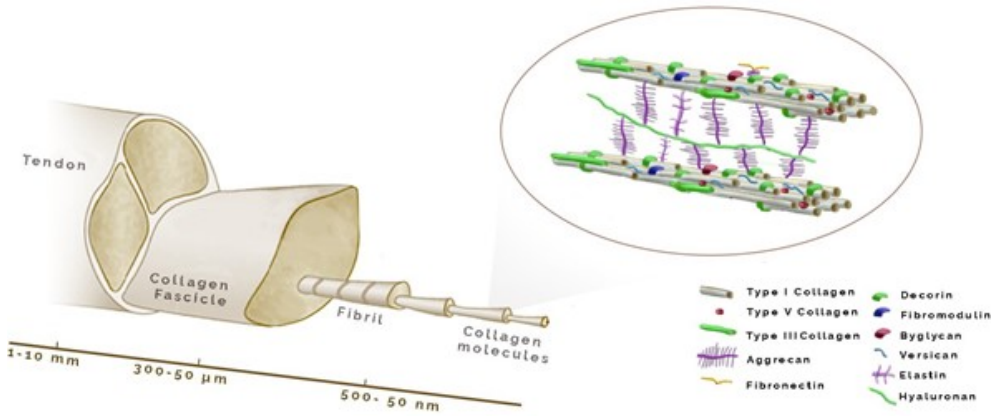

FIGURE 1.7: Hierarchical structure of tendon spanning from the single collagen molecule up to fibrils, fascicles, and whole tendon, with a focus of the structure of fibril-associated proteoglycans, the most abundant of which is decorin in tendon.

In addition, non-fibrous molecules are present on each level, the principal ones being the proteoglycans (PGs). Proteoglycans in the extra-cellular matrix (ECM) are known to regulate the assembly (i.e. fibrillogenesis) of the chief structural component of the tendon, type I collagen (Schönherr et al., 1995; Danielson et al., 1997; Kuc and Scott, 1997; Derwin et al., 2001; **?**). Decorin, the most abundant tendon PG, is considered as a key regulator of matrix assembly because it limits collagen fibril formation and thus directs tendon remodeling due to tensile forces (McCormick, 1999; Danielson et al., 1997). Aggrecan is a highly glycosylated PG playing a key role in the regulation of the osmotic pressure and thus tissue hydration which make the tissue ideal for resisting to compressive load with minimal deformation (Vogel and Koob, 1989). However, the role of those molecules is still not completely understood. Finally, ECM also contains glycoproteins including tenascin-C and fibronectin. Tenascin-C, protein presents in regions submitted to high mechanical forces, contributes to tendon mechanical stability (Martin et al., 2003) while fibronectin located at the surface of collagen molecules, contributes to wound healing (Sharma and Maffulli, 2006).

1.2.2 Tendon development

Tendon development is divided into two stages:

- the emergence of precursors/progenitors based on their origin and localization,
- the commitment and differentiation based on pivotal signaling cascades.

Interestingly, tendon is likely to require the presence of muscle for full development, with modalities depending on the anatomical site. Current knowledge (Gaut and Duprez, 2016) organizes them into three main groups depending to their position in the body: the craniofacial, the limbs and the axial tendons. Each of them has a different cell origin. The

craniofacial tendons originate from neural crest cells, while the limbs tendons have been shown to derive from the lateral plate of mesoderm. Finally, the axial tendons, associated to the segmented muscles of the vertebral column, derive from the somites (Figure 1.8). They especially come from the syndetome, a subdomain of somite comprising the tendon progenitor cells.

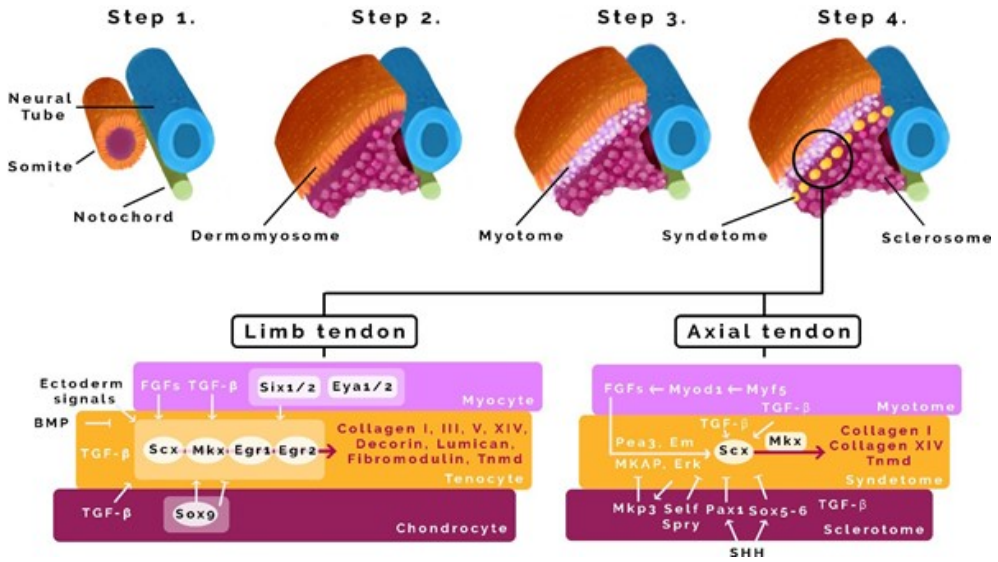

FIGURE 1.8: Development of axial and limb tendons during embryogenesis. Limb tendons are formed differently compared to axial tendons. Tendon limb progenitors are induced by ectodermal signals in the limbs and inhibited by BMP. Tendon progenitors position themselves between differentiating muscles and cartilage. Not only FGF but also TGFb can induce limb tendons. As in the axial tendon development, Scx and Mkx play a pivotal role giving the starting impulse for limb tendon formation. Early growth response 1 and 2 (Egr1/2) transcription factors act as molecular sensors for mechanical signals guiding the final steps of tendon maturation and production of collagen I, III, V, XIV, proteoglycans (decorin, fibromodulin, lumican), and tenomodulin. Axial tendon differentiation starts with upcoming FGF signaling from myotome. Signals from the sclerotome, for example, Sox9 (activated by SHH) have a negative effect on Scx induction blocking its expression. Moreover, TGFb signaling influences Scx and Mkx expression promoting axial tendon differentiation and the activation of extracellular matrix proteins such as collagen I, collagen XIV, tenomodulin, and others. Adapted from Delgado Caceres et al. (2018).

Tendon development is regulated by several factors. Among them, a few are identified to play an important role in tenogenesis: Scleraxis (Scx), a bHLH transcription factor, is the earliest known marker and regulator of tenogenesis. It promotes tendon differentiation and tenocyte specification (Alberton et al., 2011; Chen and Galloway, 2014). In axial tendon, muscle is required for the initiation of tendon development since it arises from the syndetome, a somite subdomain adjacent to the sclerotome and myotome. Scx initial expression is induced and regulated through the interplay of sonic hedgehog (Shh) and Wnt signaling in the syndetome. In the same way, fibroblast growth factor (FGF), specifically FGF8 and FGF4 from myotome, and transforming growth factor beta (TGF-β), are induced through the signaling pathways MAPK/ERK and SMAD2/3 respectively (Schweitzer et al., 2001; Havis et al., 2014). On the contrary, signals from the sclerotome lineage play a negative role. Scx induction might be blocked by Shh through Pax1 activity in the sclerotome. Mechanotransduction is also probably a key element on tendon development. The force exerted by muscles on tendons is required for the activation of FGF and

TGF-β(at the muscle-tendon interface), to maintain the expression levels of Scx, leading to tendon terminal differentiation(Maeda et al., 2011; Havis et al., 2016; Subramanian et al., 2018). Shear force generated during muscle contraction may stimulate and activate either TGF-βor integrin signaling (Subramanian and Schilling, 2015; Munger and Sheppard, 2011). However, in the limb and craniofacial area, Scx expression is initiated in the absence of muscle, in mouse, chicken and zebrafish embryos (Edom-Vovard et al., 2002; Chen et al., 2008). Further cell differentiation, maturation and segregation into individual tendons, seems induced by muscle cell migration. The absence of muscle eventually prevents further tendon development and leads to a loss of Scx expression. Scx then regulates the expression of tenomodulin (Tnmd), a late stage tenogenic marker, involved in tendon's maturation and functional performance (Dex et al., 2017). Tnmd is considered as a highly specific marker of differentiated tenocytes. Scx has also been shown to regulate positively Col1a1 transcription in mouse tendons (Shukunami et al., 2018).

Two other transcription factors, the homeobox protein Mohawk (Mkx) and the zinc finger transcription factor early growth response factor 1 (EGR1), promote final lineage commitment and differentiation into tendon cells (Liu et al., 2015; Ito et al., 2010). They activate Scx and Tnmd expression in various stem cell types and positively regulate type I collagen production in vivo (Lejard et al., 2011; Guerquin et al., 2013). Besides, Mkx activates the expression of TGF-β2 gene by binding to its promoter. It is also supposed to inhibit muscle differentiation by repressing MyoD transcription (Liu et al., 2015).

In developing tendons, tenocytes align in parallel arrays along the tendon axis and deposit large amounts of extracellular matrices including collagens, elastin and small leucin-rich proteoglycans (Kannus, 2000). The increased presence of collagen type I, is not a specific marker of tenogenic differentiation. Indeed, it is a major component of other musculoskeletal tissues such as bone and skin. However, the development of an aligned collagen structure and mechanical function can indicate appropriate tenogenesis and tendon formation (Theodossiou and Schiele, 2019).

1.3 Myotendinous Junction

The myotendinous junction (MTJ) is a highly specialized anatomic region in the musculotendinous system. The tension generated by muscle fibers is transmitted from their intracellular contractile proteins to the extracellular connective proteins in the tendon (Figure 1.9).

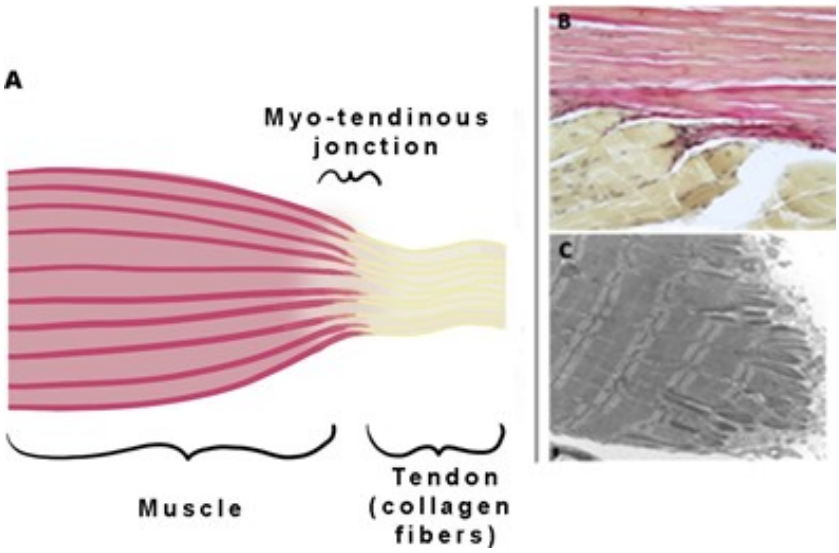

FIGURE 1.9: Representation of Myotendinous junction. (A) Schematic presentation of the myotendinous junction (MTJ) localised between the muscle and the tendon, Adapted from Human Anatomy Pt 514 with Salem at University of Southern California. (B) Dense regular CT of Muscle-tendon junction, guinea pig, stained by Hematoxylin and eosin (H&E). (C) TEM observations of rat's muscle-tendon interface, which appears very folded with many long interdigitations. The muscle ultrastructure reveals a regular disposition of sarcomeres with aligned myofilaments and Z lines, both near the MTJ and far from Bars C 0.5 µm from (Curzi et al. 2019).

1.3.1 Organization and structure

Skeletal muscle and tendon are complex, multiphasic, neighboring tissues with their own specialized structural, mechanical and functional properties as seen in §1 and §2. Thus, their disparity requires a specific interface because:

- the machinery that gives the muscle its contractile function is intracellular (Kuo and Ehrlich, 2015), while the collagen matrix that gives the tendon its connective strength is extracellular. In order to effectively transmit force generated from the intracellular contraction of the muscle proteins to the extracellular collagen fibers of the tendon, the composite junction requires contiguous transmembrane connections.
- the difference between the mechanical properties of tendon (E from 100kPa to 2 GPa) and muscle (E from 10 to 55 kPa) at the MTJ interface makes it more subject to damage (Lima et al., 2018) (Constantinos N Maganaris and Paul 1999). The muscle is the most flexible of these tissues, but also the thinnest at its insertion with the tendon. It submits the MTJ to greatest stress and exposes this area to rupture. Therefore,

to counterbalance this apparent weakness, the interface region between muscle and tendon must possess important structural features to protect the MTJ from mechanical damage during movement.

At the macroscopic scale, the muscle-tendon interface is not a well-defined separation. Muscle and tendon tissues meet in a zone where they overlap, resulting in a gradient in tissue composition.

At the microscopic level, the major structural features of the MTJ observed by electron microscopy are the extensive invaginations and evaginations of the sarcolemma with the tendon extracellular matrix (Figure 1.10). Consequently, the interdigitations known as "finger-like" greatly increase the contact area between the two types of tissues by 10 to 50 times. This feature enables MTJ to resist to the high mechanical stresses ≈1,8-3,5x10^4 N.m^{-2} generated by muscle contraction (Tidball and Chan, 1989)(Tidball and Daniel 1986). Thereby, it allows a smoother transition of mechanical strength as well as a greater dissipation of mechanical stresses, which reduce the risk of abrupt stress concentration and thus the risk of rupture.

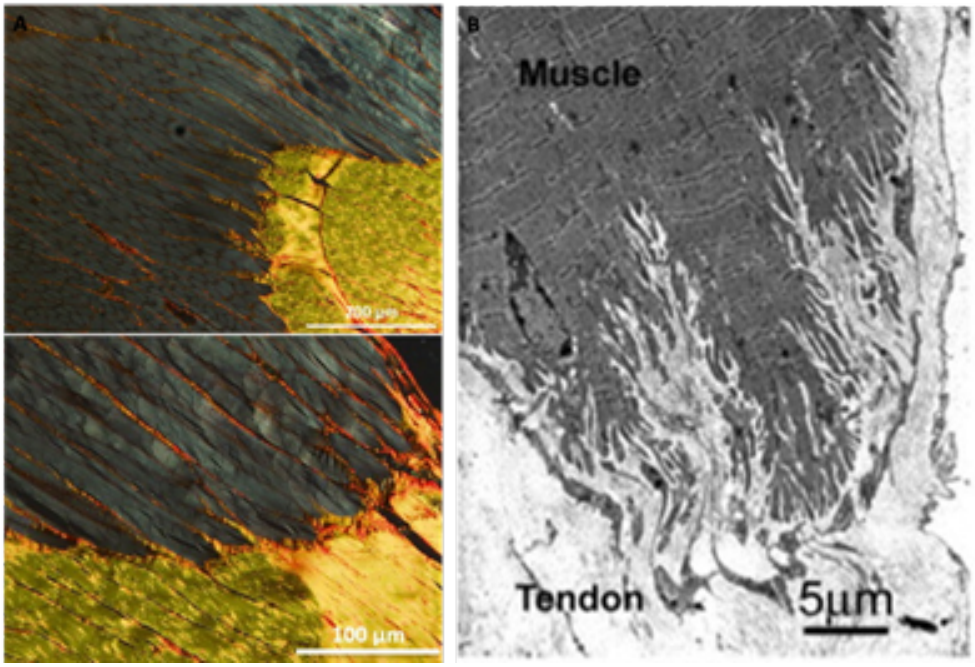

FIGURE 1.10: Microscopic observation of MTJ. (A) photograpy of the muscle–tendon interface stained with picrosirius red under polarized light shows the junction between the muscle fibers and the tendon. (Source: Pablo Moncada-Larrotiz and Lisa Larkin, University of Michigan). (B) transmission electron micrograph (TEM) of the myotendinous junction shows the network of interdigitations between the muscle sarcolemma and the tendon ECM. (Larkin et al., 2006) Copyright ©2015 Elsevier Ltd. All rights reserved. Reproduced with permission.

At the protein level, the organization of myotendinous anchoring system is also influenced by both muscle and tendon tissues and their interaction (Tidball and Chan, 1989). Adhesive complexes are essential for MTJ function since they are responsible for transmitting mechanical forces, maintaining and securing skeletal muscle fibers to tendon fibrils. Two major and distinct transmembrane linkage systems have been described in the MTJ, both constitute a structural link between tendinous extracellular matrix proteins and

myofibrils (Figure 1.11). The two anchoring systems require laminin-2 to form functional myotendinous junction (Holmberg and Durbeej, 2013). Laminin-211 is highly expressed at the MTJ level and is the only isoform present in adulthood while laminin-221 and 411 are expressed at the embryonic stage (Grounds et al., 2005).

The first linkage system contains the dystrophin-associated protein complex (DAPC) (Gawor and Prószyński, 2018). It is initiated on the muscle cell side with the binding of actin to dystrophin. Dystrophin is located at the inner surface of the cell membrane and is capable of binding to muscle cell membrane proteins. This in turn binds to B-dystroglycan and at the extracellular site, α-dystroglycan is linked to ECM laminin-2 through sarcoglycan. The sarcoglycan complex may function in stabilizing the entire complex.

The second system contains α7β1 integrin, which is the predominant integrin in adult skeletal muscles. It plays important roles in skeletal muscle development and function. The β1 subunit participates in the linkage with actin via several subsarcolemmal proteins, including αactinin, talin, vinculin, paxillin and tensin (Tidball and Lin, 1989; Turner, 2000). The α7 subunit binds ECM proteins such as collagens, fibronectin, vitronectin, and laminins in the basal lamina surrounding individual muscle fibers. The inactivation of specific adhesion proteins, such as the α7 integrin subunit, leads to severe disruption, especially to the detachment of MTJs from the ECM (Miosge et al., 1999).

ECM surrounding the MTJ is rich in collagen I and tenascin-c on the tendon side. On the muscle side, the sarcolemma is in close contact with the muscle basement membrane in which laminins and type IV collagen are the major constituents with the presence of type XIV collagen. They play an important role in the basement membrane formation. More recently, type XXII collagen, a member of the FACIT (Fibril Associated Collagens with Interrupted Triple helices) collagen family, has also been shown to be solely present at the MTJ (Jakobsen et al., 2017).

1.3.2 Development of the myotendinous junction (MTJ)

Despite their distinct embryonic origins, muscle and tendon's morphogenesis take place in close spatial and temporal association. In return, the correct assembly of the MTJ is crucial for proper muscle and tendon functions. Unfortunately, the signals mediating the connection between muscles and tendons, and the mechanism governing the establishment of the junction site have not been fully elucidated yet Charvet et al. (2012); Subramanian and Schilling (2015); Nassari et al. (2017); VanDusen and Larkin (2015), propose review of the current understanding and provide some insight into MTJ development (Figure 13).

In vertebrates, Charvet et al. (2012) categorizes the MTJ formation in five major events :

1. The earliest morphological modification at the nascent MTJ is the formation of close interactions between myogenic cells and tenoblast cells, as described by (Tidball and Lin, 1989).
2. Tenoblasts and myoblasts, initially separated by several micrometers, progressively develop interactions between themselve.

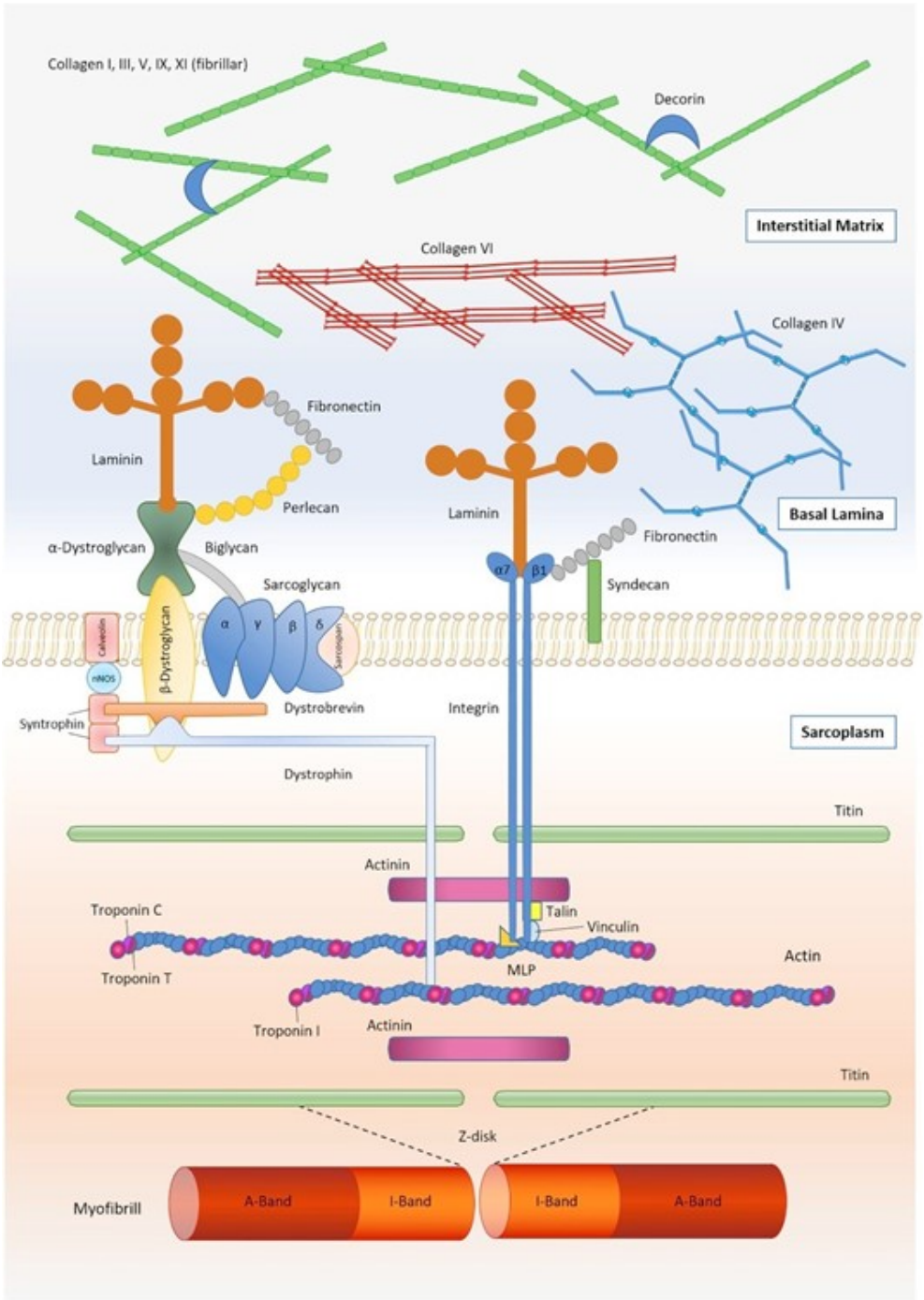

FIGURE 1.11: Schematic representation of the MTJ at the molecular level. Two types of linkage complexes are described: the dystrophin-associated protein complex (DAPC) and the protein complex containing the transmembrane α7 β1 integrin. Both complexes connect the sarcomeric actin to the tendinous extracellular matrix (ECM) via the basement membrane laminin α2, most likely assembled into the laminin 211 trimer. These complexes are enriched at the MTJ and correspond to the sub-sarcolemmal densities observable in the finger-like processes with transmission electron microscopy. Both systems are interconnected via the intracellular proteins α-actinin or desmin. From Csapo et al. (2020) CC BY.

3. Adjacent to these association processes, an accumulation of sparse fibrillar ECM components is observed between muscle fibers and tendon cells, which leads to a closer association of cells with collagen fibers.

4. Myoblasts fuse into contractile myotubes and the deposition of ECM proteins close to the sarcolemma forms the nascent basement membrane between myotubes and early on tendon development.
5. The sarcolemma starts to fold, and myofibrils associate with subsarcolemmal densities.

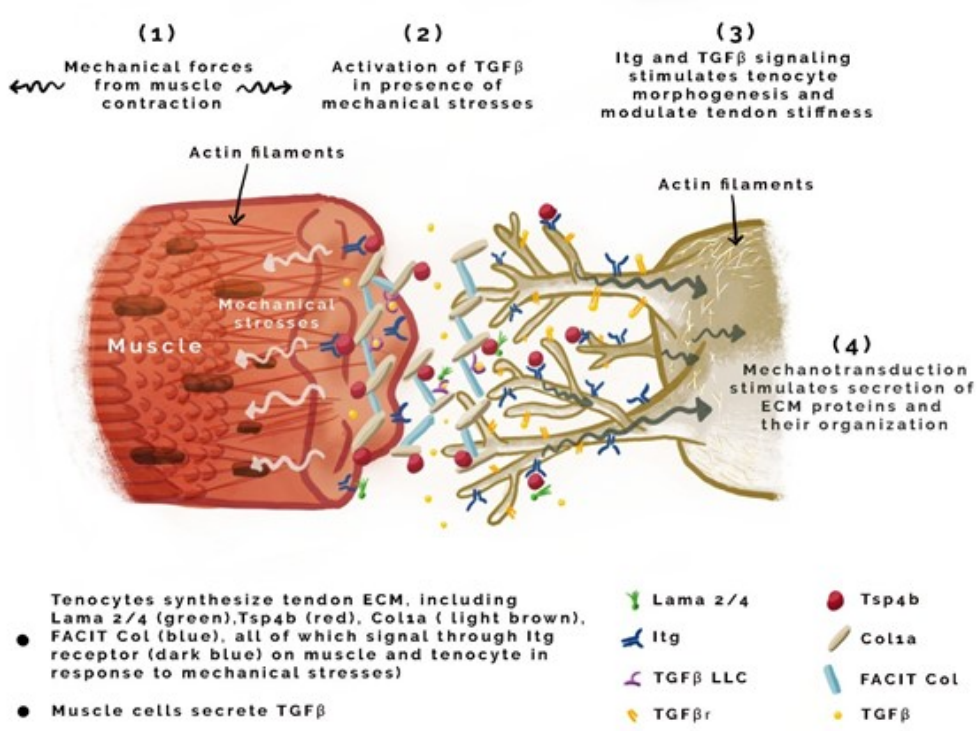

FIGURE 1.12: Myotendinous junction formation. A muscle fiber (red) secretes ECM components into its surroundings (the myomatrix), which includes the integrin ligands Tsp4 and Lama2. This ECM accumulates in the absence of (tendon precursor cells) TPCs. Some of these components overlap with those of the tendon ECM, which is secreted by tenocytes (white). Myomatrix is primarily composed of Lam trimers and Fn. By contrast, the tendon matrix is rich in Col1a trimers and thrombospondin pentamers. In the presence of tensile force from muscle contraction (1) changes in ECM organization and other factors lead to release of active Tgfβligand. Tgfβ-mediated mechanotransduction is essential for tenocyte differentiation and morphogenesis (2). Tgfβligand binds to receptors on tenocytes to increase pSMAD3 signaling (3), secretion of ECM components (4) and growth/branching of microtubule rich projections (5). Cartoon depiction of tenocyte morphogenesis in the presence of mechanical force. The myotendinous junction (MTJ) is the narrow zone in which ECM components of tendon and muscle interact. Inspired by Subramanian and Schilling (2015)

In mammalian tendons, tenocytes and collagen fibrils start organizing themselves in parallel array in response to the contractile force of the developing muscle during the late embryonic and neonatal periods. The neo-synthesized ECM provides a support, which in turn drives the thick and thin filaments of sarcomere in myotubes to organize themselves into parallel arrangement. The gradual alignment of collagen fibers results from the progressive formation of sarcomeres and increasing in contraction forces. This process suggests a mechanical crosstalk between muscle and tendon. Finally, the anchorage of collagen fibers into the sarcolemma results from the recruitment of linkage complexes of transmembrane proteins, which extends from the last Z-line. It leads to the formation of sarcolemma protrusions, leading to “finger-like” forms.

Some of the mechanisms under which muscle cells signal to the tendon cells to form and maintain a stable MTJ have been recently explained using the Drosophila model. It was shown that moleskin (Msk), known as a nuclear import protein, is conserved in Drosophila and humans. This protein is essential for muscle attachment (Liu and Geisbrecht, 2011)). Msk is synthesized by muscle cells and modulates the neuroregulin-like ligand (Vn) secretion, accumulation and localization at the site of the muscle-tendon attachment site. Vn activates EGF-signalling pathway in tendon cell precursors which induces in turn the expression of most tendon cell-specific genes, including the markers of terminally differentiated tendon cells, (β1- tubulin and delilah).

Moreover, the factor Roundabout (Robo) was demonstrated playing a role in directing muscles to their corresponding tendons. Robo is expressed in a subset of muscle fibers and acts as a guidance receptor for the protein Slit, an important tendon-specific guidance signal produced by the tendon cells (Ordan and Volk, 2015). However, the contribution of Robo on muscle patterning remains elusive.

Finally, another protein complex has been described as playing a role in guiding the Ventro- Lateral (VL) muscles. This complex includes the transmembrane protein Kontiki (Kon) located at myotube tips and signals through the intracellular adaptor complex Dgrip/Echinoid. This protein complex allows the establishment of a stable connection between myotubes and tendon cells (Schnorrer et al., 2007).

To conclude this section, the structure, composition and molecular mechanisms involved in the development of the MTJ are still unclear and not well documented. The difficulty of studying this intermediate region is due to the lack of a specific marker, as well as the difficulty of carrying out tests in humans. The emergence of diverse animal models such as mice, chicken, zebrafish or Drosophila has however facilitated the study of this junction. These models have made it possible to highlight information that had previously been difficult to access such as the "cross-talk" between muscle and tendon.

1.3.3 MTJ current repair solutions

In traumatic injuries, where the muscle–tendon interface is completely separated, simple suture has been shown to not provide adequate functional recovery. Therefore, research is directed toward the potential use of growth factors, such as insulin-like growth factor 1 (IGF-1), basic fibroblast growth factor (bFGF), nerve growth factor (NGF) or hepatocyte growth factor (HGF) (Kasemkijwattana et al., 2000; Kasprzycka et al., 2019).

The benefit of growth factors particularly for MTJ repair has not been evaluated. Furthermore, a cocktail of growth factors may act through multiple signaling pathways and have mitogenic effects on fibroblasts, thus increasing the formation of fibrotic tissue and limiting their potential of repair on the MTJ (Jones and Clemmons, 1995).

Additionally, cell-based therapies may hold potential for musculoskeletal tissue regeneration. However, such treatments have undergone several unsuccessful clinical trials because of poor cell delivery, survival, and proliferation in vivo (Bareja and Billin, 2013; Lacitignola et al., 2008; MacLean et al., 2012; Motohashi and Asakura, 2014).

Among the other current strategies to regenerate the MTJ injury, graft repair techniques are being explored. They involve either autogenic fascial patches, biological or synthetic scaffolds. However, to date, those techniques are not able to accurately replace native MTJ-like morphology. They also promote fibrotic scar tissue formation and may not result in the formation of a native-like MTJ at the repair interface, increasing the likelihood of future damage (Kääriäinen et al., 2000).

Chapter 2

Tissue Engineering approaches for the myotendinous system

Tissue engineering (TE) is a promising approach to repair tendon and muscle when natural healing fails. Biohybrid constructs obtained after cells' seeding and culture in dedicated scaffolds have been considered as relevant tools for mimicking native tissue, leading to a better integration in vivo. They have been employed to perform advanced in vitro studies to model cell differentiation or regeneration processes. Tissue engineering relies on three pillars: cells, biomaterials, and environment, ensured by chemical or physical factors (Figure 2.1).

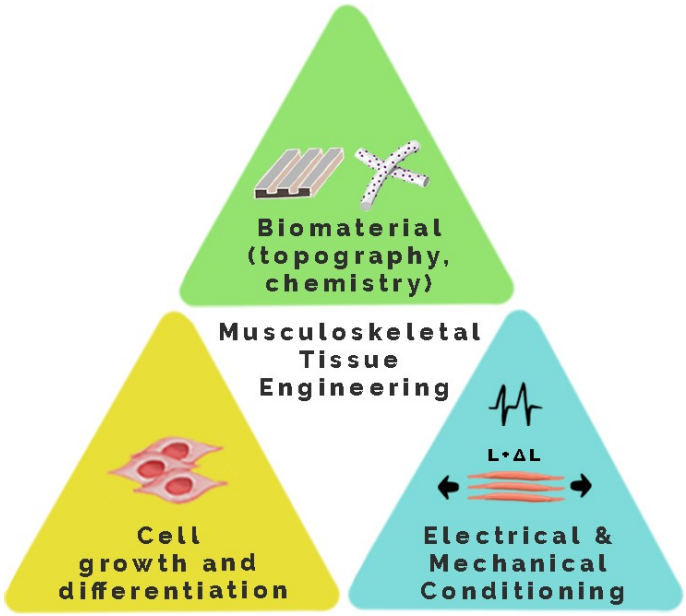

FIGURE 2.1: : The three pillars of tissue engineering. Cells are cultured on a scaffold where they can attach, proliferate, or differentiate, giving them a phenotype relevant for the renewal of tissue functions. The mechanical and biochemical environments are of prime importance for triggering specific responses.

2.1 Current approaches for myotendinous junction reconstruction

Engineering a tissue for myotendinous junction repair is a complex task, in link with the complexity of the native tissue. As explained in the previous parts, the MTJ is not a smooth continuous division between muscle and tendon to limit stress-associated failure. The gradient of structural and mechanical properties throughout the entire interface region should be replicated to mimic its functions. In addition, this tissue is always submitted to mechanical passive and active strains, that probably contribute to its specific structure. Therefore, to properly engineer a composite muscle–tendon system, those very specific biological, biomechanical and structural properties of the muscle fibers, tendon and interface must be accounted for (Figure2.2).

	E (MPa)	UTS (MPa)	SAF (%)
Native MTJ	0.2789 (±0.1509)	0.1478 (±0.01631)	122.4 (±19.18)
Muscle	0.005–2.8	–	–
Tendon	500–1850	52–120	5–16%

FIGURE 2.2: Mechanical properties of the native MTJ, muscle and tendon. In term of modulus, ultimate tensile strength (UTS) and strain at failure (SAF)(values obtained from literature. (Engler, Griffin, Sen, Bönnemann, Sweeney and Discher, 2004; Myers et al., 1998; Pollock and Shadwick, 1994; Lieber, 2002; Lima et al., 2018)

Atala's group proposes two different approaches based on a unique scaffold composed of 3 different areas (Figure 2.3). In a first study, such scaffolds are prepared by electrospinning and consisted in: i) an area of collagen/ poly-ε-caprolactone (PCL) fibers, ii) an interphase area where fibers of collagen/PCL and collagen/poly-L-lactic acid (PLLA) are co-extruded, ii) an area of collagen PLLA fibers. All the areas are randomly deposited, and fiber size is about 500 nm, independently of the electrospun material. Young's moduli are around 4, 20, and 28 MPa, respectively. When C2C12 are seeded on to PCL, they form myotubes, while NIH/3T3 fibroblasts spread on PLLA. There is no evidence of cell reorganization at the interface to form a specific MTJ (Ladd et al., 2011).

In a second study, (Merceron et al. 2015) used the co-printing of two synthetic polymers poly- urethane (PU) and PCL together with a bio-ink based on hyaluronic acid, fibrinogen and gelatin (Figure 16). The bio-ink contains C2C12 myoblasts on the PU side and NIH/3T3 cells on the stiffer PCL side. The interface is created by co-localizing the printing of PU and PCL leading to a 10% overlap. After the composite PU–PCL/C2C12-NIH/3T3 construct has been printed, the fibrin-based hydrogel bio-ink is cross-linked. The extruded fibers exhibit a diameter of about 300 µm. According to classic tensile tests, the final construct is elastic on the PU-C2C12 muscle side (E = 0.4 MPa), stiff on the PCL-NIH/3T3 tendon side (E = 46 MPa), and intermediate in the interface region (E = 1.0 MPa). Again, both cell lines grow correctly on their respective surfaces and some interfacial features

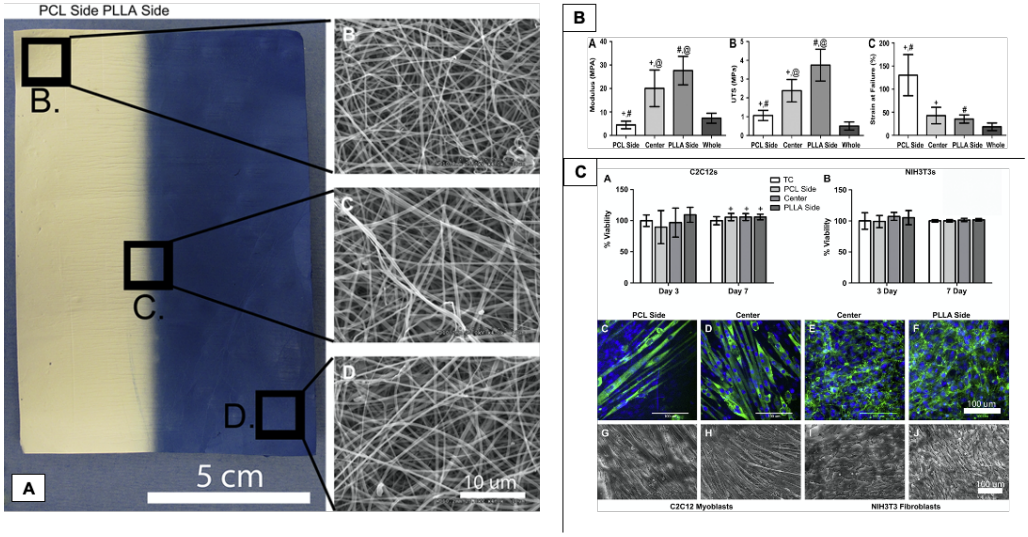

FIGURE 2.3: Co-electrospun dual scaffolding system with potential for muscle–tendon junction tissue engineering. (A) Image showing the three regions of the scaffold: PCL side, center, and PLLA side with the methylene blue dye in it. (B–D) SEM images from different regions of a scaffold showing fiber morphology and diameter (all images 4K×). (B) PCL side (549 $\pm$ 97.4 nm), (C) Center (504 $\pm$ 92.5 nm),(D) PLLA side (452 $\pm$ 40.3 nm). (B) Average parameters obtained from tensile testing to failure of each region and the whole scaffold. (A) Young's modulus. (B) Ultimate tensile strength. (C) Strain at failure. +,#, @ indicate statistical significance with $p < 0.05$. (C) (A,B) MTS assays demonstrating cytocompatibility of the scaffold regions. Data are expressed as percent viability which is the average absorbance normalized to the average absorbance of tissue culture control. (A) The scaffolds show no statistical difference in cell viability at 3 days and at 7 days there was a slight increase in percent viability in the scaffold groups, but this difference is likely due to experimental error. (B). For the fibroblasts, at both 3 and 7 days, no differences were found in viability between the scaffolds and tissue culture controls. (C–J) Confocal (C–F, all images 200×) and SEM (G–J, all images 300×) images of scaffolds seeded with C2C12 myoblasts or NIH3T3 fibroblasts. Adapted from (Ladd et al., 2011)

could be observed under confocal microscopy. This type of approach seems quite promising, because it allows to control the depositing of cells locally. It highlights the ability offered by 3D printing to deposit different cell types in precise locations, paving the way to complex multicellular scaffolds for regeneration.

In the scaffold-less tissue engineering field, Larkin et al. (2006) attempt to reconstruct the junction using so-called scaffold-free self-organized tendon constructs (SOT) . SOT consists in collagen-rich deposits and flattened, hosting longitudinally oriented tenocytes extracted from rat tendons. They are put into contact with pre-established cultures of spontaneously contracting multinucleated myotubes. The interface presents an ultrastructure that resembles the fetal/neonatal MTJ. When subjected to tensile tests, rupture is observed on the muscle side. Swasdison and Mayne (1991), produce encouraging muscle-tendon units by co-culturing embryonic tendon fibroblasts with myoblasts between fixed posts. Finally, Hashimoto et al. (2016) develop a 3D gel-patch tissue system using skeletal muscle-derived multipotent stem cells (Sk-MSCs) sheet-pellet for MTJ reconstruction. They found that their Sk-MSC sheet-pellet transplantation achieved favorable results in the reconstruction and/or reconnection of the ruptured muscles and tendons. This approach does not imply a specific scaffold but provides new insights into the mechanisms responsible for the formation and maturation of the junction, to mimic the in vivo conditions.

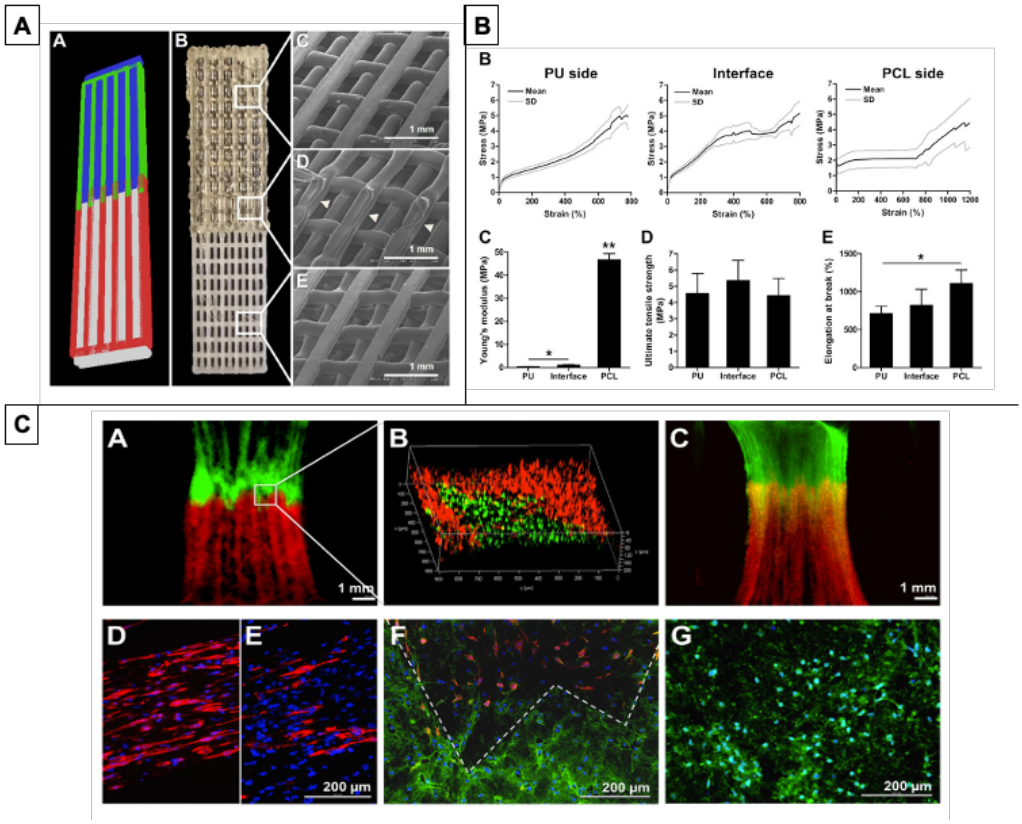

FIGURE 2.4: bioprinting of muscle–tendon unit (MTU) construct. (A): (A) MTU construct with cells (green: PU, red: PCL, blue: C2C12 cells, white: NIH/3T3 cells). (B) Gross image of MTU construct with PU side on top, PCL side on bottom, and 10% overlap area at interface in center. SEM images showing (C) PU side, (D) interface region, and (E) PCL side. (B): Tensile properties of the bioprinted MTU constructs. (A) When tensile force is applied, the PU side strains before the PCLside strains. (B) The stress–strain curves of the PU side, interface region, and PCL side. (C) Young's modulus, (D) ultimate tensilestrength, and (E) elongation at break of the bioprinted MTU constructs with different regions. (C): (A)–(C) Fluorescently-labeled dual-cell printed MTU constructs (green: DiO-labeled C2C12 cells; red: DiI- labeled NIH/3T3 cells; yellow: interface region between green and redfluorescence). (A) Constructs were imaged at (A) 1 d and (C) 7 d in cultureto show cell–cell interactions and movement. (B) Confocal microscopic image shows a 3D reconstruction of the interface region on1 d after printing. (D)–(G) Immunofluorescence of bioprinted MTU constructs after 7 d in culture. (D) and (E) On the PU side of theconstruct, C2C12 cells formed highly- aligned, multinucleated myotube structures (red, (D) desmin and (E) MHC; blue, DAPI). (F)At the interface region, depicted by the dotted line, differential expression between the two cell types is observed (red, desmin; green, c ollagen type I; blue, DAPI). (G) On the PCL side of the construct, NIH/3T3 cells secreted collagen type I (green, collagen I; blue DAPI). Adapted from (Merceron et al., 2015*b*) ©IOP Publishing. Reproduced with permission. All rights reserved.

As shown above, the bibliography is rather scarce in this field, probably because tissue engineering is still in its infancy and researchers still focus on single tissue reconstruction. To be exhaustive on the possible alternatives to build a tendon-muscle continuum, we propose hereafter a summary of these approaches proposed for tendon, as tendon reconstruction was one part of the PhD thesis of Alejandro Garcia Garcia (2019), as well as an extended review for muscle tissue engineering, as some parts of this PhD will deal also with this issue.

2.2 Current approaches in Tendon T.E

This paragraph focuses on biomaterials for scaffolds and thus for the reconstruction of the tendon- muscle continuum tissue. Scaffold for tendon tissue engineering construct (TEC) must tolerate high and impulsive forces and stresses for daily living activities. Ker et al. (1988) estimated that peak stresses can approach 100 MPa during intensive exercise. Such large forces/stresses require specific TEC materials and design to prevent rupture.

Regarding synthetic materials, only a few FDA-approved could be considered: poly-ε-caprolactone (PCL) (Naghashzargar et al., 2015)(, poly-L-lactic acid (PLLA) (Sensini et al., 2018),poly-lactic-co-glycolic acid (PLGA) (Moffat et al., 2009), or polyurethanes (PUs) (Cardwell et al., 2015). Synthetic constructs present tunable and reproducible mechanical and chemical properties. They are relatively inexpensive to produce and easy to mold into a variety of forms: meshes, foams, hydrogels, electrospun, yarns (Xu et al., 2013) , knitting (Zheng et al., 2017), and 3D printing (Park et al., 2018). However, introducing some of those materials can lead to increased inflammation and rejection after implantation.

Regarding biological scaffold, most research has focused on collagen alone or in mixture with other molecules, such as proteoglycans, as a support for tendon tissue engineering. Since, the composition and structure of tendons is mainly determined by type I collagen, different strategies have been explored to produce the ideal collagen-based scaffold, such as sponges (Müller et al., 2016), gel, extruded collagen fibers (Gentleman et al., 2003), or electrochemically aligned collagen (Uquillas et al., 2011). Collagen base-scaffold permits a more rapid infusion of cells and/or growth factors, but they are often too compliant and weak to transmit muscle forces. Therefore, some alternatives to collagen for tendon reconstruction have appeared such as silk fibroin. With this fibrous nature, silk fibroin is a biocompatible material, low immunogenicity, and remarkable tensile strength as main properties (Kuo et al., 2010). More recently, decellularized matrices of tendons from a wide range of species were proposed as scaffold. As they preserve biochemical composition, offering cells a full biomimetic environment. However, as for collagen scaffold, they present rapid degradability and low mechanical properties, which might limit their use in TE.

Finally, some hybrid scaffolds based on the synergistic effect between natural and synthetic materials have been employed for tendon TE. They combine the properties of both the biological and synthetic compound. The biological compound tends to act as cells' carrier, by stimulating proliferation and migration over the support. While, the synthetic compound provides the stiffness needed for the construct to reach mechanical properties near the tendinous native tissue Mallick and Cox (2013). More information regarding cells and environment pillars can be found in the review in annex (Beldjilali-Labro et al., 2018*a*).

2.3 Current approaches in Muscle TE

2.3.1 Cells type

(From Beldjilali-Labro et al. (2018*a*))

The choice of an appropriate cellular source is fundamental for generating functional muscle in vitro. Fishman et al. (2013) established a non-exhaustive list of criteria that cells should meet to be suitable candidates for muscle engineering. According to the literature data (Table 4), four cell types are predominantly employed in muscle engineering: the mouse C2C12 myoblast cell line (Hashimoto and Sato, 2012*a*; McKeon-Fischer and Freeman, 2011), primary myoblast-derived satellite cells (SCs) (Boonen et al., 2010; Serena et al., 2008; Langelaan et al., 2011*a*), primary myoblast from different species (Baniasadi et al., 2016; Kheradmandi et al., 2016). SCs are an appealing solution as they are relatively easy to isolate and are also the direct precursor of myoblasts. Unfortunately, SCs maintained in vitro suffer a severe reduction in their ability to produce myofibers, and a decrease in their proliferative capacity (Shadrach and Wagers, 2011). The C2C12 cell line manages to decrease the variability of primary cell isolation. In addition, using the C2C12 cell line for muscle engineering studies makes possible an objective comparative analysis with works that are published in skeletal muscle bioengineering as it mainly uses this cell type (Liao et al., 2009).

2.3.2 Modulation of the Environment

Functional muscle formation is an intriguing and highly complex process that requires features, such as cell differentiation and maturation (Bandyopadhyay et al., 2013). As shown in Figure 5, several intracellular pathways are responsible for enhancing proliferation and differentiation expression of cell genes during muscle development (Egerman and Glass, 2014). The effects of a wide variety of chemical and/or physical factors on muscle cell progenitor cultures have been investigated extensively. Many previous studies have demonstrated the ability of chemical stimulation to induce muscle cells and differentiation by studying the effect of certain growth factors (Powell et al., 2002; Bian et al., 2012; Gilbert, 2000; Kheradmandi et al., 2016). At the same time, many studies suggest the benefits of using physical factors because of their potential ability to accelerate growth and development in skeletal muscle engineering (Shadrach and Wagers, 2011; Liao et al., 2009; Egerman and Glass, 2014). Electric and mechanical factors are the most used in the literature. Electrical stimulation is of interest because of the indisputable role of the electrical cues issued by the central nervous system in the development of skeletal muscles in vivo (Mauro, 2002). The understanding of its effect and how to use it are increasingly controlled. The parameters of the electric field applied can be modulated, according to the type of response desired. It has been shown that depending on whether the regimen applied is direct or alternative, and depending on the voltage/intensity range, it accelerates sarcomere assembly, promoting cell proliferation, differentiation, and/or muscle cell alignment (Hashimoto and Sato, 2012*b*; Hosseini et al., 2012; Sirivisoot and Harrison, 2011; Ostrovidov et al., 2014; Serena et al., 2008; Langelaan et al., 2011*a*; Shin et al., 2015; Michailovici et al., 2014; Wang et al., 2008; Fujita et al., 2010). Some studies pointed out that electrical stimulation makes intracellular calcium and NO release possible (Ikeda et al., 2006). Others showed that it acts via the activation of PI3K, p38 signaling pathways (Ricotti et al., 2013; Salgarella et al., 2017). In parallel, mechanical stresses also play a role

in muscle cell growth, differentiation, and function because of the contractile and elastic nature of skeletal muscle(Campion et al., 1978). When cells grow on a scaffold, a variety of stretch regimes can be applied. Thus, by modulating the cycle, stretching elongation and duration, muscle cell changes and functionality can be modulated (Valentin et al., 2010; Pennisi et al., 2011; Boonen et al., 2010; Okano et al., 1997; Candiani et al., 2010; Wang et al., 2015; Khodabukus and Baar, 2012; Bajaj et al., 2011*a*). It seems that cell stretching induces the activation of FAK via integrin, leading to an increase in gene expression (Buvinic et al., 2009). Other studies suggest that stretching may also influence the passage of calcium via the ion channels (Eltit et al., 2006; Rahnert and Burkholder, 2011) and activate PI3K and p38 signaling pathways (Zöllner et al., 2012; Ahmed et al., 2010*a*).

It has now been clearly shown that several signaling pathways can be modulated in order to control muscle cell development in tissue engineering. The most recent studies are based on cell culture methods while using a combination of chemical and physical stimulations. More importantly, there is growing evidence that a combination of chemical and physical stimulations in addition to surface topography and scaffold composition may be a solution for generating safe and functional muscle constructs in vitro (Liao et al., 2008; Moon du et al., 2008). However, the chronology of these different stimuli actions during the development of muscle cells in vivo remains unclear. It may be of particular interest to investigate not only a combination, but also successive different stimulations (chemical, mechanical, electrical).

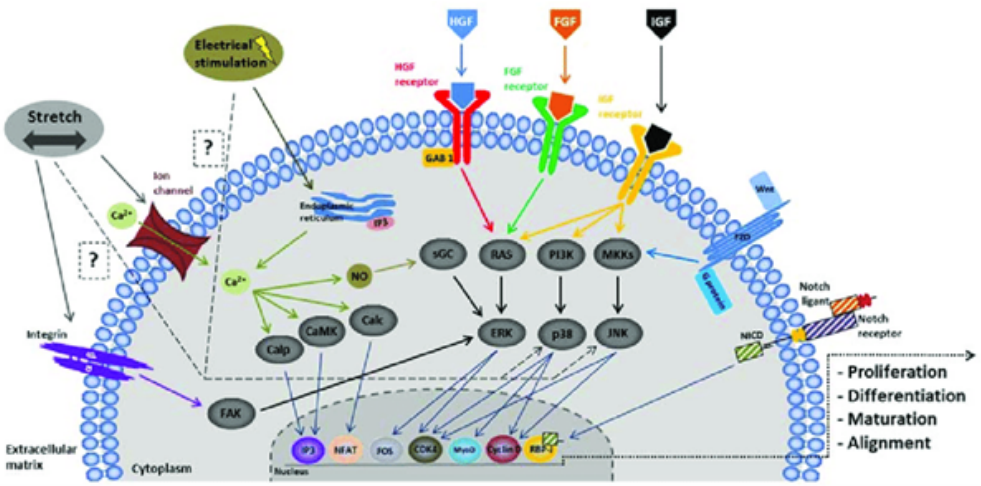

FIGURE 2.5: Schematic representation of skeletal muscle cell mechanotransduction: chemical signals initiated by growth factors such as insulin-like growth factor (IGF), Hepatocyte growth factor (HGF), and fibroblast growth factor (FGF) binding to their respective receptors to trigger RAS, phosphatidylinositol- 3-kinase (PI3K), and McKusick-Kaufman syndrome (MKKs) signaling cascades and activate Extracellular signal-regulated kinases (ERK), mitogen-activated protein kinases (p38), and c-Jun NH2-terminal kinases (JNK) pathways, respectively (Zhang et al., 2007; Hara et al., 2012; Tatsumi et al., 2002). Electrical stimulation induces calcium release from the endoplasmic reticulum (Adam et al., 2003). Calcium can act by activating either ERK (Hanke et al., 2010) or calp, camk and calc (Pavesi et al., 2015; Sørensen et al., 2008; Suzuki et al., 2000). Mechanical stretching signals involve the transmembrane protein integrin and the calcium ion channel (Walker et al., 2015). Activating integrin triggers the FAK signaling pathway. Electrical and mechanical stimulations are also likely to activate the JNK and p38 pathway. Other pathways may be involved, such as wnt/frizzled and notch. All these signaling pathwaysh up-regulate the expression of some of the genes responsible for skeletal muscle progenitor development

2.3.3 Materials of biological origin

The macromolecular composition and structure of protective sheets surrounding muscle fibers (e.g., sarcolemma, endomysium) are mostly driven by various types of collagen (Hashimoto and Sato, 2012*b*; Pennisi et al., 2011; Okano et al., 1997; Serena et al., 2008; Langelaan et al., 2011*a*; Bustamante et al., 2014; Perez-Ruiz et al., 2007). For this reason, collagen and gelatin have been widely used as materials for muscle tissue engineering (Costantini et al., 2017; Hosseini et al., 2012; Ostrovidov et al., 2014; Cárdenas et al., 2004). Non-mammalian sources of naturally derived materials have also been explored to produce suitable scaffolds for muscle reconstruction, such as alginate (Baniasadi et al., 2016; Dargelos et al., 2002), fibrin (Boonen et al., 2010; Shin et al., 2015; Friday et al., 2000; Low and Taylor, 1998), or chitosan (McKeon-Fischer et al., 2011*b*; Kjaer, 2004). They have the capacity to be configured into various shapes, including film, hydrogel, and sponge. Some of these materials are responsive to fabrication methods, such as chemical modification to add cross-linkers (Hennink and van Nostrum, 2002), or specific functional groups to improve cell attachment (Rowley and Mooney, 2002), or mechanical properties (Davidenko et al., 2015), in order to obtain structural control similar to that of native muscle.

Recently, as with tendons, scaffolds that were derived from decellularized skeletal muscle may be the optimal biomimetic biomaterials for repairing large skeletal muscle defects. In the literature, implants of decellularized muscles have been reported with contrasting results. Lin et al. (2014) showed that the enzyme detergent method for removing cells from mouse skeletal muscle, made it possible to maintain the biomechanical properties at a level that was comparable to that of native tissue. Several other authors did not observe any myoblast migration towards the scaffold in vivo (Gamba et al., 2002; Fishman et al., 2013). More recently, Porzionato et al. (2015) performed a comparative analysis between different decellularization protocols on muscles from different species, and especially on human samples. The study evaluated the integration capacity of the decellularized scaffold in vivo. They observed good integration of the scaffold surrounding the native muscle structure and signs of neo-vascularization.

2.3.4 Synthetic Materials

Most of the synthetic polymers used for muscle tissue engineering scaffolds are manufactured from polyesters, which include poly(vinyl alcohol) (PVA) (McKeon-Fischer et al., 2011*b*; Kheradmandi et al., 2016), (PGA) (Saxena et al., 1999, 2001), poly(lactic acid) (PLA) (Rimington et al., 2017; Ricotti et al., 2010), poly(caprolactone) (PCL) (Abarzua et al., 2017; Jun et al., 2009; Li et al., 2007), and their copolymer poly[(lactic acid)-co-(glycolic acid)] (PLGA) (Zhao et al., 2016; Aviss et al., 2010*a*; Abarzua et al., 2017; Shin et al., 2015; Kim et al., 2006; Xu et al., 2014). These polymers are well characterized and have been approved by the Food and Drug Administration (FDA) for certain human uses (Middleton and Tipton, 2000). They can be tailored into porous sponges, fibers, or microspheres for cell encapsulation (Kim et al., 2006). PDMS (polydimethylsiloxane) (Lam et al., 2006*a*; Fujita

et al., 2010), which is a type of silicone, is also used for other bio-microsystem applications. Although there are many applications in TE, their lack of biological cues for promoting desirable cell adhesion and responses

2.3.5 Hybird Materials

Hybrid scaffolds consist of the combination of synthetic polymer and natural derived components, to benefit from and exploit each asset. Natural components bring bioactivity, favorable environments for cell adhesion, and proliferation, along with remodeling properties,while synthetic materials can obtain the target mechanical properties. Although this type of approach is quite recent for muscle reconstruction, several configurations and combinations can be found in Table 4: PDMS and fibrin [247], PEG and fibrin (Cha et al., 2017), PLGA and collagen(Shin et al., 2015), PCL and collagen (Choi et al., 2008*a*), and PCL and silk fibroin (Wang et al., 2015).

2.4 From Biohybrid Muscle Design to Reconstructed Tissues Response

2.4.1 Films and Hydrogel: Effect of Scaffold Structure and Mechanical Properties on Biological Response

Of the materials used, collagen (Hashimoto and Sato, 2012*b*; Pennisi et al., 2011; Okano et al., 1997; Takeda et al., 2016; Serena et al., 2008; Wang et al., 2015; Shadrach and Wagers, 2011; Perez-Ruiz et al., 2007), fibrin (Boonen et al., 2010; Shin et al., 2015; Cha et al., 2017; Friday et al., 2000; Heher et al., 2015), gelatin (Costantini et al., 2017; Hosseini et al., 2012; Ostrovidov et al., 2014; Suh et al., 2017), alginate (Baniasadi et al., 2016; Ansari et al., 2016), and polymers, such as PLLA (Altomare et al., 2010), PDMS (Lam et al., 2006*a*; Fujita et al., 2010), or PEG (Wang et al., 2015; Salimath and García, 2016) generally functionalized or coated with adhesion peptides, are the most commonly found. To compensate for the mechanical weakness of hydrogels and their lack of conductive properties, which are useful in muscle tissue engineering (Salahshoor and Rahbar, 2014; Pollot et al., 2018), nanomaterials have often been added to the initial polymer. These include gold nanostructures (Choi et al., 2008*a*; Pardo-Yissar et al., 2001), graphene (Bajaj et al., 2014; Shin et al., 2015; Ku and Park, 2013), and carbon nanotubes (Sirivisoot and Harrison, 2011; Ostrovidov et al., 2014; McKeon-Fischer et al., 2011*b*; Ramón-Azcón et al., 2013; MacDonald et al., 2008). The rationale for developing conductive polymers is the need for the transmission of the electrical impulse, which in turn may influence cell behavior, specifically for cardiac and skeletal muscle (McKeon-Fischer and Freeman, 2011).

Natural polymers were first used in the form of simple coatings, to efficiently exploit the inherent capacity of cells to produce their own extracellular matrices and assemble themselves into organized and functional tissues. The gel-like structure and smooth aspect of the coating induce cells to proliferate and differentiate in a random orientation. To overcome this anarchic cell arrangement and favor myotube alignment, which is one of the

most critical factors in skeletal muscle regeneration, Vandenburgh et al. (1988) anchored the gel between two fixed points acting as an artificial tendon. Mechanical tension between the anchor points promoted myofiber alignment and stimulated muscle growth.

Several studies outlined the role of film stiffness on myotube differentiation into the physiological striated state. The best results were obtained on materials with muscle tissue-like stiffness (elastic modulus around 10 ± 4 kPa) (Engler, Griffin, Sen, Bönnemann, Sweeney and Discher, 2004; Griffin, 2004). Baniasadi et al. (2016) worked on cross-linked-oxidized alginate/gelatin hydrogels and investigated the impact of mechanical properties and degradation rate on the behavior of cultured cells. In order to contract, muscle fibers need to grow parallel (Bian and Bursac, 2009) to one another with identical anisotropy (Courtney et al., 2006). This can be achieved using a film with a specific topography to induce this behavior via contact guidance (Dalby et al., 2003).

Topographical nano- (Yang, Ieronimakis, Tsui, Kim, Suh, Reyes and Kim, 2014) or micro-patterning have thus been investigated in grooves (Sanzari et al., 2017), waves (Lam et al., 2006*a*), or more complex configurations (Janakiraman et al., 2007) to enhance rat satellite cells or C2C12 myoblast fusion thanks to alignment and myotube formation. This approach mainly applied 2D films on to which myoblasts were cultured as monolayers until the formation of mature myotubes. Then, the mature cell layer can be transfer into a 3D construct hydrogel (Lam et al., 2009), in order to be transplanted into a rat model. Several studies have shed light on the effect of optimized surface features, such as groove depth (Altomare et al., 2010), width (Charest et al., 2007), and periodicity (Lam et al., 2006*a*) on the formation of longer, functional myotubes with striated structures and contractile behavior in vitro (Qazi et al., 2015). According to these authors, optimal depth varied between 1 to 2.5 µm for a width of 10 µm, with a periodicity of 6 mm. Bajaj et al. (2011*b*) demonstrated that hybrid 30 patterned structures led to the best C2C12 cell differentiation, as assessed by myosin and nuclei staining, as well as the size and orientation of the resulting myotubes.

Hydrogels were also developed in 3D to embed/encapsulate the seeded cells. Costantini et al. (2016) prepared a chemically modified gelatin hydrogel and demonstrated the positive impact of mechanical stiffness and geometrical confinement on myoblast culture. Their results showed a parallel orientation of cells cultured in the smallest hydrogel string structure. Interestingly, the highest amount of myotube formation was obtained in a 3D hydrogel with stiffness in the range of 3 kPa, when compared to hydrogels whose stiffness was closer to that of native tissues. They speculated that C2C12 cells, when cultured in a 3D environment, exhibit specific focal adhesion configurations that influence cell polarization and signaling pathways, which were not observed in 2D constructs.

In contrast, Cvetkovic et al. (2014) produced strips of cross-linked collagen and fibrin with very high elastic moduli from 200 to 400 kPa that they placed on a specific holding tool named "biobiot". Despite the considerable stiffness of the material, cells aligned during gel compaction and formed myotubes, more specifically, under the effect of IGF added to the gel.

Hydrogels can be shaped as sponges, with an interpenetrating network structure favoring cell colonization within the 3D scaffold. For example, Bandyopadhyay et al. (2013) developed a biocompatible and biodegradable porous sponge that is made with poly(L-lactide-co-ε- caprolactone) copolymers using phase inversion. This type of scaffold, which is characterized by a pore size of around 300 µm, supports adult human myoblast growth and differentiation into multinucleated myotubes in vitro and favors cell colonization in vivo in an ectopic rat model. Similarly, Kin et al. (2007) prepared cross-linked atelocollagen sponge using a freeze-drying technique (80°C), with pores in the range of 50–100 µm, and successful cell colonization of the scaffold was achieved in an ectopic rabbit model. Although the hydrogel/sponge manufacturing process is relatively easy to implement, pore size and full interconnectivity remain difficult to control (Omidian et al., 2006; Lee et al., 1999). Another way of controlling 3D hydrogel porosity is to mold them into previously prepared PDMS structures that are designed by photolithography. In the study by Bian et al. (2012), primary muscle cells from rats were mixed with Matrigel/fibrin gel to form an elongated hexagonal structure of various sizes. They demonstrated that the networks with the most elongated pores resulted in the best cell response in terms of alignment and contractility (Cha et al., 2017).

2.4.2 Film and Hydrogel: Effect of Electrical Stimulation on Biological Response

Recently, both Kasper et al. (2018) and Rangarajan et al. (2014*a*) highlighted the attractive strategy of electrical stimulation for activating the signaling pathways that are presented in Figure 2.5. Hashimoto and Sato (2012*b*) demonstrated the effect of electric field on the differentiation and contraction of cultured C2C12 cells. More specifically, they showed that optimized parameters (1s pulse of 8V for three days) had a beneficial influence whereas higher electric stimulation damaged myocytes.

(Serena et al., 2008) aimed partly to mimic neuronal activation by means of an adequate electrical field (pulse of 70 mV/cm for 3 ms). Applying this to muscle precursor cells (MPCs) cultured in 3D collagen scaffolds, they observed enhanced proliferation when compared to non-stimulated cultures. However, ten days after implantation in mice, cell number and distribution were no different in the two conditions. Cvetkovic et al. (2014) subjected their constructs that were located on "biobots" to electrical stimulation (20 V, 1 to 4 Hz), representative of action potentials observed in vivo. They managed to coordinate the contraction of multiple myotubes in the artificial muscle strip. In contrast, (Stern-Straeter et al., 2005) focusing on the influence of electrical stimulation of primary myoblast cultures in a 3D degradable fibrin matrix, described the negative impact that is induced by their stimulation on the myogenic differentiation process, with a down-regulation of the transcription factor in the MRF-family. Coordinating the electrical stimulation within the differentiation process of muscle progenitor cells is delicate and should not be introduced too early (Langelaan et al., 2011*a*).

2.4.3 Film and Hydrogel:Effect of Mechanical Stimulation on Biological Response

A number of studies applied mechanical loading to cell-laden scaffolds in order to develop functional and structurally-biomimetic muscle constructs. Mechanical stimulation is another important factor during myogenesis (Wang et al., 2015; Bandyopadhyay et al., 2013), through the continuous passive tension applied to skeletal muscle by bone growth during both embryogenesis and neonatal development, as described in Figure 2.3. It also has a significant impact on the diameter of mature skeletal muscle fibers, as well as on cell numbers and myofiber composition (Alberts et al., 2014).

Twenty years ago, Okano et al. (1997) described the impact of cyclic mechanical stretching (frequency: 60 Hz, amplitude: 5%, for four days) on encapsulated C2C12 myoblasts in a collagen type I and reported an assembly of highly dense and oriented myotubes. More recently, Powell et al. (2002) outlined that repetitive stretch/relaxation cycles applied to muscle cells suspended in collagen/Matrigel enhanced the diameter and area of myotubes by 12% and 40%, respectively, and increased the elasticity of the muscle construct, after eight days. Pennisi et al. (2011) mobilized uniaxial or equibiaxial cyclic tensile strain (15% of stretch, 0.5 Hz) to induce assembly and differentiation in C2C12 skeletal myocytes seeded on to flexible-bottom plates precoated with collagen-I. The uniaxial strain resulted in a highly aligned array of cross- striated fibers, with the major axis of most cells aligned in a perpendicular manner in relation to the axis of the strain, and caused faster cell differentiation; on the other hand, equiaxial strain did not induce any clear orientation and it displayed signs of membrane damage and impaired differentiation(Pennisi et al., 2011).

The mechanical stimulation of muscle constructs has not been systematically associated with an improved biological response, depending on the strain parameters used (duration, frequency, direction) (Wang et al., 2015). For instance, Boonen et al. (2010) investigated the effects of a two-day uniaxial ramp stretch (2%), followed by four days of uniaxial intermittent dynamic stretch (4%) at a frequency of 1Hz on the C2C12 or MPC cells in 2D or 3D constructs. They observed either no effect or a lowered effect on the maturation and differentiation of the cells. There is thus not yet any consensus on the protocols to be applied to such constructs.

The simultaneous combination of mechanical forces and geometric constraints imposed by the substrate represents new models for understanding the mechanisms of cell response.

Ahmed et al. (2010*b*) recently designed a flat support, without any micro-grooves, functionalized by adhesion proteins to control cell orientation. C2C12 cells produce different morphological and cytoskeletal responses to mechanical stimulation depending on their alignment relative to the direction of the cyclic tensile strain: strain applied to 0°micro-pattern lines results in the most irregular actin striation when compared to the highly organized stress fiber orientation observed along the 90°micropattern. Myoblast nucleus shape and orientation seem to be determined by geometrical constraints, showing that cyclic tensile strain and geometric constraints may be competing forms of stimuli.

2.4.4 Electrospun Scaffolds: Effect of Scaffold Structure and Mechanical Properties on Biological Response

The main materials that were used to produce electrospun scaffolds for skeletal muscle engineering are biocompatible and biodegradable synthetic polymers, such as PLGA [186], PCL (Guex et al., 2013; Abarzua et al., 2017; Jun et al., 2009; Wang et al., 2015; Cha et al., 2017; McKeon-Fischer et al., 2011*b*; Li et al., 2007; Choi et al., 2016), PVDF (Martins et al., 2013), and polyurethane (Liao et al., 2008; Candiani et al., 2010; Sirivisoot and Harrison, 2011). These materials can also be of natural origin such as collagen (Takeda et al., 2016; Shin et al., 2015; Choi et al., 2016), gelatin, decorin, silk fibroin, alone or mixed (Abarzua et al., 2017; Wang et al., 2015). As for the gels, conductive elements can be added to the polymer, such as graphene (Shin et al., 2015), carbon nanotubes (Sirivisoot and Harrison, 2011; Ostrovidov et al., 2014; McKeon-Fischer et al., 2011*b*), polyaniline (PANi) (Jun et al., 2009), or gold nanoparticules (Choi et al., 2008*a*; McKeon-Fischer and Freeman, 2011).

Parallel configurations were studied to mimic the natural organization of bundles of aligned muscle fibers, which is necessary to develop high contractile forces (Okano et al., 1997). Of the parameters that could be adjusted during the electrospinning process, Li et al. (2007) showed that the rotation speed of the collector had a considerable impact on the anisotropy of the resulting fiber mesh, which in turn, influenced the mechanical properties of the scaffolds. For instance, the tensile moduli for random/aligned fibers of polyurethane (PU) were 2.1 $\pm$ 0.4 MPa and 11.6 $\pm$ 3.1 MPa, respectively.

It is well-documented that aligned fibers in electrospun scaffolds cause myoblast cytoskeletal reorganization, cell orientation along the fibers, and cell fusion into myotubes, unlike randomly oriented fibers (Liao et al., 2008; Aviss et al., 2010*a*; Martins et al., 2013; Abarzua et al., 2017). Physicochemical cues for polymers influence myoblast differentiation, hydrophilic properties, and low matrix stiffness had a beneficial effect on cell response.

Drexler and Powell (2011) investigated coaxial electrospinning methods to produce scaffolds with tunable stiffness and strength without changing the architecture or the surface chemistry. These authors demonstrated that strength and stiffness were positively correlated with the inner core diameter, with no impact on fiber diameter. This method might then make it possible to produce scaffolds with mechanical properties that are similar to those of native skeletal muscle tissue (up to 10 kPa) (Engler, Griffin, Sen, Bönnemann, Sweeney and Discher, 2004). Furthermore, hybrid composite fibers composed of natural and synthetic polymers are of great interest in order to benefit from the synergistic effect of mechanical properties and the biocompatibility of polymers in the same scaffold (Kheradmandi et al., 2016; Kim et al., 2010). Aligned PCL/collagen electrospun fibers, when compared to randomly orientated nanofibers, showed higher tensile strength in scaffolds, as well as effective human myoblast alignment and differentiation into myotubes (Choi et al., 2008*a*).

The influence of electrospun fiber diameter on skeletal muscle cell behavior remains poorly documented. Liao et al. (2008) produced polyurethane electrospun fibers with various diameters: 600 nm, and 2 µm to 10 µm by varying the polymer concentration

(7%, 10%, and 15%). They did not find any influence of electrospun fiber diameter on the differentiation of C2C12 myoblasts. Sreerekha et al. (2013) designed a multiscale composite scaffold with fibrin nanofibers (50– 500 nm) and PCL microfibers (1 to 2.5 µm). These dimensions mimic the hierarchical structure of ECM that is found in native tissues (Figures 1.3 and 1.7). Topography scale also has an effect on cell responses: hydrogel micro-patterns designed on electrospun materials or wavy imprinted materials improved C2C12 myotube formation, orientation, and length through a multi- dimensional scale (Guex et al., 2013; Cha et al., 2017). A more complex structure has been proposed in the form of a core- shell scaffold that combines aligned nanofiber yarns in a hydrogel shell to provide a suitable 3D environment successfully guiding the C2C12 myoblast alignment and differentiation (Wang et al., 2015).

Jun et al. (2009) evaluated the effect of PLCL/PANi random fibers on C2C12 myoblast culture. Mechanically, the fibers showed an increase in tensile strength and a decrease in elongation at break as the concentration of PANi increased. While having a minimal effect on the proliferation, the electrically conductive fibers appeared to have a moderate effect on C2C12 cells by increasing the number and length of the myotubes and enhancing the expression level of myogenic genes. McKeon-Fischer et al. (2011*a*) McKeon-Fischer et al. (2011) electrospun PCL with multiwalled carbon nanotubes (MWCNT) and with PAA/PVA hydrogel. The addition of MWCNT increased the mechanical properties of the "actuator" to more than the values of native skeletal muscle. Primary rat muscle cell cultures within a hydrogel were the first to display interactions among actin filaments in the large multinucleated formations. Later, McKeon-Fischer et al. (2014) implanted the same type of scaffold for four weeks on to the vastus lateralis muscle of rats. These authors showed that the scaffold displayed early signs of inflammation and fibrotic tissue formation, which decreased over time, while the number of myogenic cells and neovascularization increased, suggesting that this approach could be innovative for muscle repair.

2.4.5 Electrospun Scaffold: Effect of Electrical Stimulation on Biological Response

Electrical stimulation was recently investigated on electrospun bioconstructs to simulate motoneuron activity. Ostrovidov et al. (2014) demonstrated the positive effect of administering electric pulses (5 V, 1 Hz, 1 ms) for two days on the maturation and contractility of myotubes from C2C12 cells. These cells were cultured on gelatin electrospun fibers loaded with carbon nanotubes to promote electrical conduction. The same type of results was observed by Sirivisoot and Harrison (2011) on electrospun polyurethane/carbon nanotube scaffolds (5% and 10% w/v polyurethane), when compared with nonconductive electrospun polyurethane scaffolds after electrical stimulation (Biphasic pulses delivered at 20 Hz).

2.4.6 Electrospun Scaffold: Effect of Mechanical Stimulation on Biological Response

Candiani et al. (2010) used a bioreactor and PU electrospun scaffold to investigate the effect of mechanical conditioning on the development of murine skeletal muscle cells. They applied a unidirectional stretching phase (24 h of stretching at 0.02 mm/h, up to 960 µm of displacement) to mimic bone growth-associated muscle lengthening during embryonic development, followed by a phase of cyclic stretch (frequency 0.5 Hz, amplitude 1 mm). Cyclic stretching induced an eight- fold increase in myosin heavy chain synthesis after 10 days and contributed to myotube maintenance in a 3D environment. Also, with electrospun PU, Liao et al. (2008) demonstrated that mechanical (5% or 10% cyclic strain at 1 Hz for two days post differentiation) or synchronized electromechanical stimuli (20 V at 1 Hz starting at day 0, 4, or 7 days post differentiation) increased the percentage of striated myotubes from C2C12 cells and an up-regulation of α-actinin and myosin heavy chains. They highlighted the need to carefully consider the combination of topographical and mechanical stimuli to optimize myogenesis. More specifically, these authors showed that a 5% pre-stretching procedure applied after cell seeding and prior to the application of cyclic strain resulted in enhanced myogenic differentiation. They also evidenced that the timing of electrical stimulation application is a crucial factor for modulating myoblast differentiation.

Chapter 3

Multiscale-engineered muscle constructs: PEG hydrogel micro-patterning on an electrospun PCL mat functionalized with gold nanoparticles

Megane Beldjilali Labro a⋆, Rachid Jellali a, Alejandro Garcia Garcia a, Alexander David Brown b, Augustin Lerebours a,c, , Erwann Guenind, Fahmi Bedoui c, Claire Stewart b, Murielle Dufresne a Jean-François Grosset a, Cécile Legallais a

3.1 Abstract

The development of new, viable and functional engineered tissue is a complex and challenging task. Skeletal muscle constructs have specific requirements as cells are sensitive to the stiffness and geometry of the materials, as well as to the biological micro-environment. The aim of this study was thus to design and characterize a multi scale scaffold, and to optimize it regarding the differentiation process of C2C12 skeletal myoblasts.The significance of the work lies in the microfabrication of lines of polyethylene glycol (with different widths and spacing), on poly(ε-caprolactone) nanofiber sheets obtained using the electrospinning process, coated or not with gold nanoparticles to act as a potential substrate for electrical stimulation. The differentiation of C2C12 cells was studied over a period of seven days and quantified through both expression of specific genes, and analysis of the myotubes' alignment and length using confocal microscopy. We demonstrated that our multiscale bio-construct was easy to handle, presented tunable mechanical properties, and supported the different stages skeletal muscle cells go through, from myoblasts to myotubes. More specifically, the scaffold with 500 µm spacing between the micropatterns induced the most advanced differentiation. This model induces a higher expression of myotube markers with a 1.5-fold increase for MyoD and 2-fold for embryonic myosin heavy chain, but also improve the parallel orientation of the myotubes with a variation of

less than 15°.In contrast, the presence of gold nanoparticles did not affect the outcome of the cells. These scaffolds: i) showed the ability of sustained myogenic differentiation by enhancing the organization of reconstructed skeletal muscle; ii) could be suitable for the application of mechanical and electrical stimulation to mimic the muscle's physiological function.

3.2 Introduction

The reconstruction of the lost function or mass of skeletal muscle caused by chronic diseases and traumatic injuries is often difficult to achieve despite the highly regenerative nature of this tissue (Juhas and Bursac, 2013; Shadrin et al., 2016). As with other tissues, natural or synthetic biomaterials have been developed to replace or repair the structure of the skeletal muscle. While, none of them has successfully replaced its structure/function yet. These biohybrid constructs can also represent suitable "native-like" tissue models for in vitro investigations, leading to better understanding of the muscle regeneration process, or dedicated to the evaluation of new chemical or physical protocols for the treatment of muscular diseases or injuries. The highly organized structure of skeletal muscle in long parallel conductive fibers formed through the differentiation and fusion of satellite cells into multinucleated myotubes is undoubtedly a challenge for its reconstruction(Frontera and Ochala, 2015; Sosa et al., 1994). Controlling tissue organization in vitro by aligning myoblasts in preparation for the formation of myotubes is thus recognized as a crucial step (Wakelam, 1985). An effective scaffold for skeletal muscle tissue engineering needs to provide such fundamental elements, i.e., an appropriate microenvironment that will allow muscle cells to grow, differentiate and align to support the transmission of muscular force (Cheng et al., 2020) . In recent years, several strategies have emerged to develop such biohybrid constructs, from the design of complex architecture to the use of external stimuli to foster the formation of parallel-aligned myofibrils. Some studies focused on topographical cues at the nano- or micro-scale to promote spatial alignment of myoblasts on the biomaterial, studying the impact of the size and design of the micropatterns on cell alignment and fusion(Charest et al., 2007). Nano topography-guided approaches have been shown to promote tissue differentiation and activate specific function, using polydimethylsiloxane (PDMS) substrates patterned with parallel nanogrooves (Jiao et al., 2018; Xu et al., 2018). The electrospinning technique (Riboldi et al., 2005; Aviss et al., 2010*b*; Choi et al., 2008*b*) has also been widely used, as it provides fibers that mirror the structure of native collagen fibrils of extracellular matrix(Jiang et al., 2018; Teo et al., 2006). Yet fibers must be highly aligned in order to offer cells a parallel support to form myotubes, otherwise cells follow the random organization of the electrospun fibers(Zhong et al., 2015). Photolithography, hot embossing, and soft lithography are helpful for creating micro-topographical cues. A previous study has shown enhanced alignment of myotubes using photolithography patterned micro-channels, spaced from 5 to 100 µm apart and with varying depths(Shimizu et al., 2009). Meanwhile, other studies have investigated the effect of geometrical patterns, such as wavy, square, circle or plots, on myogenic

differentiation(Lam et al., 2006*b*; Junkin et al., 2011). They established that myotubes formed on large patterns were able to follow geometric cues in the microenvironment. Yet, the limitation of geometric guidance appeared on patterns with sharp corners, and small curve radius. Finally, other approaches involving electrically conductive materials or polymers such as carbon, gold, iron nanoparticles, polyaniline, and polypyrrole, have been investigated to mimic the natural environment and have shown they can improve the formation, maturation and guidance of myotubes **1–3**. Although substrates from nano to microfeatures are acknowledged for favoring myotube formation, they have demonstrated some limitations as guidance cues when cell–substrate interaction is overridden by cell–cell interactions (Lam et al., 2006*a*). Thus, it can be hypothesized that coupling microtopography and electrospun nanofibers could closely mimic the topographical aspect of natural muscle bundles and efficiently enable the formation of aligned myotubes over large areas. The aims of the present study is then to associate the effect of multiscale scaffolds and conductive nanoparticles to prepare nano-to-macro hierarchically organized tissue engineered skeletal muscle. The easy-to-handle construct was integrated into this design phase to obtain in fine a biohybrid construct capable of sustaining external stimuli such as stretching cycles or elect. We first manufactured a double-scaled scaffold, based on poly(ε-caprolactone) (PCL) electrospun nanofibers coated with gold nanoparticles (Au NPs) and then micropatterned it with polyethylene glycol (PEG) hydrogel lines. The PCL nanoscale fibers were expected to promote cell adhesion and guidance, while the gold particles were selected because of their nanostructure, easy surface functionalization process, and conductive properties. Finally, the PEG linear patterns were used to contribute to enhanced cell guidance. C2C12 myoblasts were then cultured on the scaffolds designed to evaluate their growth and differentiation into a new type of tissue engineered skeletal muscle.

3.3 Materials and Methods

3.3.1 Scaffold preparation and characterization

Three steps were necessary to obtain the multiscale scaffold (Figure 3.1).

Step 1: Preparation of electrospun PCL A solution of 10 wt% poly(ε-caprolactone) (PCL, MW = 80.000 Da, Sigma-Aldrich, St. Louis, MO) in dichloromethane (DCM, Sigma-Aldrich) /N,N-dimethylformamide (DMF, Reagent Plus ≥99%, Sigma-Aldrich) (80:20 v/v) was prepared under stirring for 24 h before electrospinning. Polymer solutions were loaded into a 5 mL syringe equipped with a (18G) stainless steel gauge needle. Grounded aluminum foil was used as the collector electrode. The distance between needle and aluminum collector was 15 cm and the collector had a diameter of 75 mm. Solution was fed in constantly using a syringe pump at 1.02 mL/h. The voltage applied was optimized to obtain good spinnability, with a typical value of 15 kV.

Step 2: Preparation of Au NP-doped PCL nanofibrous scaffolds The electrospun scaffolds were immersed in 2 mL aqueous solution of chloroauric acid $HAuCl_4$ (20 mM Sigma-Aldrich) for 1 h, during which the color of the scaffolds changed to purple (supplementary data). Subsequently, the Au NP-doped nanofibrous scaffolds formed were rinsed three times with deionized water and vacuum dried at room temperature for 24 h.

Step 3: Preparation of (PEG) hydrogel micropatterns on PCL nanofibrous scaffolds The resulting electrospun fibers (with and without Au NPs) were micropatterned with PEG hydrogel using photolithography. PEG-diacrylate (MW 575) was purchased from Sigma-Aldrich. For the UV photo-crosslinking process, the liquid PEG was mixed with 1% w/v of photo-initiator (2-Hydroxy-2-methylpropiophenone, Darocur 1173, Sigma Aldrich). Then the mixture was dropped on electrospun scaffolds by spin coating (SPINCOATER model P6700) and exposed to a UV light source for 20s (Kloé UV-KUB 2, 365 nm, 40 mW/cm2) through a photomask. The patterned scaffold was washed carefully in the dark with distilled water to remove the PEG precursor solution.

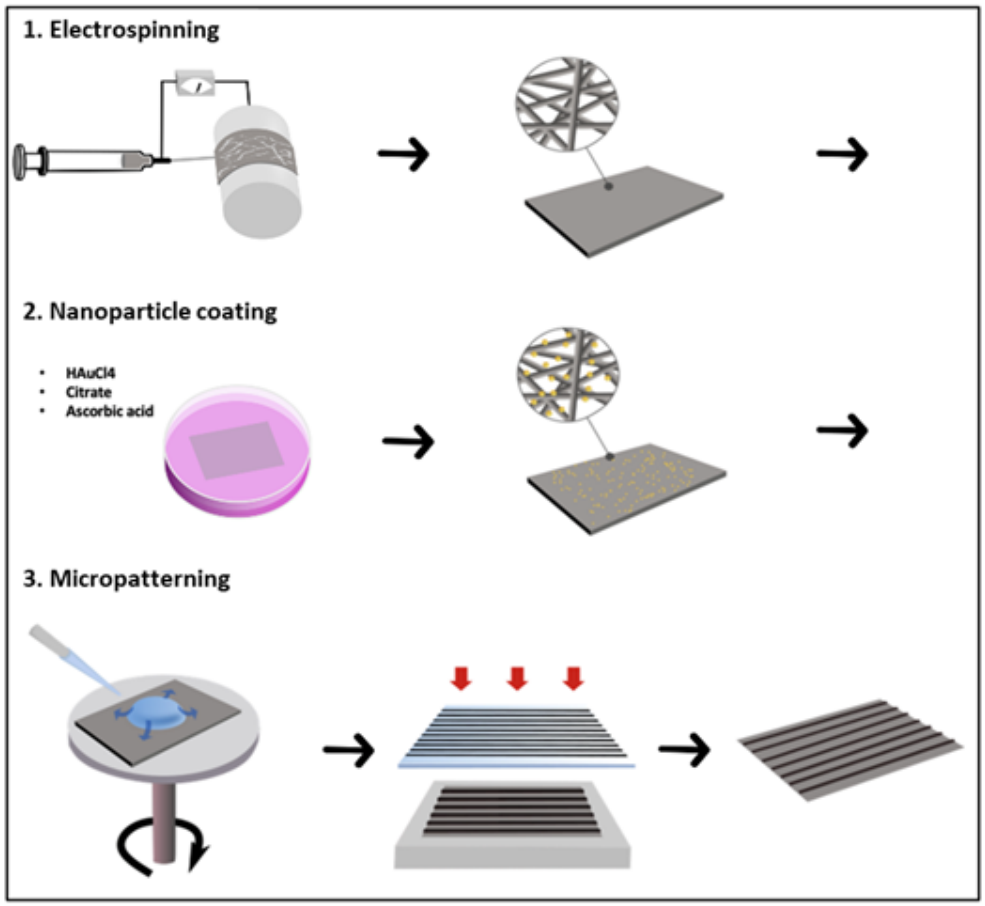

FIGURE 3.1: Schematic illustration showing the three steps in the manufacturing process: 1) electrospinning of PCL on drums at high velocity, 2) the nanoparticle coating process, including the successive addition of gold, citrate and ascorbic acid solutions to the scaffold immersed in milliQ water, 3) soft photolithography of polyethylene glycol (PEG) hydrogel, with 50 µm or 100 µm width line patterning and spaced 500 µm or 1000 µm.

3.3.2 SEM characterizatioN

The topography of the electrospun scaffolds was observed using environmental scanning electron microscopy (Philips XL30 ESEM-FEG). Fiber diameter was measured after setting up the scale bar. Average fiber diameters (n=100 fibers) were analyzed with ImageJ software (NIH, Bethesda, Maryland). The isotropy value of the scaffold (n=6) was analyzed using Mountain™ software (with smoothing and maintaining the default frequency thresholds at 5% and 80% Str ISO 25178) and the main orientations of the fibers were analyzed using the Fourier Transformation method (n=6). Gold deposits over the electrospun scaffold were investigated using Energy Dispersive X-ray Spectroscopy (EDS) analysis with the detector present in the microscope. The measurement is based on the energy and intensity distribution of X-ray signals produced by the electron beam striking the surface of the target scaffold.

3.3.3 Scaffold conductivity

Electrical conductivity was measured by a source meter (model 2602-A, Keithley instruments, Inc.) using a two-point probe method at room temperature. Three replicates of the Au NP-doped scaffolds were cut into 1 cm x1 cm squares. The contacts at both ends of each sample were copper sheets and the needle probes were held perpendicular to the contacts. In addition, in order to determine the baseline, we used PCL scaffolds without Au NPs as controls. However, because their resistivity was beyond the sensitivity of our instrument, we supposed it was non-conductive. Contact angle measurement A standard static sessile drop method (VCA Optima XE, AST Products) was used to characterize the wettability of the electrospun scaffolds. A 10 µL water droplet was dropped on to the surface of the scaffold (n=3) and a side-view photo was taken to measure the contact angles. The measurement was repeated twice.

3.3.4 Mechanical properties

The whole scaffold's elastic modulus was quantified using uniaxial tensile testing. One sample of each scaffold (n = 3) was cut into a strip measuring 1.0 x 3.0 cm, with a thickness of 100 $\pm$ 10 µm. The thickness of the scaffolds was evaluated using a precision dial thickness gauge (Mitutoyo Corporation, Japan). The samples were secured with the metallic grips of the tensile tester (Bose Electroforce 3200, TA, USA) and stretched at a rate of 0.05 $mm.s^{-1}$ using a cell load of 22N. The elastic modulus was calculated by analyzing the recorded stress-strain curve in the elastic zone, where the relationship is linear, i.e., generally between 5 and 10 % strain. The local Young modulus (E) of each scaffold was measured with a Chiaro nanoindenter system (Optics 11, Amsterdam, NL) mounted on an optical microscope. Two probes were selected based on estimation of the materials' stiffness and the manufacturer's probe selection chart. The probes selected were 5.23 N/m with a tip radius of 9 µm for mats without PEG, and with a spring constant of 47.69 N/m and a radius of 25 µm for mats with PEG hydrogel. Before testing, the optical sensitivity and geometrical factors were calibrated by indenting a hard surface (e.g., glass slide). A

fibrous mat was deposited on a glass slide and the probe was placed in contact with the scaffold where an indentation of 15µm was made. All experiments were performed at room temperature. For each condition, about 9 curves were acquired. Data were analyzed with DataViewer 2.2 software (Optics 11, Amsterdam, NL) using the Hertzian contact theory to calculate the local E.

3.3.5 Profilometry

The surface structure of the different samples was measured using an optical profilometer laser (Sensofar) on 3 samples (PCL, Au NPs PCL, and micropatterned scaffold) using a 1746 x 1313 µm zone. For each specimen, 3 measures were performed to extract roughness features: height parameters (Sv), valleys and peaks (Sp) including arithmetical mean height (Sa), root mean square height (Sq), and maximum height (Sz). Skewness (Ssk) is the degree of symmetry in the surface heights about the mean plane, while kurtosis (Sku) indicates the randomness of height and the sharpness of the structures on the surface. Specimens were also examined with SEM (accelerating voltage of 20 kV) to analyze fiber texture after the addition of hydrogel.

3.3.6 Cell seeding on scaffolds

Murine C2C12 skeletal muscle myoblast cells (ATCC CRL-1772) was cultured on T-75 flasks at 50 % of confluence with growth media, Dulbecco's Modified Eagle's Medium high-glucose (HDMEM; Hyclone, USA) supplemented with 10 % fetal bovine serum (FBS, Gibco Invitrogen, USA) and 1 % of penicillin-streptomycin (Gibco Invitrogen, USA). To evaluate the response of the cells to materials, the scaffolds were cut into rectangles measuring 30 mm × 10 mm, disinfected with ethanol 70 % (Sigma-Aldrich, USA) for 45 min, washed three times with PBS (phosphate buffered saline, Gibco Invitrogen, USA) pH 7.4 and incubated in growth media for 30 min before starting the cell culture in 6-well plates. Each scaffold was plated with a density of 5.10^3 cells for viability and proliferation tests and 5 × 105 cells for the confocal analysis. With the highest density, after 48h, culture was about 80 % of confluence. Then, the growth media was changed to differentiating media constituted of HDMEM supplemented with 2 % horse serum (HS, Gibco Invitrogen, USA) and 1 % of penicillin-streptomycin (Gibco Invitrogen, USA) and culture was prolonged for five more days.

3.3.7 Evaluation of cell adhesion, viability, and proliferation

Adhesion

On day 1, the cell-seeded scaffolds were removed from the culture media, gently washed with PBS and soaked in a buffered 4 % paraformaldehyde (PFA) solution (VWR) prior to observation using scanning electron microscopy (SEM) (XL 30-ESEM FEG, Philips, The Netherlands) to evaluate the cells' attachment and growth.

Viability

On days 2, 3 and 5, cell viability was estimated with the Far-Red fixable dead cell staining Kit (ViaQuant™, GeneCopoeia). The samples were observed using fluorescence microscopy at a wavelength of 650 nm (Leica Microsystem, Wetzlar, Germany), allowing determination of cell viability and distribution.

Proliferation

CellTiter 96®AQueous One Solution Cell Proliferation Assay (Promega) was used to evaluate the cell proliferation at different time points (days 1, 3, and 5). 100 µL MTS solution in complete culture media were added to each well (n=6). After 4 h of incubation at 37°C, the absorbance of the solution was measured using a Spark multimode microplate reader (TECAN, Swiss) at a wavelength of 570 nm and was then recorded with a 96-well plate reader. Finally, cell behavior after 7 days of culture on the scaffold was assessed through immunofluorescence. After washing with PBS, the samples were fixed in a 4 % PFA solution for 10 min at room temperature. Samples were permeabilized with a 0.2 % TritonX-100 solution for 10 min and blocked with a 2 % bovine serum albumin solution (BSA, Sigma) for 30 min. Myosin, actin and nuclei staining of cells was performed, using myosin heavy chain antibodies (1/200, Neo Biotech) for 2 hours followed by secondary staining using Alexa 594 overnight (1/200, Thermofisher), prior to Alexa Fluor 488 Phalloidin (1/200, Thermofisher) staining for 2 hours and Hoechst 33258 (1/1000, Sigma) for 15 min. The samples were finally washed with PBS before visualization using Z-stacking and mapping "Tile scan" specifications of confocal microscopy (Zeiss LSM 710). The confocal images were about 1 mm in size.

3.3.8 Myotube measurement

The influence of the biomaterials on myoblast differentiation, myotube length, orientation and total area occupied was measured using ImageJ (NIH, Bethesda, Maryland) and Cell ProfilerTM (Broad Institute) software19. Myotube length was defined as the line distance from one extremity of the myotube to the other. The total area occupied by differentiated cells was counted in 3-5 pictures, selecting an area of 2 mm x 2 mm for each sample. The percentage of cell alignment was defined based on the measurement of myotubes (n=100) aligning with $\pm$ 20° from the pattern.

3.3.9 RT-qPCR

Gene expression was studied using RT-qPCR (reverse transcription quantitative polymerase chain reaction) after 7 days of culture on the scaffolds. Briefly, samples were lysed with 350 µL of Trizol and centrifuged to extract the RNA (ribonucleic acid) according to the manufacturer's protocol (Qiagen, Germany). The RNA was retrotranscribed into DNA (deoxyribonucleic acid) using a High Capacity cDNA Reverse Transcription kit (Applied Biosystems, USA) according to the manufacturer's protocol. RT-qPCR was performed

using the SYBR Green PCR Master Mix (Applied Biosystems). Relative mRNA levels were calculated using the 2-ΔCt method. The ΔCts were obtained from Ct normalized with the Rp2b gene levels in each sample and reactions were checked before the experiments (efficiency > 80 %, R2 > 0.99). The results were normalized with the data from the basic PCL electrospun construct, to highlight the intrinsic effect of the scaffolds' modifications on gene expression. The primers used are listed in the supplementary data (Table S3).

3.3.10 Statistical analysis

Statistical analysis and graph drawing were carried out using GraphPad Instat 3.10 and Prism v 6.0 (GraphPad Software, CA. USA). All data are represented as mean ± standard deviation from at least three independent cultures ($n \geq 3$). Group comparisons were performed using the Mann–Whitney non-parametric two-tailed test and the Kruskal–Wallis non-parametric test with Dunn's multiple comparisons post-test. Significance is indicated on the graph by * $p<0.05$; ** $p<0.01$; and *** $p<0.001$.

3.4 Results

The surface area of the constructs (manufacturing process illustrated in Figure 1) was 6 cm^2, for an average thickness of 91 µm (n=9). This manufacturing process led to four different types of scaffold: (I) electrospun poly-ε-caprolactone (PCL), (II) the same coated with gold nanoparticles (PCL-Au), (III) electrospun PCL with patterning of PEG hydrogel lines (PCL-PEG), and finally (IV) an electrospun PCL coated with gold nanoparticles and patterned with PEG hydrogel lines (PCL-Au-PEG).

3.4.1 Fabrication and characterization of the basic PCL scaffold

Our first objective was to produce a flat mat of partially aligned PCL fibers. A medium range drum rotation speed of about 1000 rpm was thus applied during the electrospinning process. SEM images (Figure 2a) of the resulting PCL matrices showed smooth fibers with an average diameter of 776 ± 250 nm (Figure 2b), and a preferred orientation between -20° and 20° for 70 % of them (Figure 2c, d). Wettability of the materials was assessed by the contact angle at each stage in the preparation for cell culture. First, the dry PCL electrospun sheet showed a contact angle (ϑ) of 130°, corresponding to hydrophobic properties. After 45 minutes of ethanol treatment, the angle was about 115°, the drop on the dry PCL scaffold retaining its shape with no change over time (data not shown). Finally, on PCL incubated for 30 minutes in culture medium and dried, the drops were immediately absorbed, showing complete wetting (ϑ=0°) (Figure S1).

Coating with gold nanoparticles (PCL-Au)

During the reduction process of HAuCl4, we noticed that the white color of PCL nanofiber mats changed to purple, suggesting the formation of gold nanoparticles (Au NPs)20 (Figure S2). Scaffolds were then washed several times to remove any unbound nanoparticles

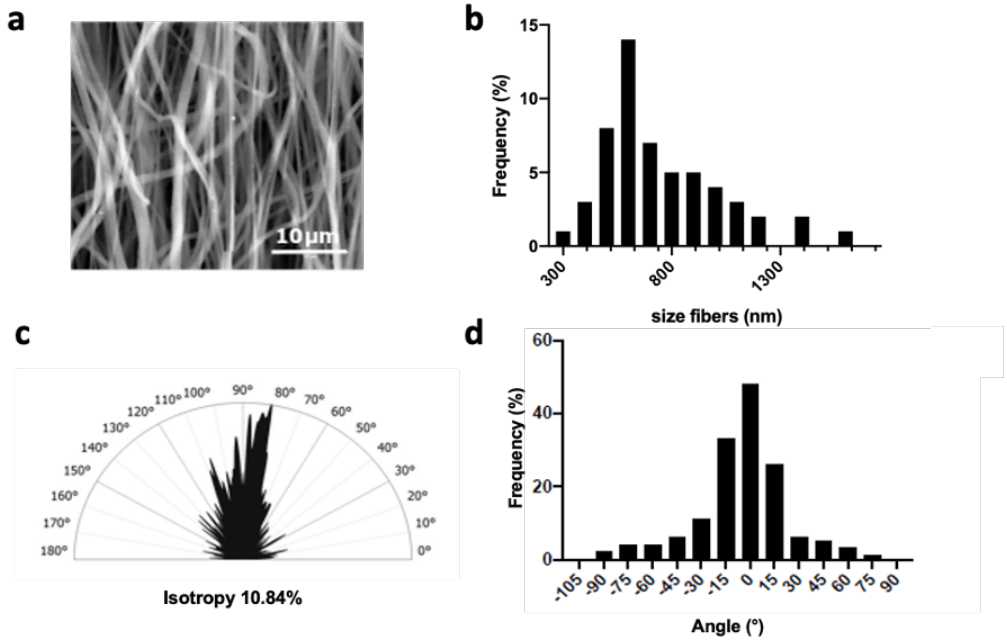

FIGURE 3.2: Characterization of electrospun fibers. (a) SEM images showing the electrospun fibers, (b) fiber size distribution (n= 100 fibers) and (c) analysis of fiber orientations according to the principal directions using Fourier transform (d) half polar smoothed curve of the orientation of the fibers from SEM image analysis (n=3).

and keep strong binding only. Nanoparticles with similar size and detailed structures of single particles were observed in high TEM resolution images. The lattice fringes of the spherical Au NPs clearly appeared with the spacing of 2.4 Åand 2.0 Å. This corresponds to the 111 and 200 lattice planes for gold, respectively (Figure 3a). Their mean diameter was estimated at 15.65 $\pm$ 6.41 nm (Figure 3b). In addition, EDS spectrometer analysis of the Au NP solution showed a peak at 520 nm (Figure 3c), confirming that the nanoparticles' size was in the range of 15 to 20 nm. SEM and EDS were then used to assess the presence of the Au NPs on the electrospun fibers. SEM observation of the morphology showed that the Au NP coating did not obstruct the porous surface structure of the material. In magnified SEM images of PCL-Au, white blots, relatively uniformly distributed along the nanofibers, were clearly observed (Figure 3d). The EDS profile of these spots presented strong gold atom signals around 2.10, 2.30 and 9.70 keV (Figure 3e).

The contact angle of the dry PCL-Au sheets was approximately 130°, the same as for the nude PCL. After ethanol treatment, the measurement fell to 102.5°. We observed that the drop was totally absorbed by the substrate in less than two minutes after the deposit. Finally, as with the PCL samples, the drops were immediately absorbed by dry PCL-Au incubated for 30 minutes in culture medium. Cell adhesion strength has been proven to vary logarithmically with an increased surface roughness for polymeric and non-polymeric materials. Analysis with a non-contact 3D surface profilometer (Sensofar®) showed that the addition of nanoparticles to the fibers had an impact on the fiber's roughness, with an increase in Sa (roughness average, arithmetical mean height) from 1.16$\pm$0.30 µm to 4.89$\pm$0.65 µm **(Figure 3.4a and b)**. Although this parameter is often used to evaluate

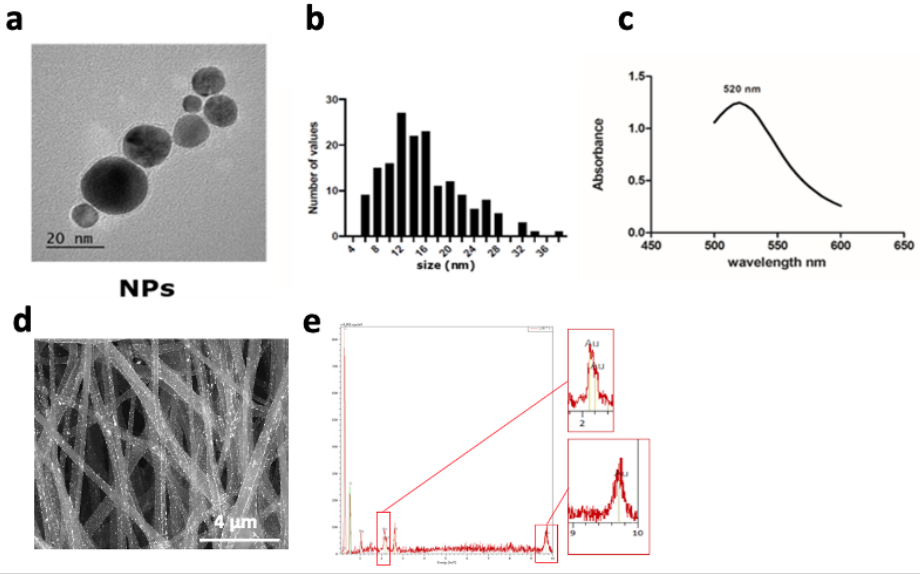

FIGURE 3.3: Characterization of the gold nanoparticles coated on the PCL scaffold. (a) TEM images of Au nanoparticles formed on the fibers, (presenting a size of 2.4 and 2.0 Å). (b) Particle size distribution from TEM image analysis (n= 30 particles) and (c) absorption spectrum of gold nanoparticle solutions using a spectrometer, with a peak of absorbance at a wavelength of 520 nm (n=3) (d) SEM images of electrospun fibers coated with Au NPs, (e) EDS spectrum showing the 3 peaks for Au elements at 2.10, 2.20 and 9,7 keV.

surface roughness, it is not enough to describe the complexity of a surface texture. The Sku (Kurtosis) characterizes the measurement of the sharpness of the roughness profile. Here, Sku was slightly higher for the scaffold without coating (Sku >3). Ssk (skewness) centered around zero for both samples, suggesting that there is a similar proportion of peaks and valleys in the samples. Although surface topography with lower skewness (Ssk) and higher kurtosis (Sku) is known to exhibit better wettability, the variations in Sku and Ssk after the coating were not enough to significantly modify it.

Micropatterning of multiscale scaffolds (PCL-PEG and PCL-Au-PEG)

Two masks with linear patterns were selected to create PEG hydrogel lines **(Figure 3.5a and c)** on the previously produced scaffolds. They were spaced either 500 µm or 1000 µm apart, with a width of 50 or 100 µm, respectively (named 500:50 and 1000:100). Photolithography made correct PEG hydrogel line deposits possible and attached well to the electrospun fibers. SEM images **(Figure 3.5b and e)** demonstrated that the hydrogel microstructure, where deposited, fully covered the PCL structure, leaving no fibers exposed at the top surfaces of the micropatterns. No damage to the morphology of the fibers located in between the hydrogels was observed (Figure 5e). We noticed a difference by comparing the masked data with the corresponding polymeric replica obtained from the electrospun fibers. Profilometry measurements **(Figure 3.5c and f)** confirmed the SEM observations. The PEG lines in both patterns had a height of about 40 µm, but their widths showed an average of 108 µm and 124 µm instead of the expected 50 µm and 100 µm, respectively. This resulted in reduced mean spacing between two lines, of 377 µm and 921 µm for

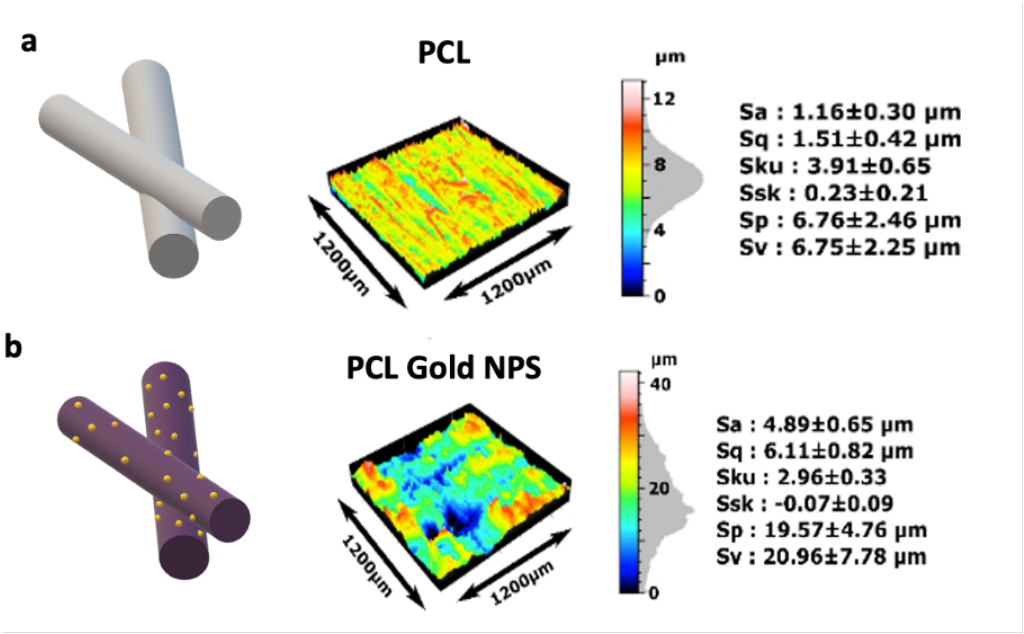

FIGURE 3.4: Topography of the PCL scaffolds coated or not with gold nanoparticles. Sensofar Confocal profiler measurement of the surface of (a) PCL and (b) PCL coated with gold nanoparticles. The features used to evaluate the surface roughness of the material were height parameters (Sv), valleys and peaks (Sp), including arithmetical mean height (Sa), and root mean square height (Sq). Skewness (Ssk) represents the degree of symmetry of the surface heights about the mean plane, while kurtosis (Sku) indicates the randomness of height and the sharpness of the structures on the surface (n = 3 for each condition).

the 500:50 and 1000:100 patterns, respectively. However, this difference was significant enough to evaluate the effect of spacing on cell behavior. The Sensofar confocal analysis demonstrated that the sheet tends to bend between the PEG lines and this effect was more significant on the 1000:100 pattern, with a variation in height of 110.40 ± 9.9 µm whereas it was only 44.46 ± 16.17 µm for the 500:50 pattern.

Mechanical properties of the different scaffolds

Figure 3.6a shows the elastic moduli of the electrospun fibrous scaffolds before and after Au NP coating or hydrogel patterning. Based on the stress-strain curves, electrospun sheets coated or not with Au NPs display similar elastic moduli of 16 ±2.5 MPa and 19.5±3.0 MPa, respectively. After the addition of PEG hydrogel lines with a spacing of (500:50) on scaffolds, the mechanical properties slightly decreased to 14.8 ±3.1 MPa for PCL-PEG and 12.2 ±2.1 MPa for PCL-Au-PEG. Micro indentation was performed to access the local mechanical properties of the fibrous part of the different scaffolds **(Figure 3.6b)**. The probe was followed by microscopy to ensure its localization on the fibers, and not on the PEG patterns. Surprisingly, the local moduli indicated a rather stiff material compared to the elastic moduli. Regarding the influence of PEG, the results were the opposite of those obtained for tensile strength. The local elastic modulus increased from 190.4 ± 96.9 kPa for PCL-Au to 764.3 ± 88.7 kPa when PEG micropatterning was added. The same trend was observed for the PCL scaffold: the local modulus increased from 124.6 ± 32.4 kPa to 495.7 ± 71.8 kPa with the PEG.

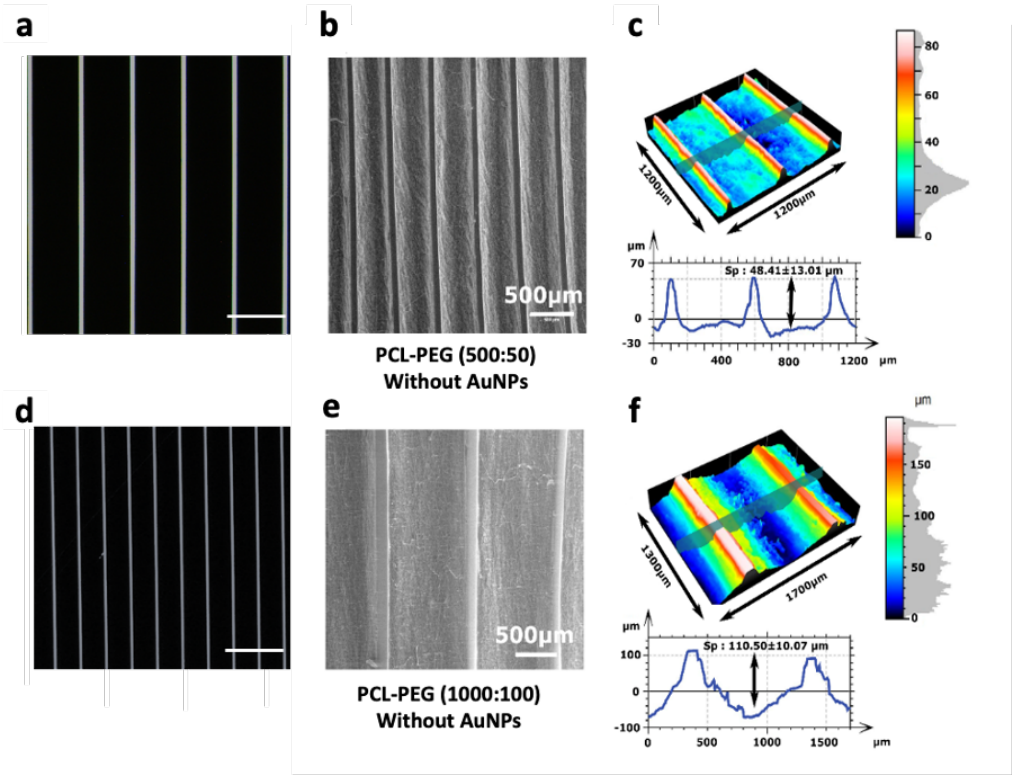

FIGURE 3.5: Characterization of the micropatterning of the scaffolds. (a,d) images of the mask used for the photolithography of 50 µm and 100 µm PEG line. (b,e) SEM images of line micropatterns with a spacing of 500 µm and 1000 µm respectively, on an electrospun mat. (c,f) Sensofar optical profiler measurements of the surface topography, height and thickness of the hydrogel line. Scale bar of (a,b) represents 1 mm.

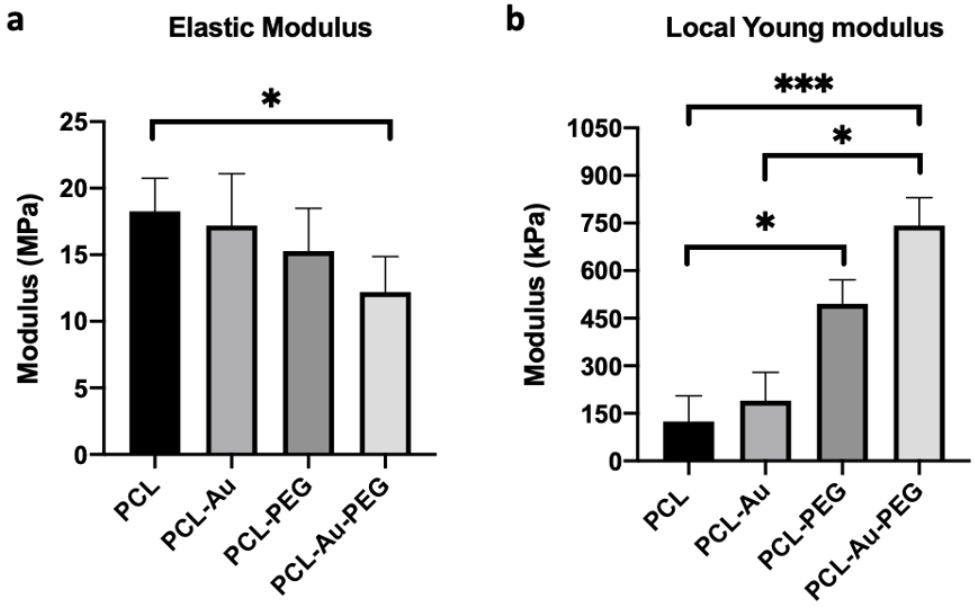

FIGURE 3.6: Mechanical characterization at the macro- and microscale levels. (a) Global elastic modulus obtained from the stress-strain curve in the tensile strength test on the four types of scaffold (n=5) (b) Local Young modulus from nano-indentation. These data were compared with Dunn's Multiple Comparisons Test: * $p < 0.05$ and *** $p < 0.001$. * indicates significant difference.

Influence of material composition on adhesion, proliferation, and cell viability

Cell adhesion was investigated on (500.50) PCL-PEG and PCL-Au-PEG. SEM images **(Figure 3.7a)** show C2C12 cells attached and distributed on the scaffolds at 24h, which confirmed that both scaffolds could support the attachment and proliferation of myoblasts. Cell proliferation assay revealed that the cells displayed the same behavior between D1 and D3 on the different materials, with threefold growth **(Figure 3.7b)**. A significant difference appeared on D5 as compared with D1 and D3, with greater proliferation of cells on the material with gold nanoparticles. A Far Red assay was performed to investigate the viability of the C2C12 cells on the composite materials **(Figure 3.7c)**. After 5 days it was evaluated that 13.2± 3 % and 20.8 ±5.5 % of the C2C12 cells were dead (red staining) on PCL-PEG and PCL-Au-PEG scaffolds, respectively. These tests indicate that neither substrate induced any cytotoxicity, above what would be expected under basal growth conditions. On these confocal observations, cell proliferation and changes in shape could also be followed from day 2 to day 5.

Cell differentiation

Finally, we evaluated the effects of spacing micropatterns (500:50 vs 1000:100) on the differentiation of C2C12 myoblasts into myotubes, as well as on their spatial orientation. On day 7, cells were immunostained with myosin heavy chain (MHC), an indicator of myotube formation. Confocal microscopy images confirmed that under partial serum deprivation (2 % of horse serum) for 5 days, myoblasts fused into myotubes on the scaffolds **(Figure3.8a and b)**. Moreover, confocal images of fluorescent stained F-actin on cells demonstrated that the actin assembly appeared perfectly oriented along the fibers and pattern structure for the PEG samples (500:50). In contrast, in some parts of the PEG sample (1000:100), on the apparent strata of cells, the actin could appear disordered. Yet, it was interesting to observe that those cells that were not in direct contact with the PCL fibers, but lay on other cells tended to assemble and arrange into spiral-like patterns **(Figure3.8a)**. In comparison, the cells in direct contact with PCL nanofibers formed elongated myotubes assembled according to fiber orientation into parallel patterns. Muscle-like cells were found to be arranged mostly in parallel with the patterned hydrogel. For the PCL-PEG (500:50), i.e., the narrow configuration, all angles formed by the myotubes with the direction of the PEG lines were found in the range -15° / + 15°, with a mean value of -0.9°± 5. When the space between two PEG lines increased (PCL-PEG 1000:100), only 72 % of the angles were in this range, with a mean value of 7.35°± 21,95° **(Figure3.8c)**. Analysis of the confocal images in Figure 8d showed that the length of the myotubes was not significantly higher with the wider spacing patterns. Finally, myotubes that formed on PCL-PEG (500:50) covered 8 % more surface area than on the PCL-PEG (1000:100) **(Figure3.8e)**.

Finally, we followed the main stages of myogenesis for these mammalians skeletal muscle cell precursors using RT-qPCR analysis **(Figure3.9)**. Muscle gene expression varied depending on the type of scaffold. On PCL-Au-PEG, IGF-I expressed a two-fold increase

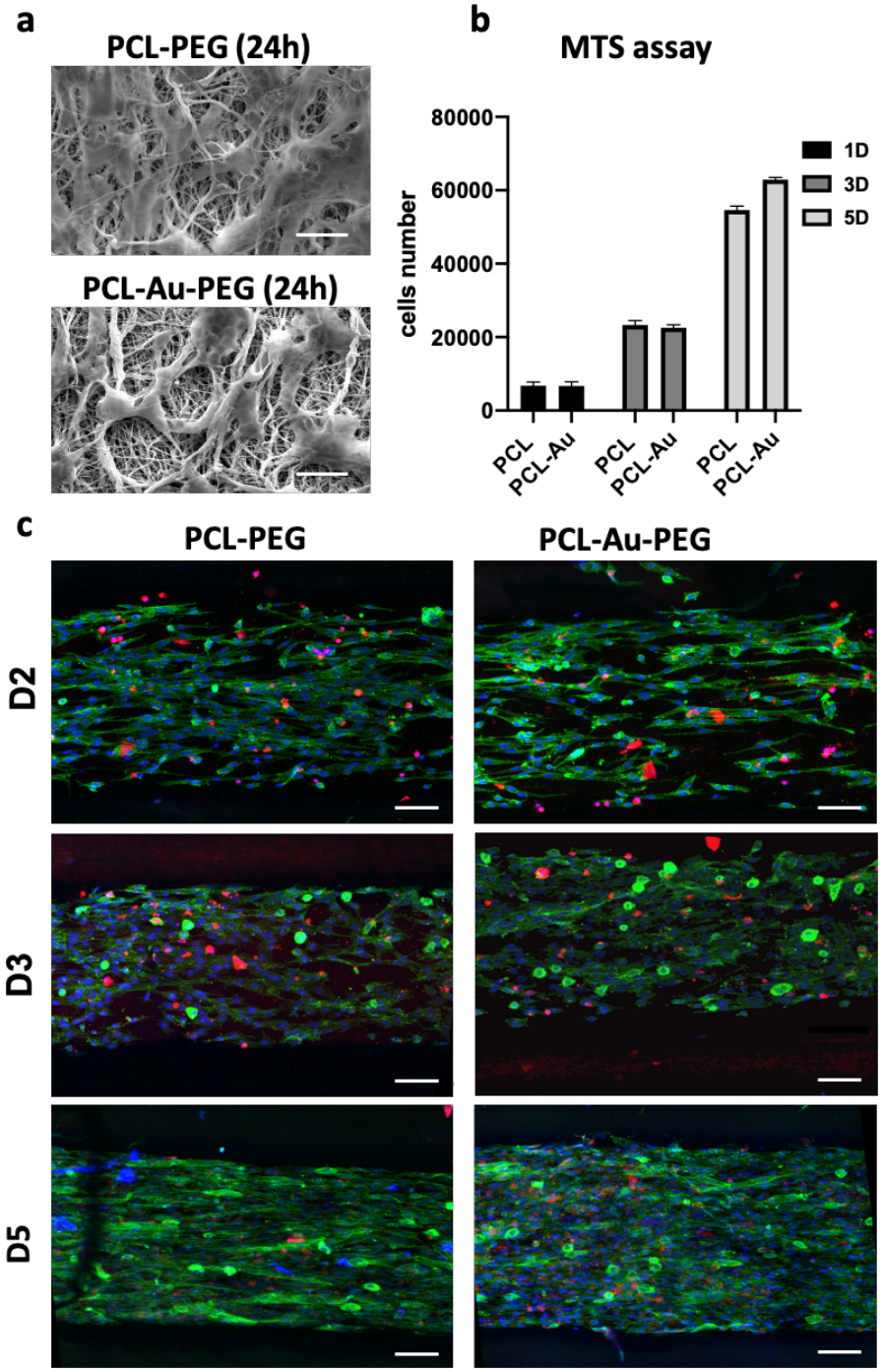

FIGURE 3.7: Cell adhesion and proliferation on the scaffolds. (a) MEB images of C2C12 myoblasts adherent to the scaffolds coated or not with gold nanoparticles, 24h after cell seeding. Scale bar 20 µm; (b) MTS assay illustrating cell proliferation was followed at D2, D3 and D5 (n=6); (c) the viability was observed by confocal images with dead cells emitting in red fluorescence (Far Red), nuclei in blue fluorescence (Hoechst-33258) and F-actin in green fluorescence at 48h, 72h and 5 days. Scale bar represents 100 µm. (The data obtained for MTT were compared with the Mann-Whitney non-parametric statistical test: there was no statistical difference between the conditions PCL and PCL-Au.)

compared to the PCL reference scaffold. MyoD XX fold reduce in the PCL-Au-PEG construct as PCL-PEG (500:50) and PCL, although the differences were not statistically significant. For myogenin, a 10-fold subexpression of the gene was observed in both

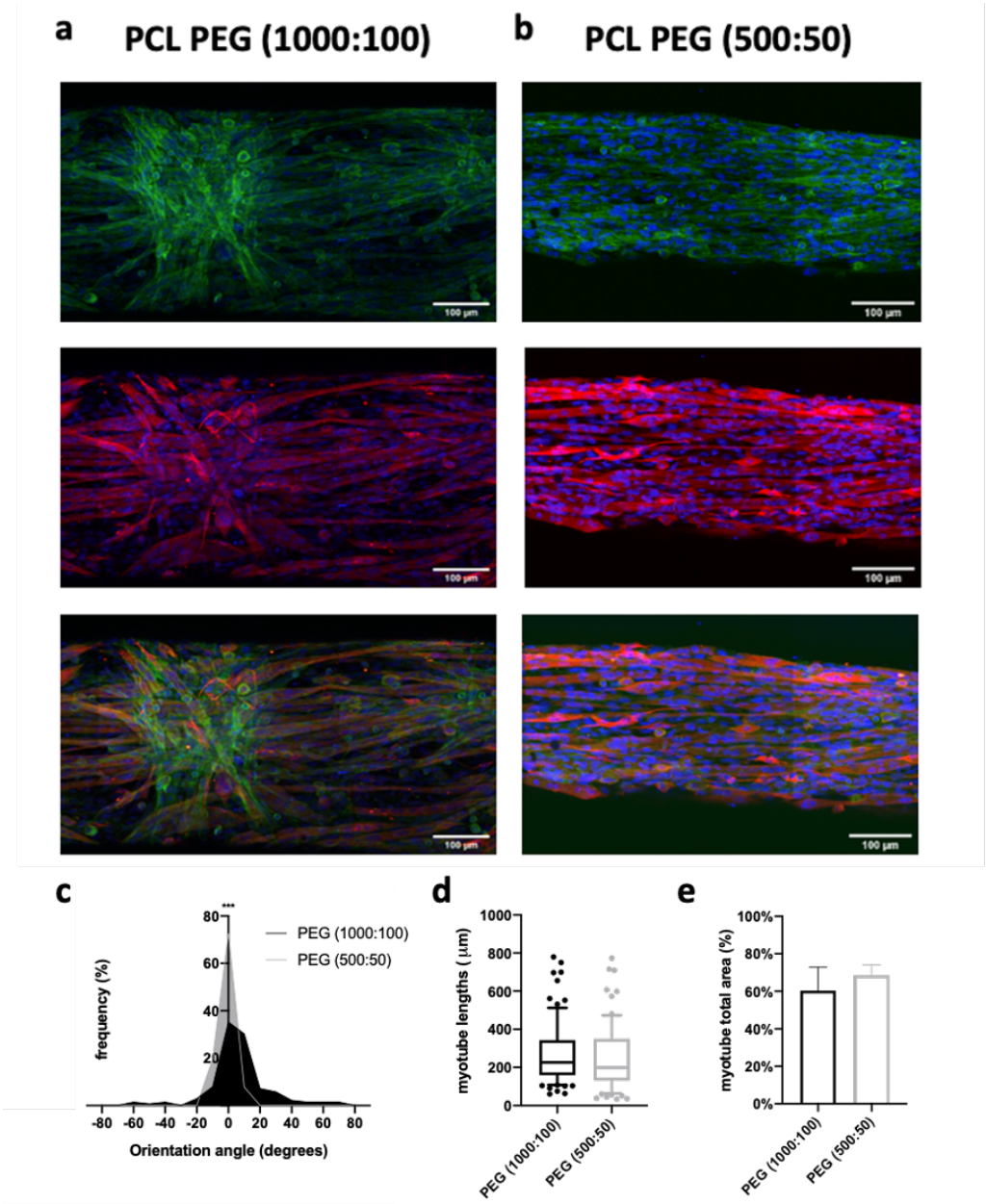

FIGURE 3.8: Myotube morphology on the scaffolds. Confocal images of C2C12 cells after 7 days of culture on scaffolds coated or not with gold nanoparticles with a space of (a) 1 000 µm or (b) 500 µm between the hydrogel lines. Nuclei in blue fluorescence (Hoechst 33258), F-actin in green fluorescence and myotubes by anti-MHC antibodies in red fluorescence. Scale bar: 100 µm. Quantification of the (c) orientation (significance analyzed by Mann–Whitney non-parametric two-tailed test), (d) length and (e) total area occupied by the myotubes as a function of the space patterning (n = 50 myotubes). There was no statistical difference between the conditions for the orientation, length or area of the myotubes. $p < 0.001$. * indicates significant difference.

scaffolds with PEG. MYH3 expression increased two-fold for the constructs with PEG and further for the PCL-Au-PEG construct. Finally, Desmin was not expressed in the 3 samples; PCL, PCL-PEG and PCL-Au-PEG as compared with PCL alone.

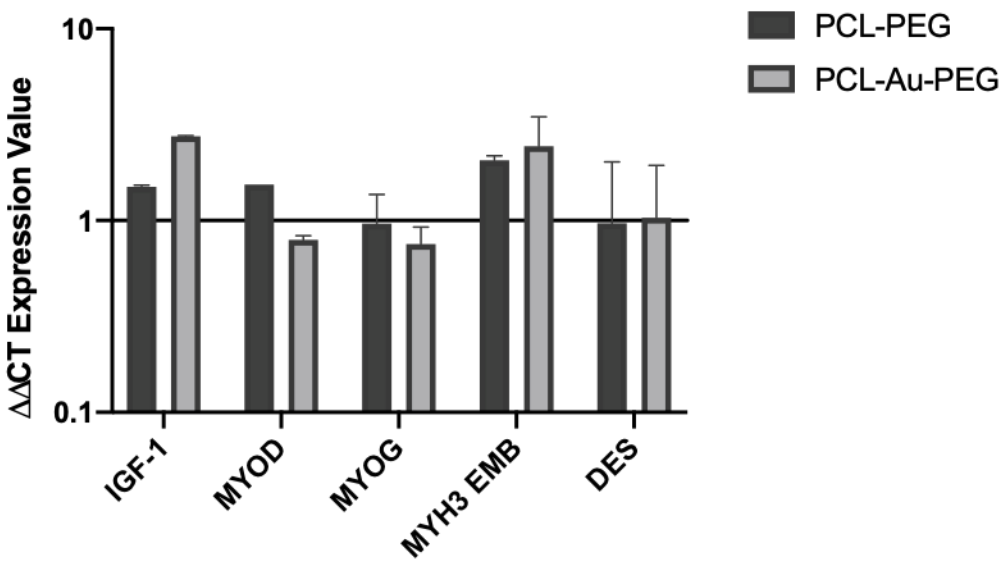

FIGURE 3.9: RT-PCR analysis on bio-constructs. A one-week-old construct made of C2C12 cells on electrospun PCL with PEG hydrogel (500:50) and electrospun PCL coated with gold nanoparticles and PEG hydrogel (500:50) were cultured under static conditions. The constructs were analyzed for various muscle gene expressions: IGF-I, MyoD, Myogenin, MYH3 emb and Desmin by means of RT-PCR analysis. The mRNA levels of C2C12 on electrospun PCL were normalized to 1 and used as the control (n=2).

3.5 Discussion

To date, many attempts have been made in tissue engineering to reconstruct skeletal muscle tissue in vitro. Current consensus states that controlling myoblast orientation is essential for achieving successful regulation and differentiation of skeletal muscle cells in vitro (Wakelam, 1985; Huang and El-Sayed, 2010). Most studies have thus focused on designing appropriate scaffolds that mimic the structure of native tissue to support the formation of highly oriented and functional myofibers. Bioinspiration could be found at the nanoscale level (mimicking the size and orientation of the matrix fibers) or at the microscale level (guiding the direction of cell proliferation). However, other key aspects of bioengineering could not be neglected, such as the handling of the biohybrid construct, and the capacity to perform dynamic stretching to promote cell differentiation. This required the production of scaffolds with adequate mechanical resistance. The multiscale approach proposed in this study aims to satisfy all these requirements, through hydrogel micropatterning of sheets of a mat of electrospun nanofibers, which can be coated with gold nanoparticles. As the basic material, poly(e-caprolactone) (PCL) was selected. This polymer is FDA approved for its biocompatibility and the absence of inflammatory or cytotoxic (Dennis and Kosnik, 2000; Ignatius and Claes, 1996). The PCL electrospinning process was tuned to produce matrices with fiber diameters of around 700 nm, to be similar to individual myofibrils (1µm)(Gunatillake and Adhikari, 2003; , Joyce). Using a drum collector rotating with a tangential speed of 3.9 ms-1 resulted in 70 % parallel-aligned fibers. PCL is also known to be highly hydrophobic and can present poor cell attachment in vitro(Leung et al., 1983). Therefore, the fibers were coated with gold nanoparticles to

increase the wettability of the scaffold and to potentially implement electrical conductivity properties. The coating method consisted in soaking the PCL sheets in chloroauric acid. This easy handling method resulted in a relatively uniform distribution of the conductive particles. PCL-Au sheets also showed improved wettability when treated with ethanol for sterilization while the PCL alone remained hydrophobic to organic liquid (supplementary data)(Zhang et al., 2009). The gold nanoparticles could be functionalized with biological peptides or proteins such as collagen to improve the adhesion and proliferation of the cells on the polymeric electrospun mats(Park and Shumaker-Parry, 2014). However, functionalization was not necessary in the present study as we showed that myoblasts indifferently attached to the nanofibers, coated or not with gold nanoparticles. Once attached to the fiber surface, C2C12 myoblasts spread out and multiplied, forming layers of cells that followed the direction of the PCL fibers, confirming previous reports. Regarding substrate stiffness, the majority of electrospun matrices described in the literature show elastic moduli in the range of tens or hundreds of MPa(Tang et al., 2019). In this study, the elastic modulus of the electrospun scaffold was reduced to a range of 10-20 MPa, values that remain very high compared to the elasticity of native tissues (10-50 kPa)(Ren et al., 2008; Ogneva et al., 2010; Discher et al., 2005, 2009). It is nevertheless in the same range as other scaffolds dedicated to muscle tissue engineering and will favor handling and further application of constant stretching or more complex mechanical stimulation10,11. Interestingly, the presence of PEG lines modified the mechanical properties of the scaffold, mostly at the microscale level, where an increase in the surface's elastic modulus, from about 150 kPa to approximatively 630 kPa was measured. It can be hypothesized that PEG residues were still present and cross-linked within the electrospun mat when exposed to surrounding UV light, thus trapping the fibers deep inside and modifying the properties of the material. The surface elasticity was still far from that of soft hydrogel matrices classically used for C2C12 proliferation and maturation. In the literature, stiffness between 1 and 45 kPa (Yn et al., 2018) is suggested as being close to normal muscle tissue elasticity. Previous work has reported an optimal material stiffness between 8 and 11 kPa, to support a proper maturation and the emergence of myotube's striation, resulting of an ultra-structural level organization (Boontheekul et al., 2007). Certain improvements could thus be proposed to reduce the mechanical properties of our scaffold. It has been shown that by modifying the solvents used to dissolve the polymer prior to electrospinning, a modulus of 36 kPa, suitable for soft tissues, could be achieved **(Engler et al., 2006)**. As already stated, in the present study nanoscale and microscale levels were investigated simultaneously to facilitate the alignment of the cytoskeleton and the formation of myotubes. As myofibers can reach a few hundred microns in diameter, a linear pattern with PEG hydrogel (40 µm height, 50 or 100 µm wide) spaced 500 to 1000 µm apart was developed. The multiscale scaffolds designed were successful for myoblast adhesion, proliferation, and most importantly fusion and differentiation into myotubes. The patterns with 500 µm to 1000 µm spacing positively affected cell organization and alignment, when coupled with a nanofibrous structure. Most of the previous studies with micro-structured hydrogel implemented patterns that created interspaces from 5 to a few hundred microns(Lam et al.,

2006*a*; Elamparithi et al., 2016; Altomare et al., 2010). A decrease in cell alignment for interspaces of more than 200 µm has been reported in the literature(Ahmed et al., 2010*a*; Patz et al., 2005). Here, by coupling the nanopatterning from the fibers and the hydrogel micropatterning, the myoblasts jointly "sensed" the topographical barrier imposed by the micropattern and the nanofiber direction, and developed highly organized stress fibers along the pattern axis. In fact, several studies have demonstrated the complementarity and benefit of combining these different scales. Previous work has established a method to pattern multiple desired topographic surfaces on electrospun nanofibers via solvent-loaded agarose hydrogel stamps(Aubin et al., 2010). In addition, through a hierarchical patterned topography of microgroove and nanopore structures hNSCs was successfully directing into neuronal differentiation**(Hu et al., 2016)**. In the same way, skeletal muscle cell behaviors on nano- and micro-alignment combined scaffolds with different angular combinations was monitoring(Yang, Jung, Lee, Lee, Kim, Song, Cheong, Bang, Im and Cho, 2014). To go further than their morphological observations, we monitored the behavior of cells through the expression of specific genomic markers. The expression of the myosin heavy chain, a mature muscle marker, demonstrated that the multiscale scaffold allowed differentiation of the C2C12 myoblasts into myotubes. Maximizing the formation of dense and cohesive myotubes promoted their fusion to form larger myofibers. The cell behavior observed in these experiments was corroborated by the increase in expression of various genes selected because they are known to play a part in myogenesis. Insulin-like growth factors (IGF) have growth-promoting activity during development and are also involved in tissue differentiation by positively regulating myogenic transcription factor MyoD(Cha et al., 2017). The increase in expression in both constructs of IGF-I and MyoD, apart from a decrease in MyoD expression for the construct containing the nanoparticles, reinforces the theory that specific scaffolds, adopting a biomimicry architecture, play an essential role regarding cell response. The MYH3 gene, which provides instructions for making a major contractile protein called embryonic skeletal muscle myosin heavy chain 3, is overexpressed on the combined scaffolds, which is corroborated by the confocal images of myosin protein. Desmin is only synthesized in fusing or multinucleated cells. However, it is often observed that the concentrations of desmin filaments correspond to the assembly of myofibrils, or the organization of myofibril bundles **(Em et al., 2003)**. Given the levels of expression of desmin close to baseline in our different materials, we can estimate that we are at an early stage of maturation where the myotubes have not yet formed myofibrils. Altogether, it can be estimated that our culture system was suitable for providing initial guidance and mechanical support for further use, such as investigating the effect of external stimulation. The effectiveness of electrical and mechanical stimulation on muscle cells has been established, with an increase in the formation of myotubes and their alignment, as well as improved contractile properties(Gard and Lazarides, 1980; Liao et al., 2008). Therefore, the combination of our multiscale material and stimulations could have a synergistic effect on the formation and maturation of myotubes. This could also lead to a gain in function in cell performances48.

3.6 Conclusion

In this study, we presented a simple and direct approach for controlling cellular alignment and elongation in a tissue engineered construct. We propose a hybrid method for manufacturing a multiscale scaffold. By using a simple photolithography process on the electrospun scaffold, we obtained an effective micropatterned polymeric surface. We performed an analysis of C2C12 cell behavior on two types of substrate, coated or not with gold nanoparticles and two ranges of patterning. Correct cell attachment and tissue formation were obtained in each substrate. Moreover, cell alignment was induced simultaneously by the nanofibers and linear micropatterning. The best results for differentiation parameters were observed on the scaffold coated with a micropatterning spacing of 500µm. Immunofluorescence analysis indicated the formation of myotubes, corroborated by gene expression. This work has produced promising results that further studies could enhance by investigating the effect of different external stimuli, such electrical or mechanical stimulation(Rangarajan et al., 2014*b*).

3.6.1 Acknowledgements

The authors specially thank X X X

3.6.2 Funding

This work was carried out and funded in the context of the Labex MS2T (Challenge Interfaces). It was supported by the French Government, through the program “Investments for the future” managed by the National Agency for Research (Reference ANR-11-IDEX-0004-02).

Chapter 4

Effect of mechanical or electrical stimulation applied to multi-scale cell-seeded electrospun construct for skeletal muscle tissue engineering

Beldjilali Labro M., Jellali R., Brown A., Stewart C., Lerebours A., Farhat F., Dufresne M., Grosset J-F., Legallais C.

4.1 Introduction

The process of skeletal muscle regeneration through tissue engineering has been subject to extensive research over the last decade. The aim is the development of strategies to promote cells' proliferation and differentiation for further clinical applications, but also to better understand physiology, physiopathology or even development (Witherick and Brady, 2018). However, the design of an efficient biohybrid construct is particularly challenging due to the complex cellular organization and specific functions of the native tissue (Shadrin et al., 2016). Moreover, obtaining in vitro mature skeletal fibers is a complex process influenced by cells interactions, as well as the biomaterial and more generally by the chemical and physical environment. Under optimal differentiation conditions, single myoblasts fuse to form multinucleated and mature myotubes to synthesize contractile proteins such as myosin and α- actinin (Sanger et al., 2002). Mature skeletal fibers are characterized by sarcomeric structures and the ability to perform repetitive contraction(Sweeney and Hammers, 2018). In order to engineer biomimetic skeletal muscle that resembles the highly anisotropic structure of native muscle fibers, numerous scaffolds with different shapes have been developed. The most commonly used techniques to produce them are hydrogel formation, 3D printing and electrospinning (Beldjilali-Labro et al., 2018*b*). Natural extracellular matrix (ECM) derivatives such as collagen or polysaccharides have the advantage of generally being biocompatible and prime for enzymatic degradation and cells adherence. While synthetic polymer presents more flexible material properties (Gibas et al., 2010; Catoira et al., 2019). Finally, biological-synthetic hybrid

constructs can merge the properties and advantages of each of the components and overcome some of their limitations (Klok, 2005). Additionally, to enhance spatial alignment of myoblasts, some studies incorporate patterns at the nano- or micro-scale produced by soft lithography (Patz et al., 2005; Wang et al., 2010). Based on this last approach, we designed a multi-scale scaffold of poly(ε-caprolactone) (PCL) electrospun nanofibers covered with linear micropatterns made with polyethylene glycol (PEG). It has already shown promising results regarding myotube formation and alignment. However, biomaterial strategies developed so far have been shown to be not sufficient enough to successfully engineer highly functional muscles. In this context, researchers also investigate the potential biological effect of electrical, mechanical, flow, or electromechanical stimuli on muscular cells to further enhance the development of skeletal myotubes (Rangarajan et al., 2014*b*; Qin and Hu, 2014; Handschin et al., 2015). As mechanical stimulus, electrical stimulation draws lots of attention in muscle tissue engineering. Indeed, since skeletal muscle is stimulated in vivo by neuron activity, electrical stimulation appears to augment the development and maturation of the tissue in vitro. It induces the remodeling of the cellular environment, promoting myosin synthesis, myofibers formation and functional properties (Ito et al., 2014). Concurrently, works have also shown that providing mechanical stimulation to skeletal muscle engineered tissue may support its maturation and development. Applying cyclic strain to the muscle tissue helps organizing muscle fibers into parallel arrangements which more appropriately mimic a functional unit of a native skeletal muscle (Boonen et al., 2010). When optimized, these external cues are expected to synergistically and dynamically activate important intracellular signaling pathways. It thus leads to accelerate the development of skeletal tissue, and to stimulate somehow some mechanotransduction occurring during embryogenesis. Based on our previously developed scaffold, we propose to investigate whether the use of stimulation mimicking neuronal or mechanical activity during myogenesis can promote the proliferation, maturation and differentiation of C2C12 myoblastic cells, as well as influence the expression of myogenic transcription factors and myosin heavy chain (MHC).

4.2 Materials and Methods

4.2.1 Scaffold preparation

A solution of 10 wt% poly(ε-caprolactone) (PCL, MW = 80.000 Da, Sigma-Aldrich, St. Louis, MO) in dichloromethane (DCM, Sigma-Aldrich)/N,N-dimethylformamide (DMF, Reagent Plus ≥99%, Sigma-Aldrich) (80:20 v/v) was prepared under stirring for 24 h before electrospinning. Polymer solutions were loaded in a 5 mL syringe equipped with a stainless-steel gauge needle (18G). Grounded aluminum foil was used as collector electrode. The distance between needle and aluminum collector was 15 cm. Solution was constantly fed using a syringe pump at 1.02 mL/h. Applied voltage was optimized to obtain good spinnability, with typical value of 15 kV. The resulting electrospun fibers were micropatterned with PEG hydrogel using photolithography (PEG-diacrylate (MW

575), Sigma-Aldrich). For the UV photo-crosslinking process, the liquid PEG was mixed with 1% w/v of photo-initiator (2-Hydroxy-2-methylpropiophenone, Darocur 1173, Sigma Aldrich). Then the mixture was dropped on electrospun scaffold by spin coating and exposed to a UV light source for 20s (Kloé UV-KUB 2, 365 nm, 40 mW/cm2) through a photomask. The patterned scaffold was washed carefully in the dark with distilled water to remove residual PEG precursor solution.

Cells

Murine C2C12 myoblasts cell line was used in this study (ATCC, CRL-1772). The growth media was Dulbecco's Modified Eagle's Medium high-glucose (HDMEM; Hyclone, USA) containing 10% fetal bovine serum (FBS, Gibco Invitrogen, USA), and 1% of penicillin-streptomycin (Gibco Invitrogen, USA). The cells were cultured onto a T-175 flask at 50 % of confluence in a CO2 incubator (5% CO2 atmosphere at 37 °C) and used for experiments before they reached 5 passages.

Cell seeding on scaffolds

The scaffolds were cut into rectangles measuring 40 by 10 mm, disinfected with ethanol 70% (Sigma-Aldrich, USA) for 45 min, washed three times with PBS (phosphate buffered saline, Gibco Invitrogen, USA) at pH 7.4 and incubated in growth media for 30 min before starting the cell culture experiment. After 48h, growth media was changed to differentiating media constituted of HDMEM supplemented with 2% horse serum (HS, Gibco Invitrogen, USA) and 1% of penicillin-streptomycin (Gibco Invitrogen, USA) to induce the differentiation. Each scaffold was plated with a density of 5.10^5 cells.cm^{-2}.

4.2.2 Experimental setup

Figure 4.1 shows the experimental setup, which includes a custom-built electronic circuit with electrodes and a generator and a CellScale MechanoCulture T6 (Waterloo, ON, Canada) bioreactor to apply the different stimuli on the cells construct.

Cell culture with electrical stimulation device

In order to impose electrical stimulation on the cell-seeded construct, a custom-made device was developed. The electrodes have been designed in an "L" shape and sized to fit a 6-well plate (fig. 4.1). They were laser cut from a carbon plate. A hole has been drilled in the upper part to allow the passage of a platinum wire (diameter 0,5mm 99,9% sigma Aldrich) which is connected to the generator. The electrodes are then held in place by a polydimethylsiloxane (PDMS) mold. The gap between both electrodes is fixed of 1.5 cm. The electrodes inserted in the PDMS mold are then sterilized by autoclave. The freshly sterilized scaffold is placed in a 6-well plate. Then the cells are seeded and cultured for 48 hours in growth medium (HG-DMEM; 10% FBS). After this time the medium is changed to differentiation medium (HG-DMEM; 2% HS) and the electrodes are placed on the sheet.

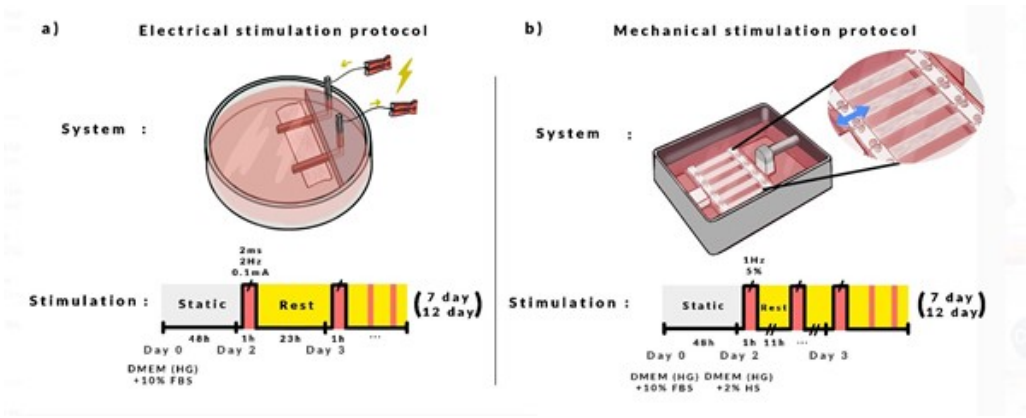

FIGURE 4.1: the experimental setup for electrical and mechanical stimulation of skeletal myoblasts. (a) the electric stimulation system with carbon electrodes embedded in a PDMS mold connected to the generator by platinum wires. (b) the tensile bioreactor, CellScale MechanoCulture T6, allowing to have six samples stimulated in the same time. Overview of stimuli parameters applied (c) with a electrical stimulation of 2 Hz for 2 ms at 0,1 mA for 1h during 5 or 10 days (d) and a 5% strain mechanical stretching, twice a day for 1h at 1Hz with 11h of rest between each cycle for 5 or 10 days following up two days of static culture under growth media.

The custom-built electronic circuit was designed to deliver an output frequency electrical stimulation of 2 Hz for 2ms at 0,1mA for 1h during 5 or 10 days. These outputs were fed to a Bipolar field generator. Finally, the medium is changed after each stimulation.

4.2.3 Cell culture with mechanical stimulation

Mechanical stimuli were applied by imposing cyclic stretch. Each construct is placed in the CellScale MechanoCulture T6 (Waterloo, ON, Canada) bioreactor, consisting of an actuator and screw-driven clamp grips mounted inside a cell culture chamber capable of applying uniaxial stretching to 6 parallel samples. The chamber is sterilized by dry heat. After two days of culture in a six-well plate in the growth medium, the samples are placed in the chamber and fixed between the clamps. The bioreactor is then filled with 150 mL of differentiating media to immerse the cells constructs. The cells sheets are subjected to 5% strain twice a day for 1h at 1Hz with 11h of rest between each cycle for 5 or 10 days. The stretching device was set in a CO2 incubator to culture the scaffolds in a 5% CO2 atmosphere at 37°C.

4.2.4 Evaluation of cell morphology

Cell behavior was assessed through immunofluorescence after 7 days of culture on the scaffold. After washing with PBS, the samples were fixed in a 4 % PFA solution for 15 min at room 94 Chapter 4: Effect of mechanical or electrical stimulation temperature. Samples were then permeabilized with a 0.3% TritonX-100 solution for 10 min and blocked with a 3 % Bovine Serum Albumin solution (Sigma) for 30 min. Myosin, actin and nuclei staining of cells were performed using respectively, anti-Myosin Heavy Chain antibody (1/200, Neo Biotech) for 2h followed by secondary staining using Alexa 594 overnight at 4°C, Alexa Fluor 488 Phalloidin (1/200, Thermofisher) for 2 hours, and Hoechst 33492 (1/1000,

Sigma) for 15 minutes at room temperature. The samples were finally washed with PBS before visualization using Z-stacking and mapping "Tile scan" specification of confocal microscopy (Zeiss LSM 710). The confocal images recorded were about 1mm in length.

Myotubes measurement

The influences of the biomaterials on myoblast differentiation, myotube length, orientation and area occupied and nuclei per myotubes were measured using ImageJ (NIH, Bethesda, Maryland), and Cell Profiler software's. Myotube length was defined as the line distance from one extremity of the myotube to the other. Total area occupied by differentiated cells was counted in 2 images (1mm of length) of each sample. The percentage of cell alignment was defined based on the measurement of myotubes (n=50) aligning with $\pm$ 15°from the pattern.

RT-qPCR

Gene expression was studied using RT-qPCR (reverse transcription quantitative polymerase chain reaction) after 7 days of culture on the scaffolds. Briefly, samples were lysed with 350 µl of Trizol and centrifuged to extract the RNA (ribonucleic acid) according to the manufacturer's protocol (Qiagen, Germany). RNA pellets were resuspended in 30 µl of RNA storage solution (Ambion, Paisley, UK) and analysed (Nanodrop, ThermoFisher Scientific, Paisley, UK) for quantity (mean $\pm$ SDEV; 6671 $\pm$ 3986 ng) and an indication of quality (260/280 ratio of mean $\pm$ SDEV, 1.95 $\pm$ 0.09). The RNA was retrotranscribed into DNA (deoxyribonucleic acid) using a High Capacity cDNA Reverse Transcription kit (Applied Biosystems, USA) according to the manufacturer's protocol. RT-qPCR was performed using the SYBR Green PCR Master Mix (Applied Biosystems). Relative mRNA levels were calculated using the 2-$\Delta\Delta$Ct method. The ΔCts were obtained from Ct normalized with the Rp2b gene levels in each sample and reactions were checked before the experiments (efficiency $>$ 80%, R2 $>$ 0.99). The results were normalized from the data of PCL electrospun construct, i.e. data were plotted as a ratio to a cell-only control group, highlighting the intrinsic effect of the scaffolds on the gene expression. The primers used are listed in supplementary data.

4.2.5 Statistical analysis

Statistical analysis and graph drawing were carried out using GraphPad's Instat 3.10 and Prism v 6.0 (GraphPad Software, CA. USA). All data are represented as mean $\pm$ standard deviation from at least three independent cultures (N $\geq$ 2). Group comparisons were performed by the Mann–Whitney non-parametrictwo-tailed test and the Kruskal–Wallis non-parametric test with Dunn's multiple comparisons post-test. Significance is indicated on the graph by * $p < 0.05$, ** $p < 0.01$ and *** $p < 0.001$.

4.3 Results

4.3.1 Implementation of the stimulation's protocols

A wide range of protocols for electric pulse stimulation (EPS) or mechanical stretching of muscle cells in culture have been proposed over the years. However, to date no consensus has been reached. We thus tested four different EPS conditions, to establish one stimulation that could recapitulate plastic changes on the gene expression level. **Figure 4.2a**, show that after 5 days of culture under biphasic or continuous field at 2V or 3V, biphasic field under 2V causes significantly less cytotoxic effect on cells than other stimulation conditions. More so, when compared to static culture, there is no significant difference in viability. **Figure 4.2b**, shows fluorescent images of C2C12 myotubes formed under electrical stimuli and static condition. Morphological differentiation could be observed. Indeed, the myotubes subjected to electrical stimulation are more elongated with an average length of 246 µm, it exhibits a greater number of nuclei per myotube 30±9 compared to static 16±11 at 7 days of culture. Finally, they appear to align in the direction of stimulation as seen in **Figure 4.2b**.

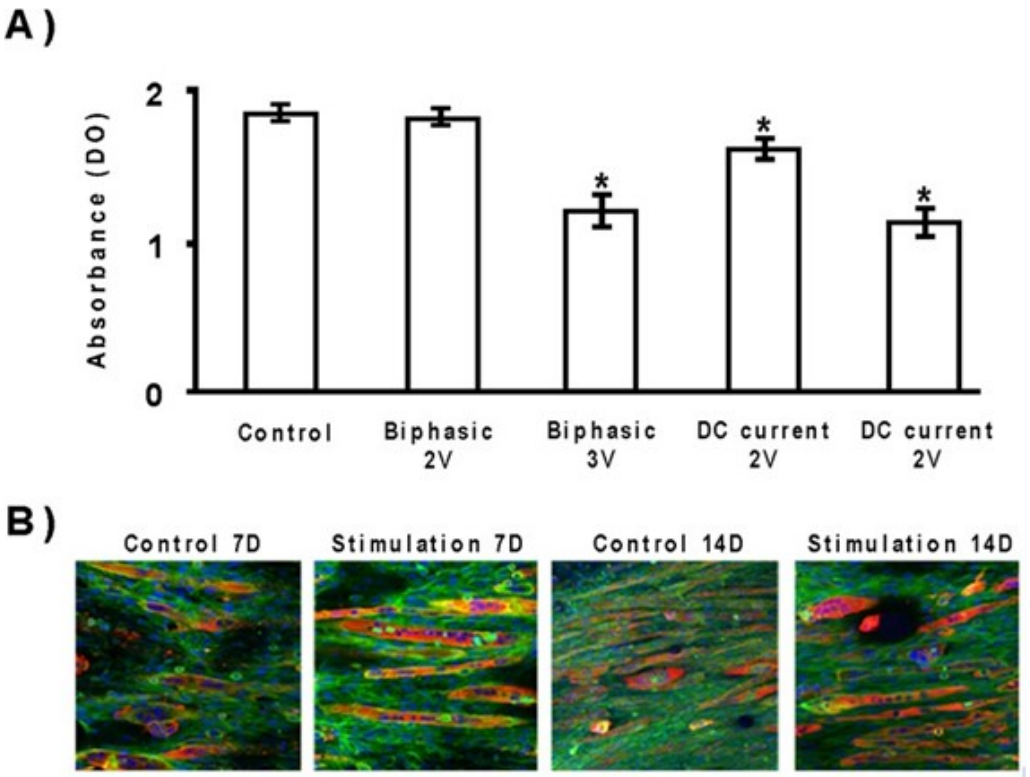

FIGURE 4.2: Preliminary investigations for electrical stimulation: (A) Effect of applied current on cytotoxicity: MTT assay (n=3). The data obtained for MTT of the cells cultured with stimulation were compared to those of the control cells (whitout stimulation) with the Mann-Whitney nonparametric statistical test. The p-values are indicated for the tests, showing a significant difference between the conditions (*$p < 0.05$). (B) C2C12 response after 7 and 14 days of culture on PCL layer with and without electrical stimulation (1 hour/day, tension 2V, pulse duration 2ms, frequency 2Hz). (Confocal microscopy, G=10x20). Blue: nuclei; red: myosin; green: actin).

4.3.2 Effect of stimulation on C2C12 behavior on PCL based scaffolds

The influence of electrical or mechanical stimulation on cell proliferation on the different constructs is then examined. The formation of myotubes is observable under all conditions to a greater or lesser extent. Firstly, on simple PCL sheet alone **Figure 4.3a**, the results showed that the cells with electrostimulation exhibited a different level of proliferation and differentiation as compared to those without stimulation or under stretching. On PCL sheet without stimulation,myotubes are oriented in a fan shape, with an orientation varying from -70°to 85°along the main axis. The application of stimulation appears effective to align the myotubes, with a focus around 10.06°± 9.26°from the axis under electrical stimulation and 24.4°± 11.64°under stretching (**Figure 4.4**). An increase in myotubes length could be observed from 351.36 ± 165.95 µm to 468 ± 280 µm with the electrical condition while, mechanical stimulations seem to reduce myotubes length formed with a mean of only 200.94 ± 149.71 µm (Figure 4). No difference was found in term of the myotubes area between the electrical stimulation and the culture in static, with mean around 13500 ±1500 µm2 (**Figure 4.4**). However, cells that have undergone mechanical stimulation are found to have an area 2,5-fold smaller. Accordingly, the number of nuclei per myotube also decrease with the mechanical stimulation and appear to be similar for the two other condition (Figure 4). Moreover, under mechanical stimulation, some cells expressing myosin heavy chain appear with a round shape, integrating several nuclei. This provides a disorganized structure to the tissue (**Figure 4.4a**). The presence of micropatterns especially with a theoretical spacing of 500 µm (PCL-PEG 500:50) show clearly the discrepancy in myotubes behavior under the 3 conditions (**Figure 4.3b**). Without stimulation, the topography promotes myotubes' alignment with an orientation diagram centered on 0.38 ± 4.97°. Mechanical stimulation seems efficient in this configuration, with very long and thin myotubes. However, they appear to be sparsely distributed when compare to the other two condition, the number of nuclei can reach 50 per myotubes. Still, electrical stimulation appears more effective, with the fusion of myotubes forming large arrangement, corresponding to a further step in muscle maturation. Consequently, the number of nuclei is going up to 185 per myotubes, with a length of 426 ± 68.15 µm compare to 248 ± 20.95 µm with the mechanical condition and 185.60 ± 19.90 µm for the myotubes formed under static condition. The surface area of myotubes is also more than 2-fold wider than the myotubes grown without stimulation (**Figure 4.4b**). With more space between micropatterns (PCL-PEG 1000:100), myotubes' are able to align, thus when there is an upper layer of cells, the myotubes formed might be more disorganized (**Figure 4.3c**). Some clusters of non-oriented fibers exist, but on the other hand, very long myotubes up to 1 mm with significant number of nuclei up to 110 can be found in the conditions (**Figure 4.4c**). Again, electrical stimulation is likely to offer the best improvement as compared to static and mechanical culture.

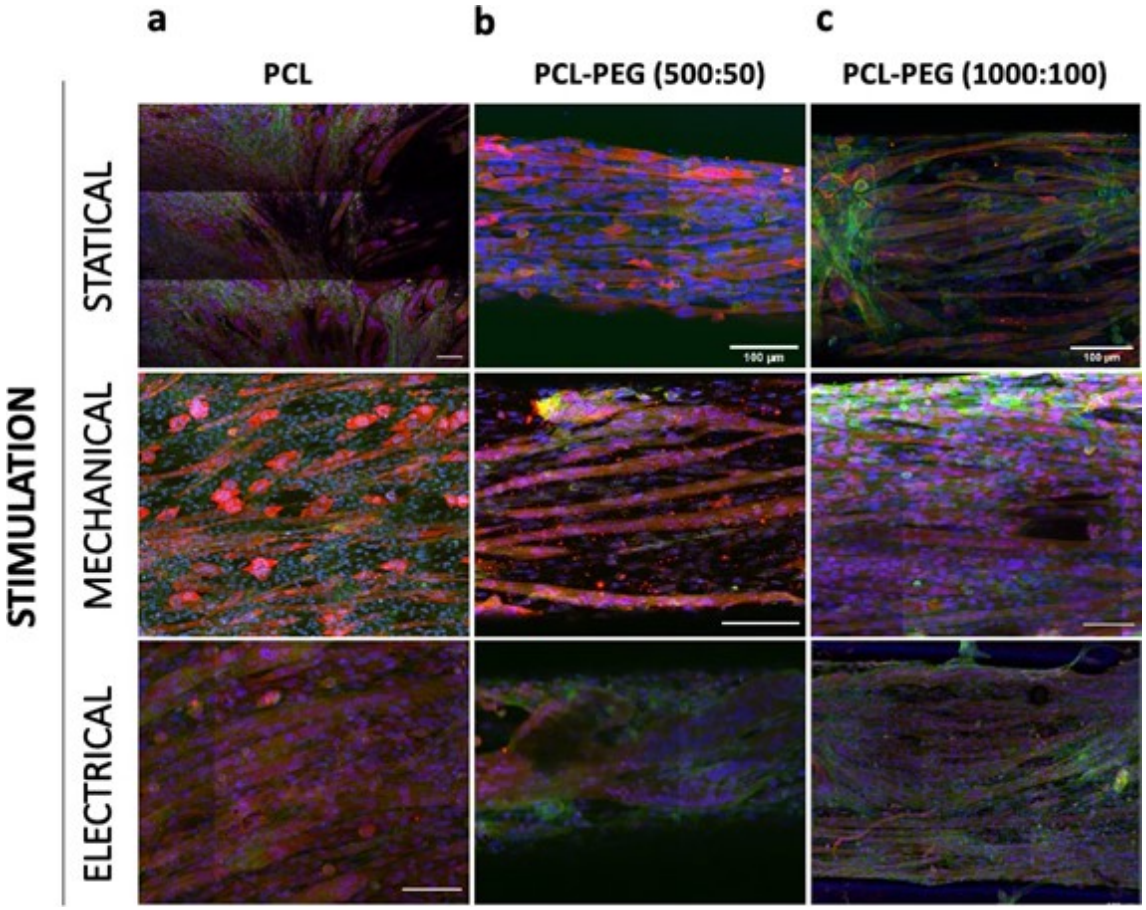

FIGURE 4.3: Confocal images of C2C12 cells after 7 days of culture on scaffold under statical, electrical, and mechanical stimulation with a space of (a) 1000 µm or (b) 500 µm between the hydrogel lines and (c) without hydrogel. Nuclei in blue fluorescence (Hoescht 33258), F-actin in green fluorescence and myotubes by anti-MHC antibodies in red fluorescence. Scale bar: 100 µm.

4.3.3 RT-PCR analysis

The maturation and differentiation of C2C12 myoblasts cells, after 7 and 14 days of culture on electrospun mats under different conditions is evaluated by RT-PCR (**Figure 4.5**). The expression level of MRF genes MyoD, Myogenin, and other genes implied in muscle development such as IGF-I, IGF-II, URB5, MYST, MYH3, and Desmin is followed. PCL-PEG construct increases the expression of most of the genes when compared to the control PCL scaffold at day 7 when no stimulation is applied. MYH3, URB5 and MYST genes expression demonstrate a two-fold increase, while Myogenin and Desmin are expressed similarly as the baseline PCL (**Figure 4.5a**). When the biohybrid PCL samples are exposed to electrical or mechanical stimulation, changes in gene expression profiles were observed (**Figure 4.5b**). Only IGF-II and URB5, exhibit a higher expression compare to static PCL control, with a 2-fold increase for URB5 expression and a moderate increase in IGF-II expression. MYST gene is more than 2-fold expressed, but only under electrical stimulation. Uncommonly, the MRF gene family follow by MYH3 and Desmin are down regulated with both stimulations, with more or less important variations depending on the stimulation applied on the PCL construct. For MyoD the expression is of (0.87 $\pm$

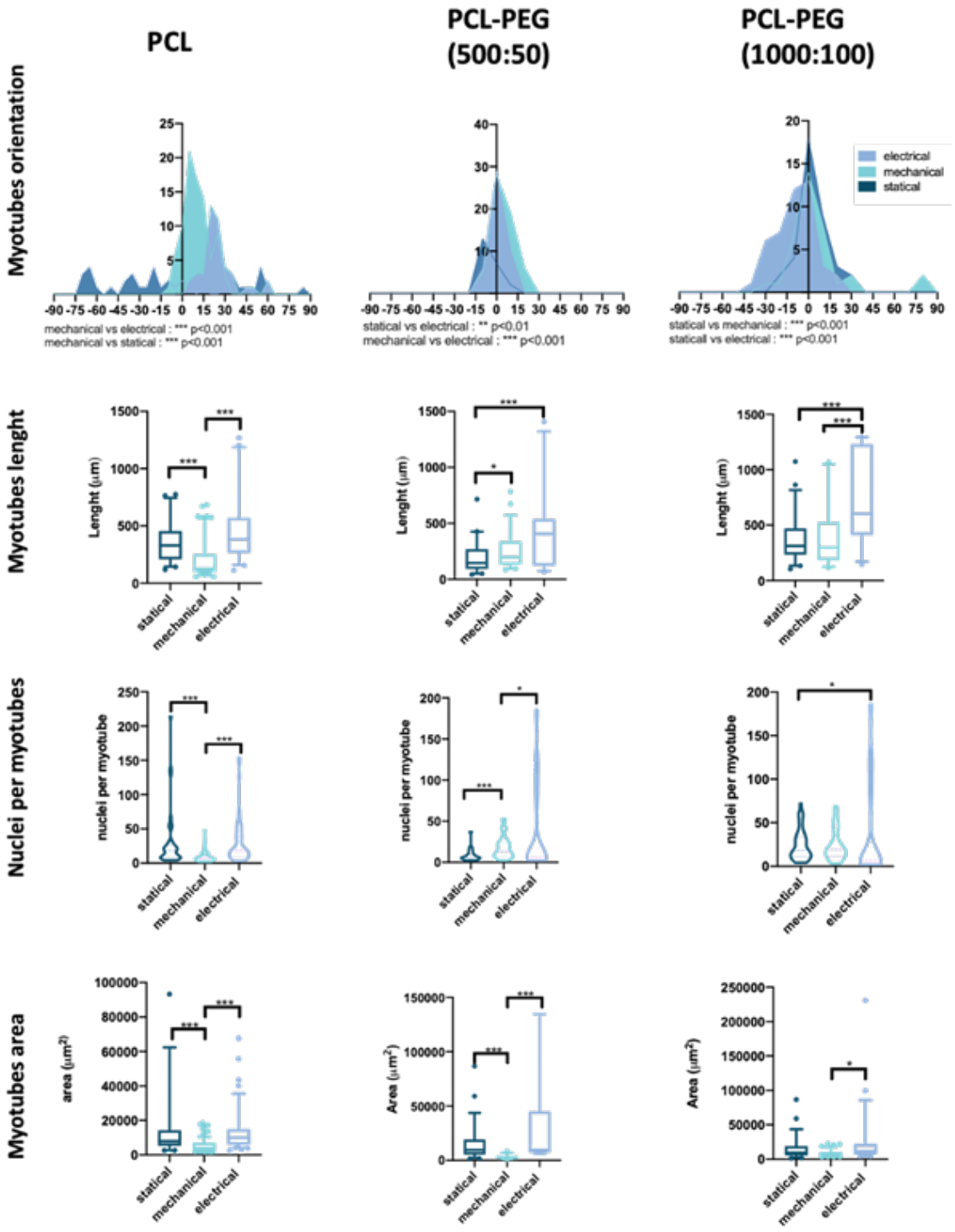

FIGURE 4.4: Quantification of C2C12 myotubes, on (A) PCL, (B) PCL-PEG(500:50) and (C) PCL-PEG(1000:100) construct, through, orientation, length, number of nuclei and total area occupied by myotubes as function of the stimulation condition applied on the different scaffolds (n$\geq$ 30 myotubes). Kruskal–Wallis non-parametric test with Dunn's multiple comparisons post-test was used for statistical analysis (p-value: * $p < 0.05$, ** $p < 0.01$, *** $p < 0.001$).

0.43) and (0.47 $\pm$ 0.43) and for MYH3 (0.62 $\pm$ 0.11) and (0.31 $\pm$ 0.13) for respectively, electrical and mechanical stimulation. Furthermore, the addition of patterns combined

with electrical stimulation appear to have an antagonistic effect on the regulation of these genes, with a 100-times less expression of MYH3, 80-times less for Myogenin and 5-time less expression of Desmin than the baseline. Additionally, after 12 days (i.e. D12), PCL construct demonstrates a divergence in the gene expression when compare to this homologue (7 days). An increase in IGF-II and MYST expression compared to D7, with IGF-II (3,21$\pm$ 0.71), MYST (3.29 $\pm$ 0.25), URB5 expression remain constant (2.35$\pm$2.57). Furthermore, the Desmin expression, which is at baseline levels at day 7 increase at day 14 (2.47$\pm$ 0.46), while Myod, Myogenin and MYH3 decrease of 2.3, 1.4 and 1.6-times than the 7-day construct respectively (**Figure 4.5c**). Interestingly, we can observe that the gene regulation is different for the PCL construct following to 10 days of stimulations, with an increase in IGF-I and IGF-II expression in both conditions and the maintenance of the level of expression of URB5 and MYST. However, it appears that 10 days of stretching results in more pronounced down regulation of MyoD and MYH3, while electrical stimulation show an increase of desmin expression from (0.41 $\pm$ 0.22) at 7 days to (1.84 $\pm$ 0.57). Finally, PCL-PEG combined with 10 days of electrical stimulation show result along the one obtained with its 7-day equivalent, a down-regulation tendency in all the genes is observed (**Figure 4.5d**).

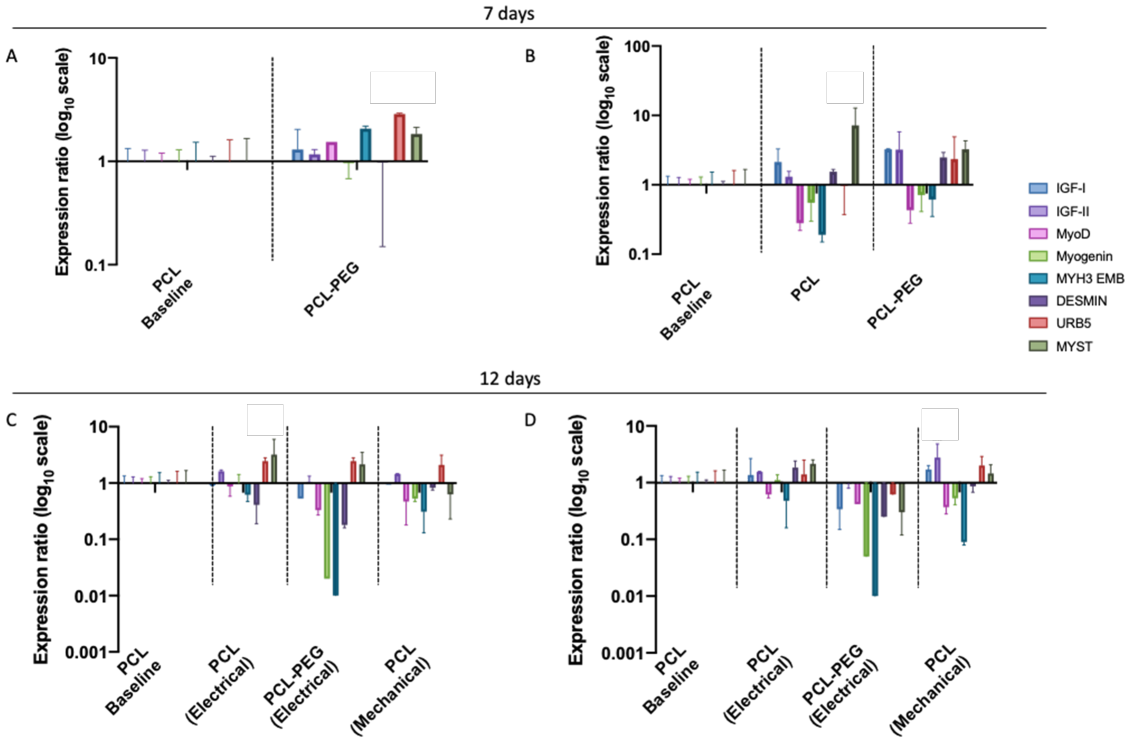

FIGURE 4.5: Expression of IGF-I, IGF-II, MyoD, MYH3 EMB, MYF4, Myogenin, MYST, URB5 and Desmin transcripts in PCL construct by RT-PCR analysis. The construct made of C2C12 cells on PCL electrospin or PCL electrospin with PEG hydrogel (500:50) were culture for (a,b) 7 days or (c,d) 12 days under (a,c) statically condition and (b,d) external stimulation (electrical or mechanical). The Results of the different genes are reported as -ΔCts between each miRNA and the endogenous control (small nucleolar RNA RP2B). The mRNA levels of C2C12 on PCL electrospin were normalized to 1 and used as control.

4.4 Discussion

Striated muscle tissue engineering has followed a long way since the very first attempts to culture and maintain muscle cells in vitro. Better control and sophisticated biomaterials prepared thanks to the progress in micro/nanotechnology, potentially combined with the use of electrical and mechanical stimulations, are promising approaches. In theory, these stimulations mimic natural skeletal muscle cells stimulation, to achieve cell differentiation and the generation of highly functional biomimetic muscle tissues. However, there is presently no consensus about an optimized muscle tissue engineering process. Thus, to continue to advance on an optimal skeletal muscle tissue engineering process, we investigated in the present work different strategies including scaffold topography, mechanical stimulation electrical stimulation, alone or combined to promote cell differentiation of a PCL based scaffold created by electrospinning. Our PCL-PEG constructs exhibit myotube-related parameters, such as fusion index, myotube length, orientation angle similar to those obtained from highly oriented electrospun (Ricotti et al., 2012), or other technique such as topographic guidance (Kim et al., 2019) or 3D printing(Costantini et al., 2017). Our work has shown that mechanical and electrical stimuli favor the formation of myotubes and thus enhanced the length and index of fusion. In addition, they also promote the orientation of the myotubes in the direction of attachment between anchoring points, similarly as works using different stimulation parameters (Langelaan et al., 2011*a*; Ahadian et al., 2012; Tanaka et al., 2014; Handschin et al., 2015). However, when the materials have a stiffness similar to that seen in the native tissue, the formation of cross-striations is then observed (Boonen et al., 2010). For optimal tissue growth and maturation, different types of stimuli should be tested, and optimal operational parameters should be carefully selected. Such tissue engineering protocols necessitate an adequate follow-up to understand clearly the mechanisms of the effect involved. As an example, the schedule for applying the stimulation still need to be refined. In our work, the stimulation was initiated together with the shift from proliferation medium to the deprived serum medium that fosters cell differentiation in classical 2D culture. Langelaan et al. (2011*b*) suggested waiting for 2 days after this medium change to start the stimulation. The number and the type of cells could also influence the response to the stimuli. The differentiation of myoblasts into myotubes, in fact, depends on two critical and related events: interruption of proliferation (Olson, 1992)and end-to-end contacts between myoblasts (Clark et al., 2002). The high number of myoblasts could could thus be considered, in this case, as a favorable condition for a more sustained differentiation process. However, preliminary tests (supplementary data) shown that cells in contact with the biomaterial form myotubes and are rapidly covered by layer of non-differentiated myoblasts. The use of muscle progenitor cells could be an alternative although a strict purification protocol should be defined. Finally, the effect of concomitant mechanical and electrical stimulation should be evaluated, as it might be implemented for the final myotendinous junction (Liao et al., 2008). To evaluate such advanced tissue engineering approaches, the understanding of potential synergistic or antagonistic effects of different biophysical stimuli on engineered muscle structure and function is requested.

Therefore, in this study, mRNA analyses were carried out to test the expression of genes broadly recognized as important for skeletal muscle development. Given the role of the MyoD family of myogenic regulatory factors (MRFs) in the transcriptional activation of the muscle program in vertebrates, we examined MyoD, myogenin expression. In addition to the transcription factors, proteinases, and extracellular matrix components are also known to play important roles in the regulation of myoblast differentiation. We evaluate the myogenesis process with the following scheme, where some genes' activities are clearly linked.

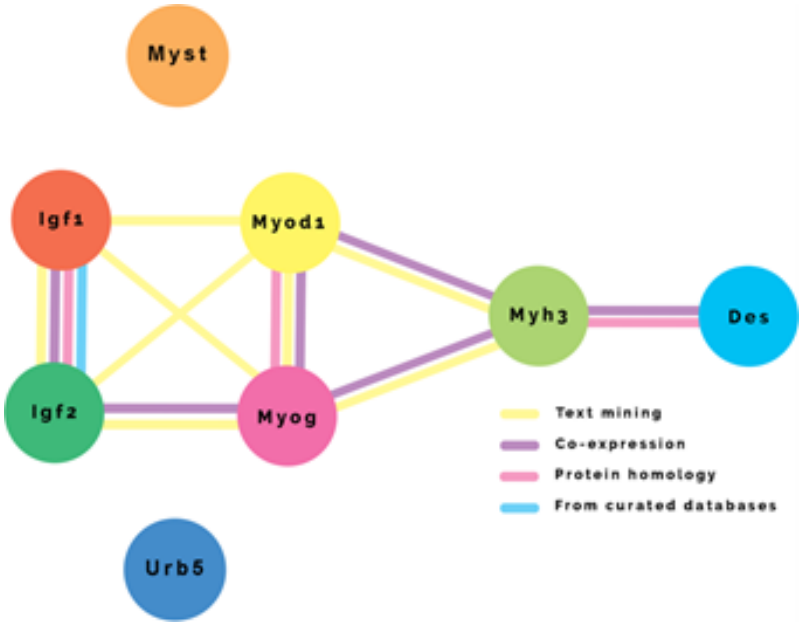

FIGURE 4.6: Figure 6: Genomic signaling pathways involved in the control of skeletal muscle maturation.

Insulin-like growth factors (IGF-1/IGF-2) are essential for normal growth and development. They are among the major fetal growth hormones in mammals (Agrogiannis et al., 2014). They positively regulate myogenic transcription factor MYOD1 function by facilitating the recruitment of transcriptional coactivators, thereby controlling muscle terminal differentiation. IGF-1 acts via a transmembrane tyrosine kinase receptor and exerts an anabolic effect on skeletal muscle (Shavlakadze et al., 2010). In our case, IGF-I/IGF-II gene were expressed with varying levels throughout the different models, at the exception of PCL-PEG under electrical stimulation. Studies in cultured myotubes suggest that IGF-1 promotes muscle hypertrophy by activating PI3K/Akt signaling (Chakravarthy et al., 2001; Rommel et al., 2001). Indeed, in vivo infusion of IGF-1 into muscles of 10-week-old mice increases protein synthesis (Bark et al., 1998) and the muscle-specific overexpression of IGF-1 results is muscle hypertrophy (Barton, 2006). This could support the conjoined expression of IGF-I/IGF-II and URB5 observed in our different conditions and constructs. E3 ligase called UBR5, previously uncharacterized in skeletal muscle, is an epigenetically regulated gene hypomethylated after resistance exercise-induced muscle hypertrophy in humans. Previous study, have shown that the level of UBR5 gene expression was positively and strongly correlated with the increases in lean leg mass during periods

of training and retraining (Hughes et al., 2020; Seaborne et al., 2019). As part of the MRF family, Myogenin and MyoD are proteins that bind to the regulatory region of several skeletal muscle genes and can activate their transcription differentiation (Brennan and Olson, 1990; Olson, 1992). MyoD (Weintraub et al., 1991) regulates muscle cell differentiation by inducing cell cycle arrest, a prerequisite for myogenic initiation. The protein is also involved in muscle regeneration. Indeed, it activates its own transcription which may stabilize commitment to myogenesis (Sartorelli and Caretti, 2005). Myogenin is a muscle-specific transcription factor that can induce myogenesis in a variety of cell types in tissue culture (Hernández-Hernández et al., 2017). During terminal myoblast differentiation, it plays a role as a strong activator of transcription at loci with an open chromatin structure previously initiated by MyoD (Du et al., 2012). When the myoblasts are at their terminal differentiation level, Myogenin and MyoD are down-regulated by the innervation process, and more specifically the associated electrical stimuli Eftimie et al. (1991). Their results could confirm our observations regarding the sub-regulation of the myogenin and MyoD genes in prolonged and stimulated cell cultures. Moreover, Recent studies have demonstrated that histone acetyltransferases HATs (MYST) provide a link between the signal transduction pathways that regulate muscle cell differentiation and the transcription factors that activate muscle genes directly. The association of HATs (MYST) with MyoD and MEF2 transcription factors which act cooperatively can control the activation of the muscle differentiation program (McKinsey et al., 2001, 2002; Utley and Côté, 2003; Shibata et al., 2010). Therefore, we expected a correlation in the expression of the MYST and MyoD genes by RT-PCR and the immunostaining of MHC in confocal microscopy in our studies. However, we noticed that while MYST was globally expressed in all the conditions at exception of the PCL construct subject to 5 days of mechanical stimulation and PCL-PEG having undergone 10 days of electrical stimulation, MyoD were downregulated in all conditions, except for the PCL-PEG construct culture or 7 days in static. Ultimetly, developing skeletal muscles express unique myosin isoforms, including embryonic and neonatal myosin heavy chains (MHCs: MHC-emb and MHC-neo), coded by MYH3 and MYH8 genes, respectively. These myosin isoforms are transiently expressed during embryonic and fetal development and disappear shortly after birth when adult fast and slow myosin's become prevalent. The upregulation of these genes is apparently controlled by the activity of the myogenic regulatory factors MyoD and myogenin. MHCs gene activation during embryonic myogenesis is accompanied by parallel upregulation of myosin like chains (MLCs) and other contractile protein genes. The switch from developmental to adult fast MHCs takes place also in in vitro cultured muscle cells. It has been reported that C2C12, when induced to differentiate upon transfer to low serum medium, first express MHC-emb, MHC-neo, and MHC-slow transcripts, starting at day 1 and peaking at day 2–4 then decreasing, whereas MHC-2A, MHC-2X, and MHC-2B transcripts start to increase at day 2–4 and peak by day 8 (Brown et al., 2012). These results suggest a possible explanation as to why in all the constructs, at the exception of PCL-PEG under 7 days of static culture, MYH3 EMB is under-regulated, whereas the presence of myotubes is corroborated by immunostaining of the myosin heavy chain in

confocal images. Finally, Desmin gene encodes a muscle-specific class III intermediate filament. This protein is essential for proper muscular structure and function. It plays a crucial role in maintaining the structure of sarcomeres, inter-connecting the Z-disks and forming the myofibrils, linking them not only to the sarcolemmal cytoskeleton, but also to the nucleus and mitochondria, thus providing strength for the muscle fiber during activity (Hnia et al., 2015). Desmin has also been postulated to play a critical role at different early steps of myogenesis both during myogenic commitment and differentiation. Studies carried out with C2C12 cells demonstrated that myotube formation could be blocked by desmin antisense RNA in vitro ((Zheng et al., 2017)). Unexpectedly, in our study the RT-PCR analysis of the selected gene suggests that adding electrical stimulation on the micropatterned cell-seeded scaffold is likely to inhibit gene expression related to myogenesis. Electrical stimulation would thus be antagonist to cell maturation ensured by the aligned microstructures. However, these assays are not in agreement with the morphological observations, where anti-MHC antibodies clearly outline the presence of long and parallel myotubes. These observations may suggest that in this configuration, the analysis that was performed in the present study at 7 days and even more at 12 days takes place too late and is not able to report the early changes in gene expression. It would then be suggested to perform a kinetic study in the first days after cell seeding instead of initiating follow up at 7 days. In addition, it could be of particular interest to also investigate MRF4, another gene of the MRF family, and other gene illustrating contraction pathways (such as MCU coding for the calcium uniporter protein or Camkk1). For the morphology analysis, desmin and α-actinin and sarcomeric myosin should also be stained to illustrate the organization and formation of crossed- striation in the myotubes.

4.5 Conclusion

In this study, we evaluated the potential benefit of mechanical or electrical cyclic stimuli on the differentiation of C2C12 cells into myotubes, in combination or not with the micropatterning of the PCL electrospun scaffold. This study shows that mechanical or electrical stimulation positively impact myotubes' maturation and alignment on the different construct. Interestingly, electrical stimulation seems leading to better results as compared with mechanical stimulation. Therefore, the synergic effect of coupling both of those stimulations should be investigating in future work. As, the protocol of mechanical stimulation used in the present study was similar to those already developed for tendon tissue engineering. This in order to investigate the formation of the myotendinous junction by co-culturing both types of cells on the same sheet.

Chapter 5

Towards the reconstruction of the junctions in the musculo-skeletal system

5.1 Introduction

The challenge "Interfaces in the musculo-skeletal system", launched in 2015, aims at reconstructing the bone-tendon-muscle system, including each tissue as well as the bone/tendon interface and the tendon/muscle interface (see Figure 1 in General introduction).

Our general approach is first to reconstruct each tissue on the same type of support, i.e. electrospun PCL scaffold with specific topography or submitted to physical stresses. Then, to follow how co-cultures take place and interact with one to another and how cells can rearrange themselves to form a continuous reconstructed tissue.

This part aimed at putting together the work performed by a previous PhD student, A.Garcia Garcia et al. (2018), for bone and tendon tissue engineering , and Christopher Y. Leon-Valdivieso, post-doctoral fellow with Dr F. Bedoui at Roberval laboratory, regarding the production of electrospun scaffold with different regions, and mine (Leon-Valdivieso et al., 2020). In parallel with the work on the myotendinous, as initially forecast for my PhD, I had the opportunity to invest myself on the first evaluation of a specific electrospun scaffold designed for the osteo-tendinous junction.

Here, we will thus present the first co-cultures of tendon and muscle cells and an alternative approach based on hydrogel. Finally, the multi-region scaffold for the bone/tendon junction is evaluated in a preliminary study for the culture of mesenchymal stem cells.

5.2 Towards the myotendinous reconstruction on electrospun scaffold

5.2.1 Concept

Co-culture systems have been used to the study of multiple tissue population interactions (Dietze et al., 2002; Mikos et al., 2006) improving culture conditions (Ekwueme et al., 2016; Ostrovidov et al., 2017; Hinds et al., 2013; Kalman et al., 2015) and material studies

(Agrawal and Ray, 2001; Bitar et al., 2005; Shim et al., 2011; Ladd et al., 2011). Engineered constructs require a cell source capable of forming the structures and processes associated with in vivo tissues, in addition current tissue engineered systems rely on other numbers of conditions such as substrate/scaffold or stimulation in order to allow the successful culture of various tissues. One of the factors of favorable culture is the nutrient medium in which the cells grow. In a multi-lineage system (muscle-tendon, tendon-bone), each cell type has different specific requirement for proliferation, maintenance. The basic conditions to facilitate proliferative and differentiative stages of skeletal muscle and tendon have been extensively studied separately and the results translated across to facilitate the creation of combined engineered models. Myogenic differentiation requires muscle progenitor cells, or myoblasts (MPCs, L6, C2C12), to exit the cell cycle. In vitro, this is generally met through a shift from foetal bovine serum to horse serum, which can also be combined with a reduction in serum content to induce cellular fusion (Martin et al., 2013). Similarly, the addition of ascorbic acid, bone morphogenetic proteins (BMP-12 and 14) with transforming growth factor beta (TGF-β) and vascular endothelial growth factor (VEGF) has been shown to induce/enhance tenogenic differentiation in BMSC cells (Yin et al., 2016; Bottagisio et al., 2017). In this part, I firstly attempt to adjust the scaffold and the operating conditions to form the myotendinous junction. I plan to associate, for the tendon side, BMSC cultivated under stretching conditions and, for the muscle side, C2C12 possibly submitted to electrical stimulation. The purpose is to follow how both tissue-like structure will join and possibly form the myotendinous junction. To ensure that each tissue can develop, cells first need to be physically separated for differentiation, and then able to contact once the barrier is removed (Figure 5.1).

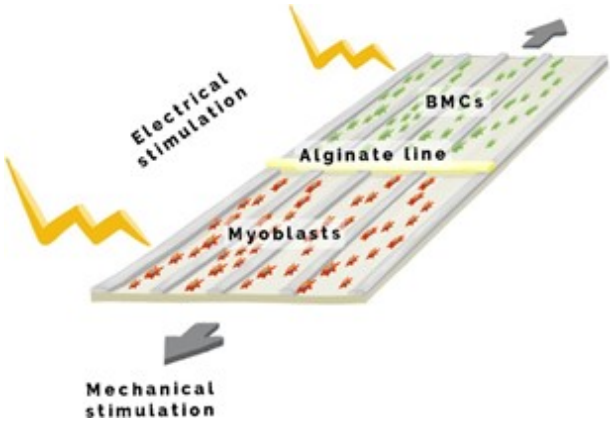

FIGURE 5.1: Concept of dedicated scaffold to study the formation of the myotendinous junction: on the right side, BMSC in green color, with differentiation promoted by cyclic mechanical stretching; on the left side, myocytes in red color, to be differentiated into myotubes with electric or mechanical stimulation and/or micropatterning.

First of all, it is necessary to compare the effects of these media combinations on each cell type to define a suitable protocol for muscle-tendon co-culture. Although these medium supplements have been shown to induce desirable characteristics in both

myogenic and tenogenic cultures, their relative effects on each other has not yet been reported. To produce a co-culture of muscle- tendon tissues, an individual medium which allows for proliferation and differentiation of both cell types must first be identified.

5.2.2 Materials issues: how to temporary separate the compartments ?

The conditions were established to favor cell differentiation towards tendon and muscle fate separately. The common culture support is electrospun PCL with a semi-aligned orientation. On the "muscle" side, micropatterning could be added to faster myotubes formation. To make the barrier between tendon and muscle cells, I propose to deposit an alginate hydrogel line in the middle of the sheet, and to remove it at a specific schedule during the cell culture process. Alginate was chosen since it has been widely used in biomedical applications and can be easily un-gelled under conditions that are not toxic for the cells, i.e. using calcium chelating agents such as citrate. Finally, alginate does not possess cell adhesive properties, thus each cell type will be kept in a confined area (Figure 5.1).

For the preliminary assays, the scaffold is first impregnated with the gelation solution ($CaCl_2$ 115 mM). Then, the viscous alginate solution (1.5%) is extruded with an ultrathin pipette cone (Figure 5.2), which explains some heterogeneity, in a direction perpendicular to the sample's length, and thus of the micropatterned PEG lines. Finally, the full support is immersed in the same gelation solution for 5 min. Bright microscopy and profilometry analysis show the presence of the alginate line, with a thickness of about 30 µm and a width of 745 µm. The PCL fibers as well as the PEG micropatterns clearly appear.

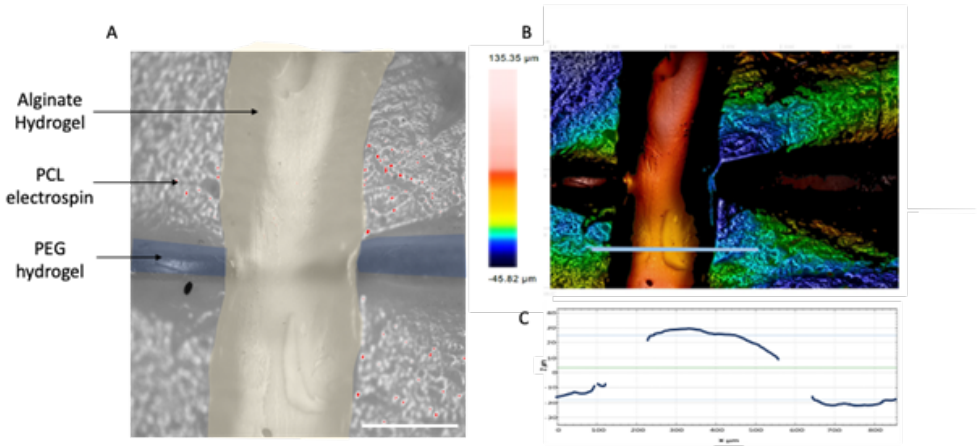

FIGURE 5.2: Alginate line deposited on the electrospun PCL scaffold. (A) bright field microscopy, scale bar 500 µm. (B) confocal profilometry analysis of topographic image colored with the depth of the material. (C) profile of the measured depths.

For future works on musculo-tendinous junction, it is suggested to deposit this alginate line by laser photolithography using the Kloé Dilase 250®apparatus (accuracy $\approx$ 5 µm) (recently acquired by the laboratory).

5.2.3 Cellular issues for the co-culture

Cell trackers to follow each population

Although muscle cells and BMSCs have a distinct morphology, it is necessary to make a clear distinction between them when they are in a common environment. For this purpose, the fluorescent markers CMFDA (5-chloromethylfluorescein diacetate) CellTracker™are used to image BMSC with a green fluorochrome and C2C12 with a red one. These fluorescent dyes are designed to freely cross cell membranes and been transformed into reaction products impermeable to cell membranes. They are retained in living cells for several generations, allowing multigenerational monitoring of cell movement. For our experiments, the cells are suspended in serum-free culture medium at a density of 106 cells. mL^{-1}, to which 5µL of solution containing the markers per mL is added. The solution is incubated for 20 minutes at 37°C. It is then centrifuged at 1500 rpm for 5 minutes. The supernatant is removed, and the pellet is re-suspended in culture medium containing serum. These last two rinsing steps are repeated three times

Co-culture conditions in multi-well plates: choice of a common culture medium

Commonly, when each cell type is cultivated separately, a different medium is used following the specificity of each cell type for an optimal cell culture. For the muscle cells, the optimal? medium is DMEM with high glucose content HG-DMEM. A change and reduction of serum content is used to enhance the fusion of the cells (from 10% FBS to 2 % HS). To induce a tenogenic differentiation of the stem cells, the ascorbic acid complement was added to the basic αEM enriched with 10 % FBS. In order to allow the successful culture of both tissues, a medium that can sustain the growth and differentiation of both cell types must first be identified. Therefore, six candidate media were evaluated for 7 days with the two cell types separately (Figure 5.3):

- M1 (HG-DMEM, 10% FBS, 1% PS),
- M2 (αEM, 10% FBS, 1% PS),
- M3 (HG-DMEM, 4 % FBS, 2 % HS, 1% PS),
- M4 (αEM, 4 % FBS, 2 % HS, 1% PS),
- M5 (50 % HG-DMEM, 50 αEM, 10% FBS, 1% PS),
- M6 (50 % HG-DMEM, 50 αEM, 4 % FBS, 2 % HS, 1% PS)

To assess the effects of each medium composition on each cell population during attachment and proliferation, each cell type was initially seeded onto a 12-well plate at 10.000 $cells.cm^{-2}$ for C2C12 myoblast and 5000 $cells.cm^{-2}$ for the BMSC. Observation of the C2C12s proliferative phase shows full confluency is reached after approximately day 3 after which cell fusion occurs (Figure 5.4). During this period, MTT quantitative measure of cell growth, of each culture condition were taken at 24h, 48h, 72h, 96h, and 5 days post seeding (Figure 5.5).

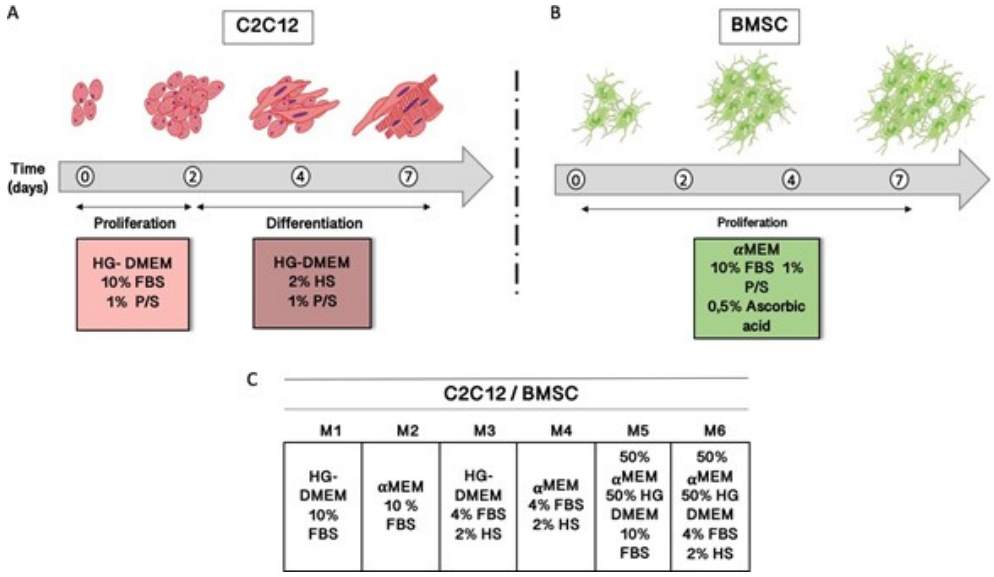

FIGURE 5.3: Experimental step of culture media selection for C2C12 (A), BMSC (B), where each cell type is cultivated separately. (C) Composition of the six different media to investigate their potentials effects on proliferation rates and morphologies on both C2C12 murine MPCs and BMSC.

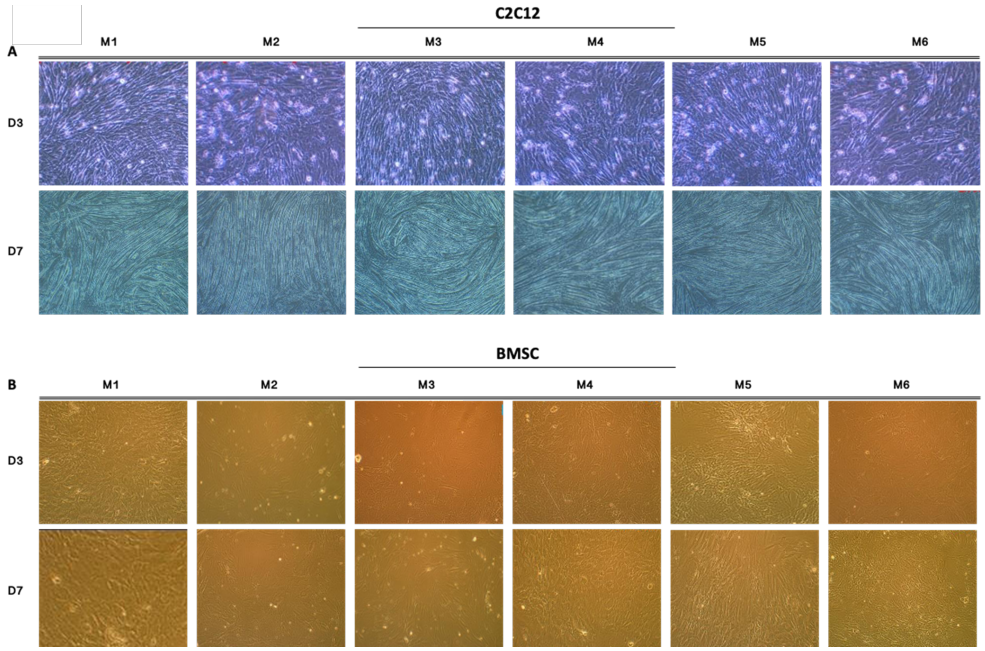

FIGURE 5.4: C2C12 and BMSC cells proliferative timeline. Culture in six different growth media (M1, M2, M3, M4, M5, M6). Pictures by phase contrast microscopy at 3 and 7 days of culture. Initial seeding at 10.000/cm2 for C2C12 Cells and 5 000.cm^{-2} for BMSC cells. The pictures are acquired at X40 magnification for the C2C12s and x100 for the BMSCs.

For C2C12, M1 (HG-DMEM, 10% FBS, 1% PS) is the classical medium, exhibiting the best proliferation as well as myotubes formation. Overall, their behavior is not affected by the other media condition, at the exception for the media M5, where cell growth is the lowest, and M2 for which myotubes appear thinner and with a reduced number.

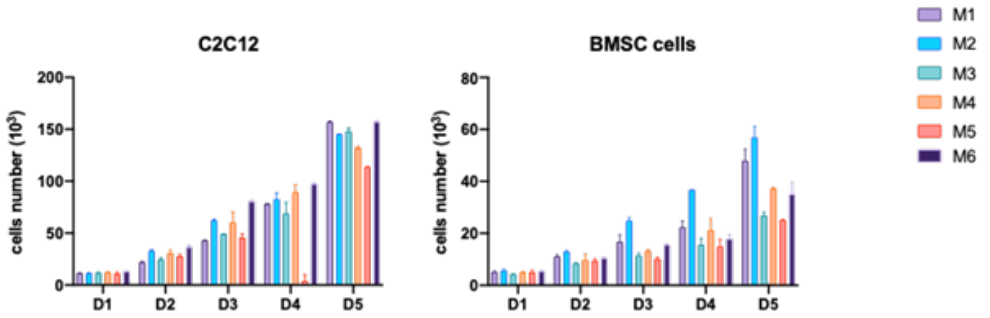

FIGURE 5.5: MTT assay illustrating (A) C2C12 and (B) BMSC cells proliferation in the six different media. The kinetics is followed every day for 5 days after seeding. M1 (HG-DMEM, 10% FBS, 1% PS), M2 (αEM, 10% FBS, 1% PS), M3 (HG-DMEM, 4 % FBS, 2 % HS, 1% PS), M4 (αEM, 4 % FBS, 2 % HS, 1% PS), M5 (50 % HG-DMEM, 50 αEM , 10% FBS, 1% PS), and M6 (50 % HG-DMEM, 50 αEM, 4 % FBS, 2 % HS, 1% PS).

For BMSC, the classical medium is M2 (αEM, 10% FBS, 1% PS). However, these cells' proliferation is much more affected by the medium composition as compared with C2C12 cells, while the morphology (stellate spread shape) is not changed with the different media. Considering the results regarding cell proliferation, M6 was chosen as co-culture media (50 % HG-DMEM, 50 αEM, 4 % FBS, 2 % HS, 1% PS). It corresponds to a 50:50 mixture of αEM and HG-DMEM supplemented with 4% FBS and 2% of HS.

Further analysis using RT-PCR or Western blot should be performed to ensure that BMSC are not engaged in a non-adapted differentiation lineage. Another interesting assay, especially in the case of sequential co-culture would be to submit one cell type to the medium conditioned by the other cell type culture.

5.2.4 Preliminary investigations using slide channels

The selected culture medium (M6: 50 % HG-DMEM, 50 αEM, 4 % FBS, 2 % HS, 1% PS) is then used as a basis for the development and optimization of the BMSC/C2C12 co-culture on the different investigated supports.

Slide channels were firstly used to perform the first co-culture assays, without the presence of a physical barrier. This choice is motivated by the ability for visualization offered by this technique. Each cell type is seeded using a dedicated port (Figure 5.6). 10.000 and 5.000 cells are injected, respectively for C2C12 and BMSCs.

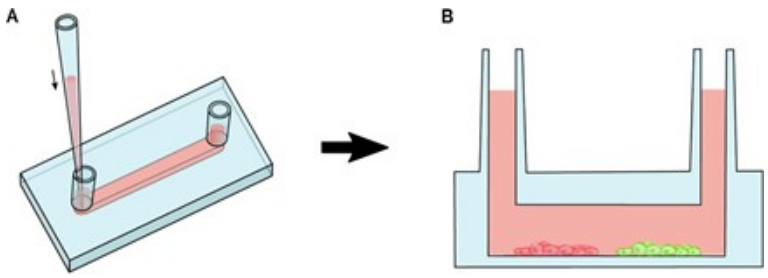

FIGURE 5.6: Schematic representation (A) of the channel slide "µ-Slide I 0.4" from Ibidi manufacturer with a growth area is of 2.5 cm^2 and a channel volume of 100µl. (B) Each cell type was seeding through the opposite reservoir.

On (Figure 5.7), one can observe that near the ports, a unique cell population is present: C2C12 colored in red and BMSC colored in green with the fluorescent dyes. They proliferate and reach almost confluence after 3 days of culture. In the middle of the channel, both populations mix (Figure 5.7), partially because the medium is not viscous and cannot ensure a well-defined border during the seeding step, resulting in a mixture of media and cells. At day 1 and day 2, the cells are still physically separated in the middle of the channel. As they proliferate, they appear to get in contact, BMSCs showing cytoplasmic extension towards C2C12 cells. After 4 days, myotubes are formed and BMSCs appear elongated and located in-between the myotubes. Epifluorescent images at day 5 show a decrease in dye fluorescence, limiting the pursuit of the experiment.

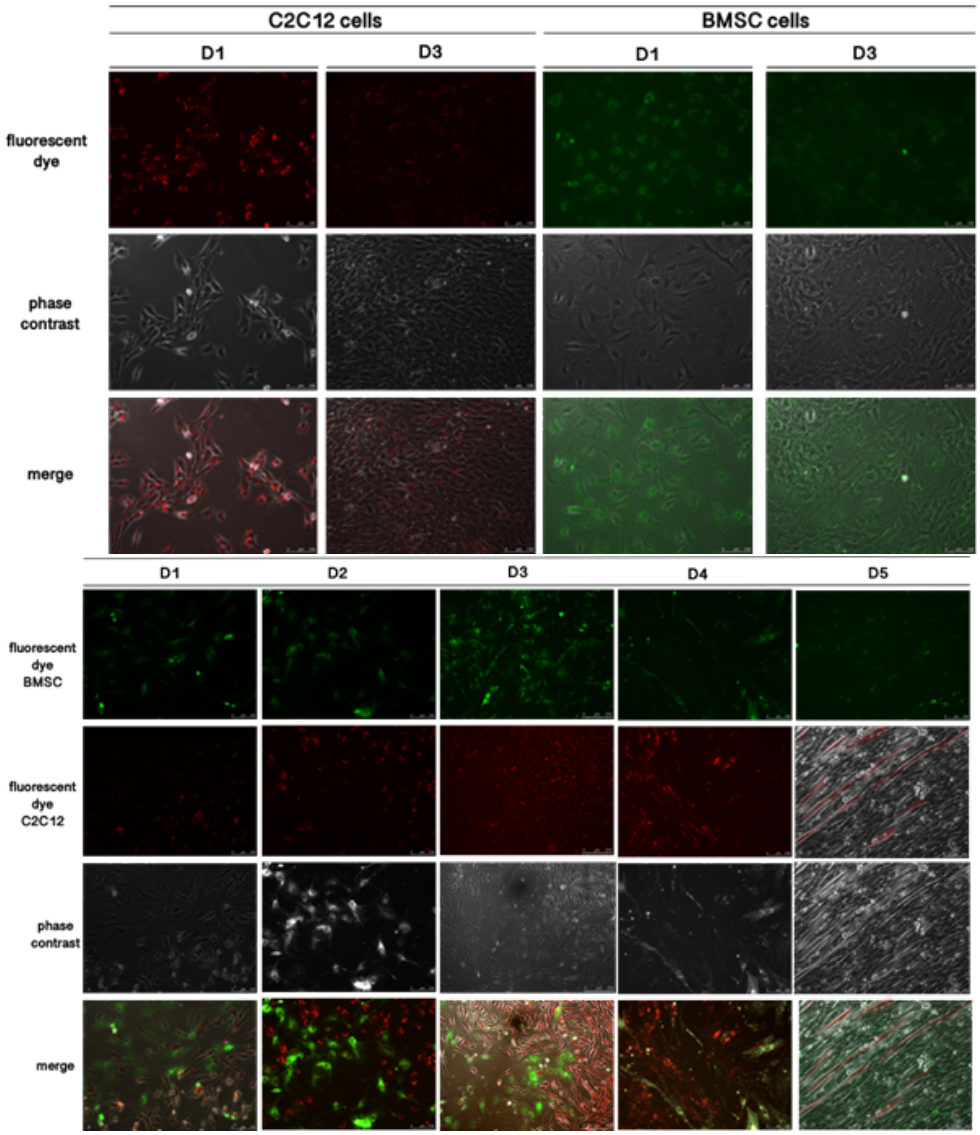

FIGURE 5.7: Epifluorescence images of C2C12 in red fluorescent dye and BMSC in green fluorescent dye, cells were culture for 5 days in a channel slide "µ-Slide I 0.4". the contact area of both cells was observed.

These preliminary results are very encouraging. Indeed, they demonstrate that the co-culture is feasible. As already stated, more analyses are requested to follow the fate of BMSC.

In future work, to improve the culture at the musculo-tendinous junction area, I propose to seed the cells in a collagen solution rather than in culture medium to contain cells locally and prevent any blending. These assays would allow to follow up each population and potential markers describing the myotendinous junction. However, cell differentiation might be limited since neither physical stimulation, nor specific biomaterials can be implemented in such a device.

5.2.5 Conclusion

In this part, I manage to demonstrate the feasibility of direct co-culture of BMSC and C2C12 cells, establishing a common culture medium and possible ways to put them in contact. For time limitation, the co-culture using the specifically tuned scaffold has not been implemented yet, but all the key components are now available and characterized. With the PCL scaffold, a specific limitation should be pointed out. Due to the non-transparent nature of the polymer, it is not possible to follow with time lapse the cell behavior and the specific area of the junction. Therefore, we investigate hereafter another type of biomaterial to avoid this limitation.

5.3 Co-culture in hydrogels for the musculo-tendinous junction: a preliminary study

5.3.1 Concept

With the aim of visualizing in real time the co-culture, we propose to use hydrogels as culture support. In the bibliography study (chapter 1), hydrogels are indeed listed among the potential materials to cultivate both tendon and muscle cells (Chattopadhyay et al., 2016; Ahmed et al., 2010*b*; Pollot et al., 2018). I suggest forming a core shell alginate tube with a cross section of max. 1mm in diameter to allow the exchange of nutrient to avoid the formation of necrotic core within the hydrogel. The extrusion process should allow to switch for one cell type to another in a single procedure. In the end, leading to a tube containing on one half C2C12 and on the other half BMSCs (Figure 5.8) (Merceron et al., 2015*a*; Ford et al., 2006; Hunt et al., 2009; Yang et al., 2018; Cui et al., 2019).

5.3.2 First attempts with microfluidic device to produce the fiber

We manufactured in the lab microfluidic devices with 3 entry points from Eric Leclerc's design, one dedicated to cell seeding, and two for alginate solution in view of achieving a flow focusing system with cells entrapped in the alginate gel. Three different designs are proposed (Figure 25). Only design A was kept, as the size of the other channels could not support the passage of too viscous solution.

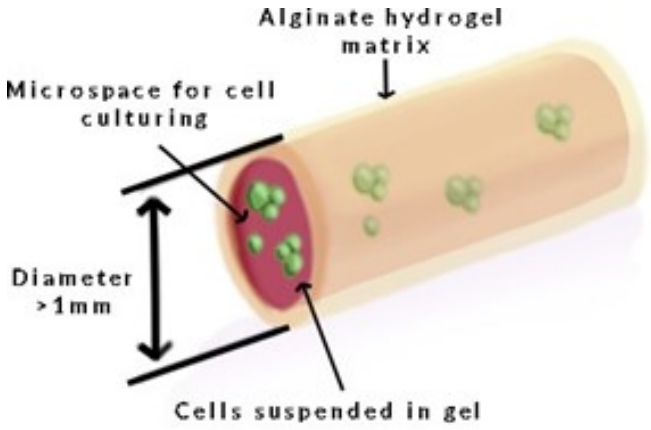

FIGURE 5.8: Schematic representation of core shell structure expected from the following microchip and coaxial experimentation.

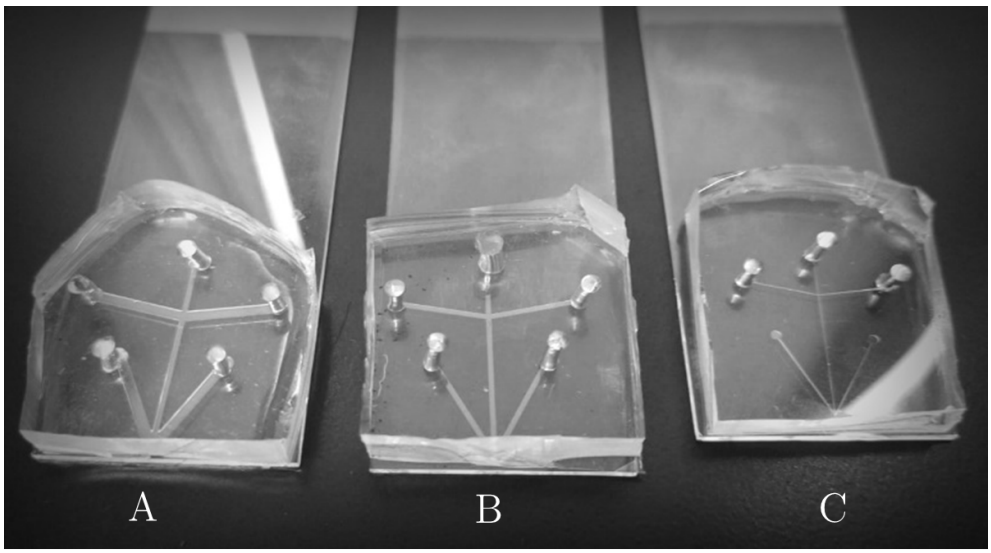

FIGURE 5.9: photography of the 3 design of microchips with (A) a central channel of 500µm and side channels of 1 mm, (B) all channels have a width of 500µm (C) has a width of 100µm. All three designs have angles of 80°upwards and 30°towards the outlet.

During the production process, cells were mixed with a 2% gelatin solution before being injected in the middle port at a flow rate of 0,5 mL.min^{-1}. Alginate 1% solution was introduced by the two-external port at a flow of 0,2 mL.min^{-1}. Unfortunately, it appears that the solutions are not able to mix. Indeed, the two surrounding channels formed by alginate do not manage to merge, and thus the tube cannot be sealed. Therefore, the result obtain is that cells are escaping in the surrounding medium (Figure 5.10).

To optimize this type of system, it could be recommended to mix cells directly with alginate, as already performed by Zhao et al. (2018) and Jiang et al. (2017), however, it was not our choice. We hypothesized that the core of the fiber should not contain alginate to offer the cells an environment where they can freely proliferate and differentiate. Depending on this concentration, alginate may in opposite limit cells proliferation and not promote myotubes formation. Another option would be to extrude the cell-containing polymer with a co-axial needle.

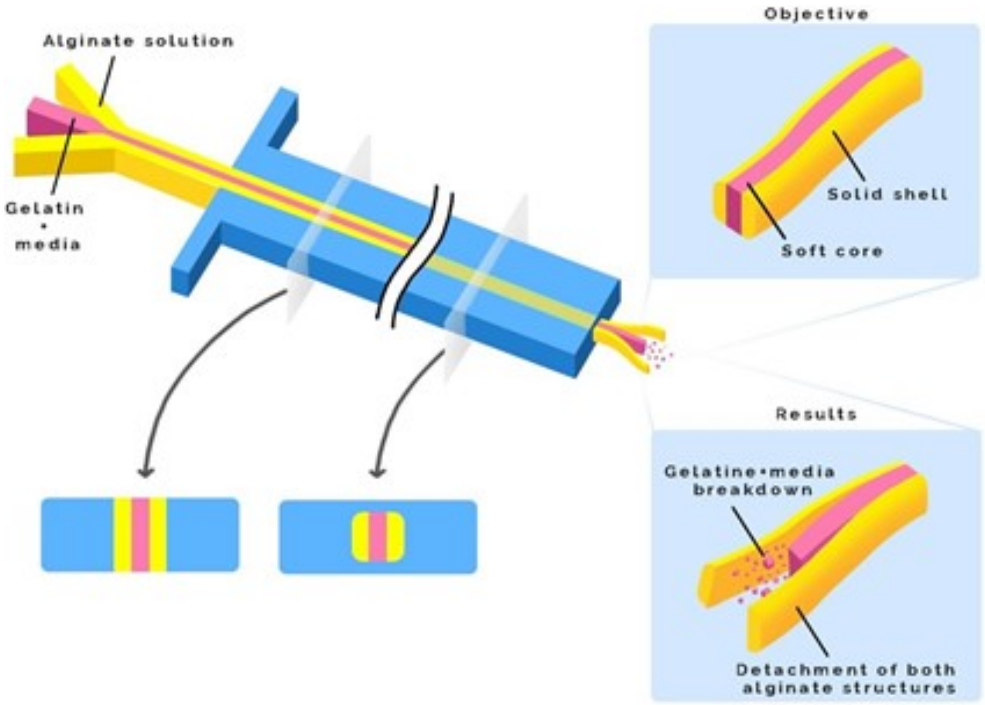

FIGURE 5.10: Schematic representation of the core shell of alginate and gelatin process from microfluidic device.

5.3.3 Second attempt with the co-axial needle

As already explained, the target for future works is to manufacture an alginate fiber with a core of cells, which was not possible in the present study. Thus, we decided to turn back to more classical option using a co-axial needle (Figure 5.11).

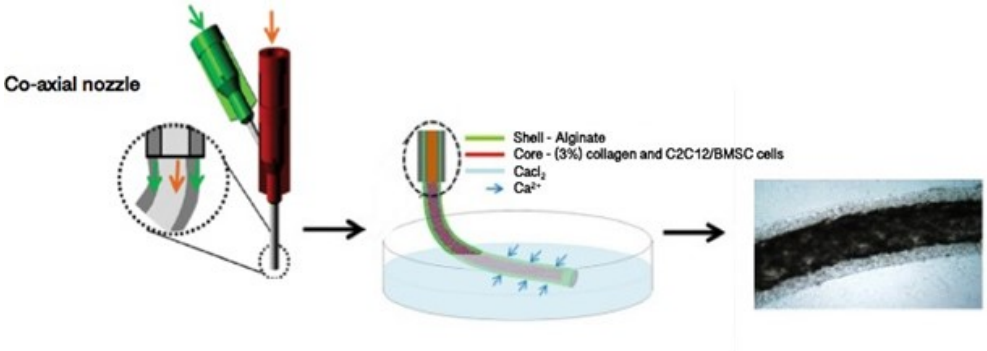

FIGURE 5.11: The encapsulation was performed with a home-made system based on a coaxial nozzle system, 1,5% alginate solution (in green nozzle) and 3% collagen containing cells (red nozzle) was rapidly extruded through a 24 G nozzle and the tube fell into a gelation bath (NaCl 154 mM, HEPES 10 mM and CaCl2 115 mM, pH 7.4). tubes produced were allowed to settle for 15 min in the gelation bath to ensure gel formation.

Production of alginate fiber with gelatin core

First, I attempt to implement the same parameters as those described above regarding the solutions, i.e. cells mixed with gelatin injected in the central needle, and alginate solution in the surrounding needle (Figure 5.12) with a flow rate of 0.8 ml.min^{-1} for the alginate and 0.65 ml.min^{-1} for the gelatin with the cells.

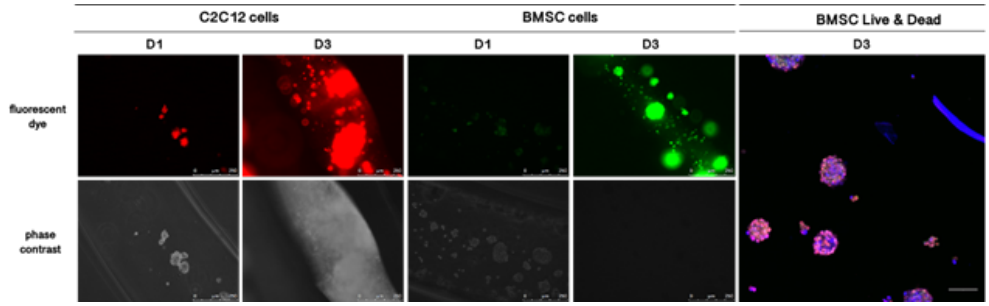

FIGURE 5.12: core shell hydrogel obtained from co-axial nozzle device with alginate 1% and gelatin 2%, C2C12 stained with red fluorescent dye and BMSC stained with green fluorescent dye for 3 days, follow by a live and dead test on BMSC at day 3.

At day 1, small aggregates of cells, either C2C12 or BMSCs, are formed in the gelatin core. They grow in number and in size as observed at day 3. The advantage of this culture method is the capacity to monitor identification by fluorescent dyes and proliferation over time, under fluorescence microscopy. However, we also observe that the resulting spheroids are not viable at day 3. Since gelatin did not polymerize, cells could not be anchored to the biomaterial resulting in the formation of aggregates. In the literature, successful culture of these cells appears to be achieved with high gelatin concentration or mostly with the presence of collagen and/or fibrin (Bansai et al., 2019; Ahn et al., 2015).

On a logistic point of view, the handling of the resulting fibers is difficult after 5 days of culture, the mechanical properties of the cell seeded scaffold being very weak.

Feasibility study with collagen

We thus implement the extrusion of cells within a 3% bovine collagen solution, keeping the 1.5% alginate solution in the surrounding needle. The cells do not aggregate in this configuration and still manage to proliferate, as shown on Figure 5.13. Moreover, Live/Dead assay demonstrate a very good cell viability at day 3. Mechanical tests have not been performed, but the fibers did appear more handleable.

These results are very encouraging. Co-culture assays can be envisaged, in static and further under external stimulation.

5.3.4 Conclusion

This new approach is completely different from the way followed initially in this PhD and even in the whole research program. Nevertheless, it should be continued, to guide us towards a final optimized biomaterial design. Indeed, as already stated, the culture in hydrogels allows to perform time lapse follow-up of the cells' distribution, proliferation

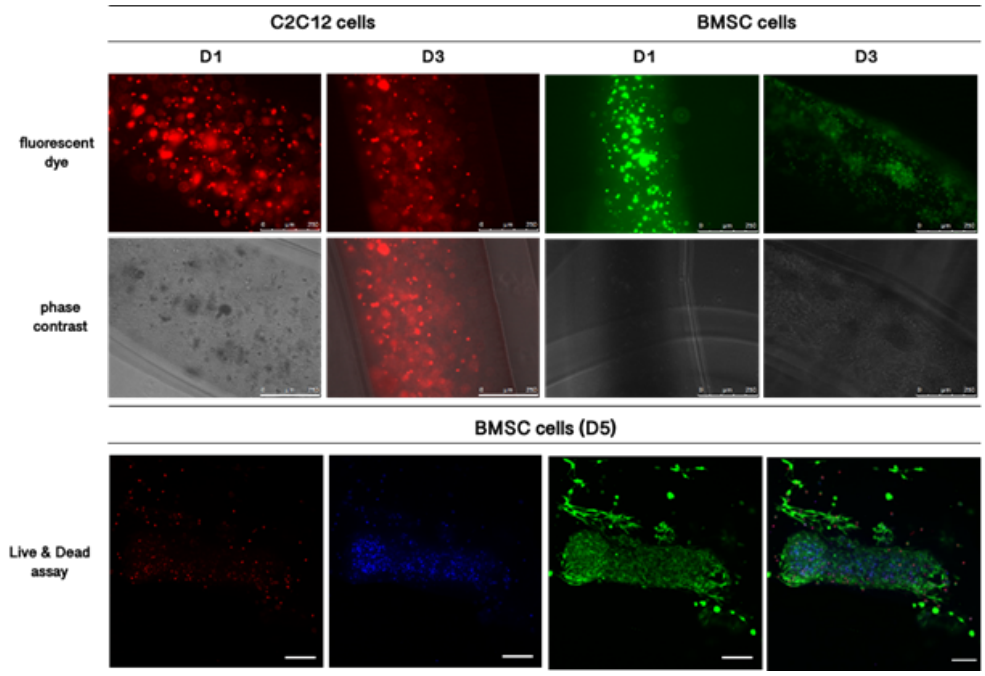

FIGURE 5.13: Core shell hydrogel obtained from co-axial nozzle device with alginate 1,5% and 3% collagen I, C2C12 stained with red fluorescent dye and BMSC stained with green fluorescent dye for 3 days, follow by a live and dead test on BMSC at day 3.

and differentiation, and moreover to localize the site of potential formation of the junction. The absence of visualization is really a drawback using the electrospun PCL scaffold. We suggest implementing this "culture in fiber" to identify the junction and define potential markers of interest. Once this established, a more complex and physically model could be advantageously investigated.

5.4 Behavior of the multi-region PCL based scaffold for the osteo-tendinous junction

5.4.1 Concept

To generate an osteo-tendinous junction, our concept is to produce a single PCL scaffold with areas whose specific topography should promote specialized cell differentiation according to the culture location. In the previous PhD work of A. Garcia Garcia, it was demonstrated that a honeycomb structure functionalized with hydroxyapatite nanoparticles guide C3H10 and BMSCs cells towards osteogenesis. In vivo, the osteo-tendinous junction can also be characterized by a gradient in term of extracellular matrix.

5.4.2 Material design and methods

Consequently, a biomimetic scaffold was designed and produced by Yusef Leon-Valdivieso during his postdoctoral stay (Figure 5.14). This multiscale structure is made of PCL only, with no hydroxyapatite on the honeycomb area. One can observe a gradient in the surface topography, starting from large honeycombs (800 µm) to small ones (100 µm), adjacent to an area of random fibers. Thus, I conduct the biological tests on the biohybrid construct.

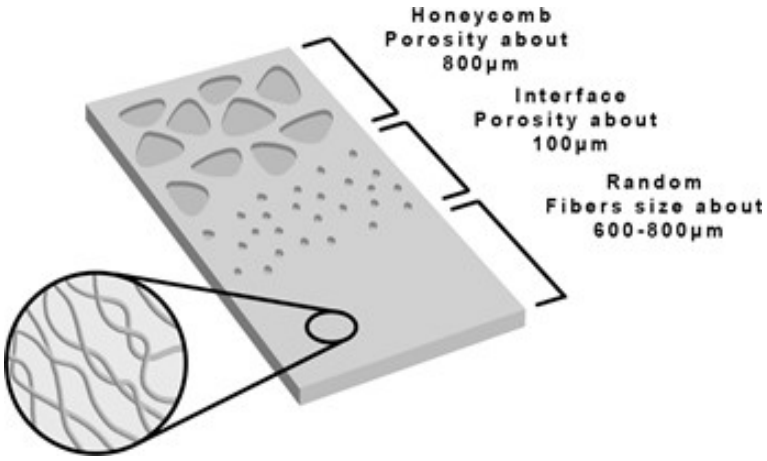

FIGURE 5.14: schematic representation of the biohybrid scaffold for the enthesis junction (bone-tendon junction) containing 3 parts, honeycomb topography with a porosity of 800µm, an interface area with a porosity about 100µm and a random fibers structure.

5.4.3 Preliminary culture of BMSC under static conditions

Rat BMSCs are seeded on the multiscale PCL sheet at a density of 105 cells.cm^{-2} and cultivated for 5 days in classical αMEM medium supplemented with 10% FBS in the absence of any differentiation factor. After 5 days, cell viability was excellent on any type of surface, as shown by the Live/Dead assay presented on Figure 31. On the honeycomb surface, cells first colonized the bottom of the structures, and then grow on the walls. Cell colonization is not affected by the material topography.

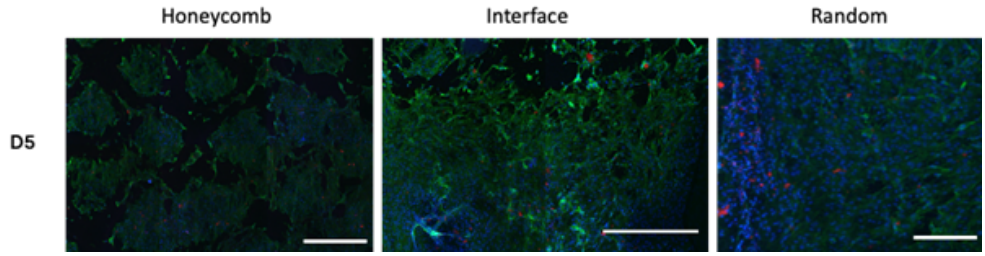

FIGURE 5.15: viability test performed by a Live/dead assay on each part of the biohybrid scaffold with BMSC cells at day 5. (scale bar: 500 µm)

Cells were then stained for alkaline phosphatase and calcium (alizarin red), as markers of osteogenic differentiation and can be observed under bright field microscopy (Figure 5.16). Tenomodulin, as marker for tenogenic differentiation, is observed by immunostaining under confocal microscope. Pictures are taken of the three different areas of the

sheets, as for the Live/Dead assay. After 7 days, one can observe that some cells express these osteogenic features while other are strained for tenomodulin, in the same area. After 14 days, cell proliferation still takes place as well as cell differentiation, since the colors appear qualitatively more pronounced. There is thus no effect of the surface topography on BMSCs differentiation. This result is not really surprising for several reasons: first, honeycombs produced here are much larger (4 times) than those previously shown to favor osteoblast differentiation (Garcia Garcia et al., 2018). In addition, there was no hydroxyapatite functionalization for the "bone side". This clearly demonstrates that such NP are requested to promote osteogenic differentiation. On the "tendon" side, as no mechanical stimulation is performed, cells do not align.

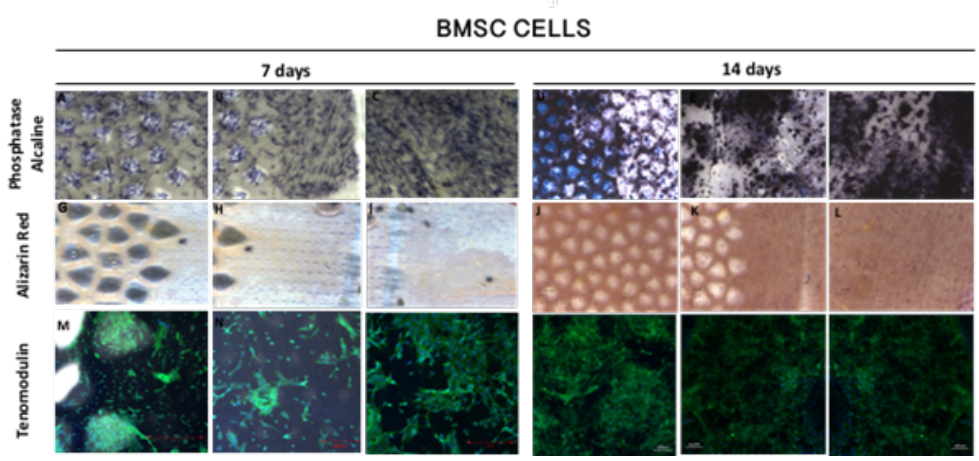

FIGURE 5.16: BMSC cells were cultured for 7 days to 14 days on the biohybrid construct. Phosphatase alkaline, alizarin red and tenomodulin staining were performed at day 7 and day 14.

5.4.4 Preliminary culture of BMSC under dynamic conditions

I thus performed the next preliminary investigations using the T6CellScale bioreactor, to submit the biohybrid construct to the same mechanical stretching described in chapter 3, i.e 5% strain applied during 1h with a 1Hz frequency, followed by 11h rest. After 7 days, cells cover the whole surface. I observe color staining regarding osteoinduction similar to that of the 14 days experiment under static conditions. However, tenomodulin expression was not found under confocal observation, in any of the areas, even in the random part where it is expected to be located (Figure 5.17).

The increase of osteoinduction is in agreement with literature analysis, as already performed in our group (Baudequin et al., 2018). The apparent absence of tenocyte like cells is more surprising, compared to our previous results. It should be further analyzed, repeating the experiments and following the expression of type I collagen that is normally synthesized.

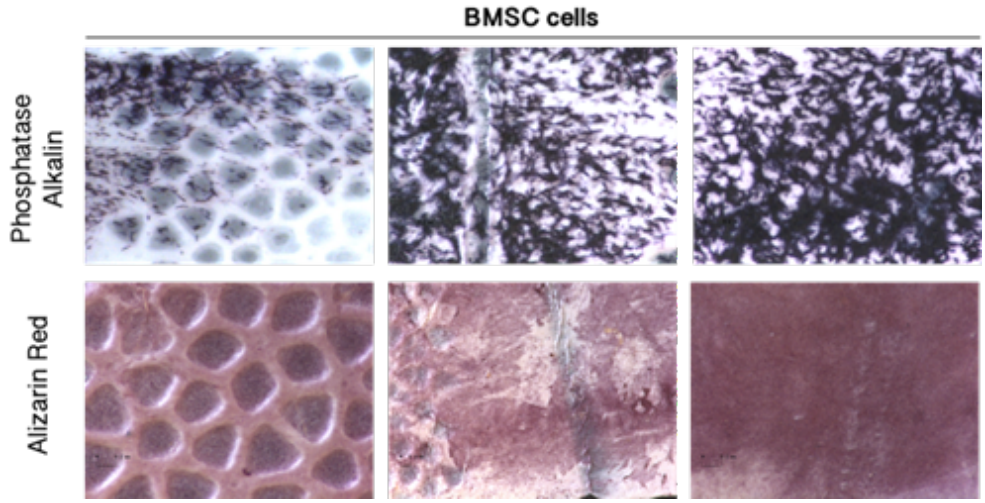

FIGURE 5.17: BMSC cells were cultured on the biohybrid construct for 5 days under mechanical stimulation. Phosphatase alkaline, alizarin red staining was performed at day 7.

5.4.5 Conclusion

The aim was to demonstrate that a material with a gradient in topography can be produced by electrospinning and seeded with cells. Some choices have been made to alleviate the production process, as compared to the honeycomb scaffolds produced in collaboration with the team of G. Schlatter at ICPEES by A. Garcia Garcia. Indeed, this process requests to alternate electrospinning of PCL and electrospraying of hydroxyapatite nanoparticles. Here, I demonstrate that the presence of large honeycomb alone is probably not efficient to drive cells towards clear osteogenic differentiation, since cells expressing tenomodulin are present in the same area. The addition of stretching favor osteogenic differentiation but not in a specific area and tendon differentiation seems to be hindered.

Starting from this promising approach, we suggest to go back to the production of a more adapted scaffold, still based on a PCL sheet, with the following requirements: one area with honeycombs with diameter around 200 µm, one interface potentially with smaller honeycombs but also with a decreasing gradient in hydroxyapatite nanoparticles cover, and one area with aligned fibers with a diameter around 500 nm. This biohybrid scaffold could thus be operated in the bioreactor with mechanical stimulation, to manage to produce a biomimetic osteo-tendinous junction.

Chapter 6

Conclusion and perspectives

In this thesis project I particularly focused on the development of a 2.5D tissue engineered skeletal muscle and a co-culture platform to study the establishment of the myotendinous junction between the muscle and the tendon. My approach consisted on the development of a construct, able to take into account the biological and mechanical properties of each tissue by tissue engineering. To carry out this objective, the versatility of electrospinning appeared to be appealing to achieve the continuum between each subsystem. Rather than directly focusing on the interface between reconstructed tissues (muscle, tendon, and bone), I wanted to ensure that the future built-up continuum was achievable using electrospinning methods adapted and evaluated for each type of tissue. Moreover, for clinical perspectives, I also postulated that cell differentiation towards different lineages (here muscle and tendon) should be obtained without any differentiation factor (that are specific for each tissue), playing only on cell-materials interactions and mechano-transduction.

First, the development and characterization of a material for muscle tissue regeneration was achieved using a combination of semi-oriented PCL electrospun sheet and different design of PEG hydrogel micropatterning. This configuration was defined on purpose to create an environment that supports biological activity based on the structure-function premise to finally accentuate the cell differentiation. The proof of concept of this new scaffold was performed with the murine myoblasts cell line C2C12. I demonstrated the viability, the proliferation of cells in the 2.5D bioconstruct. Specific immunostaining of the myosin heavy chain protein (MyCH) showed an improvement of the differentiation of the myoblast into myotubes in the new construct, as well as a better alignment of this newly formed myotubes. Then, the potential effect of cyclic stretching or electrical stimulation on the cells construct was investigated. So far, the results obtained with both stimulations are promising with C2C12. A greater differentiation and alignment of the myotubes under the electrical stimulation was found as compared with cyclic stretching. Still, it is of interest to continue with mechanical stimulation as well, since Alejandro Garcia Garcia's, a previous PhD student working on the tendinous part, has given promising results with an alignment of the BMSC on a random scaffolding and the production of an extracellular matrix. Finally, during this PhD, I had the opportunity to explore several ways to investigate the development of the different junctions (see Chapter 5). For the myotendinous, I firstly developed a common medium to allow the culture of both C2C12

and BMSC cell lines: a combination of 50% high glucose DMEM (HG-DMEM) and 50% αMEM supplemented with 4% FBS, and 2% horse serum. This medium has shown to promote the proliferation of myoblast and tendon cell like populations, while allowing C2C12 differentiation. The primary approach to investigate the development of the junction was to perform the co-culture on the electrospinning construct. However, as the electrospun scaffold is an opaque material, it was difficult to estimate the optimal culture time allowing cells to grow, differentiate and subsequently reach each other. Therefore, in parallel, I worked on a core shell hydrogel of alginate and collagen by way of co-axial nozzle technique. The result obtained is promising, as I demonstrated the viability and proliferation of each cells type. These observations suggest that a full tissue engineered musculotendinous junction is possible. As demonstrated in previous studies (Garvin et al., 2003; Sawadkar et al., 2013), tendon as well as skeletal muscle formation in a collagen hydrogel is possible and culture of such a model in the same medium is achievable. For the enthesis junction, located between the tendon and the bone, we have pursued the work of a post-doctoral, Leon-Valdivieso, member of Roverval laboratory and supervised by Dr F. Bedoui. He was at the initiative of the design of the scaffold for the future biohybrid construct. Afterwards, previous works investigated first cellular assay for tendon tissue development. My first observation was that specific topography coupled with mechanical stimulation (passive cyclic stretching) was not able to differentiate the stem cells into clear lineage as tenogenic as well as osteogenic markers were expressed. Thus, following to these works on bone-tendon cells, the biohybrid models needed to be optimized, mainly concerning the size and structure of the honeycomb. Moreover, the addition of a gradient of hydroxyapatite could be of particular interest as present in the in vivo tissues.

Prior to the creation of a skeletal muscle and tendon co-culture platform, both models need to be optimised according to cellular characteristics and adjustments to best enhance the flexibility of the system. The skeletal muscle model requires a broad and precise analysis to determine and measure differentiation. However, measuring morphological characteristics of myotubes is a laborious and time-consuming task that requires a large number of images generated mainly by confocal microscopy. Alternatives, protein analysis or gene expression through qRT-PCR, following the timeline of expression of markers such as myogenin and MyoD1, MRF4 could be performed (Player et al. 2014; Smith et al. 2012; Mudera et al. 2010). Additionally, protein markers could be used to indicate the progression of the skeletal muscle model (such as sarcomeric protein or calcium signaling) (Chemello et al., 2011).

To improve the in vitro follow-up of the skeletal muscle built up, we suggest, following the literature, to use C2C12s cells labeled with a green fluorescent protein (GFP) control virus allowing the real-time observation of fusion (Millay et al., 2013). Anti-Myogenin antibody could also be employed, as it only marks nuclei in fused cells. This would allow a non-invasive assessment of fusion but would still require a lengthy quantitative determination. Finally, characterization of the muscle fiber contraction is the only absolute

assessment of skeletal muscle progression. Therefore, the measurement of the contractibility of the construct should be assess. Similarly, for tendon model, no specific marker of maturation exists, hence the use of multiple markers is necessary to create a timeline of tenogenic differentiation progress of the BMSC.

The work presented here, has enabled to take a new step towards the realization of the myotendinous junction, opening many doors to optimization and further studies. The biomaterials developed enables the use of external stimulation that, given the ability to differentiate and align cells, could meet multiple applications, for MTJ but also for the entire musculoskeletal system reconstruction. In the future, it could represent a reliable in vitro model to study the impact of different stimulations with protocols, closer to those used in human therapy. Moreover, it could be used as a physiological or pathological model to study how conjoint tissue are form and evolve, but also help understand more specific aspect such as the effect of sport, injury, recovery, aging on a global system.

Glossary

AuNPs Gold Nanoparticles.

bHLH Basic Helix–Loop–Helix.
BMBi Biomechanics & Bioengineering.
BSA Bovine Serum Albumin.

C2MUST Characterization and personalized Modeling of the Musculo-Skeletal System.
CBB Cells, Biomaterials, Bioreactors.

DC Dichloromethane.
DM Differentiate Media.
DMF N,N-dimethylformamide DNA: DeoxyriboNucleic Acid.

E Young Modulus.
ECM Extracellular Matrix.
EPS Electric Pulse Stimulation.
ERG1 Transcription factor Early Growth Response factor 1.

FACIT Fibril Associated Collagens with Interrupted Triple helices.
FAK Focal Adhesion Kinase.
FBS etal Bovine Serum.
FDA ood and Drug Administration .
FGF Fibroblast Growth Factor.

GM Growth Media.

HDMEM Dulbecco's Modified Eagle's Medium high glucose.
HGF Hepatocyte Growth Factor.
HS Horse serum.

IGF-1 Insulin-like Growth Factor 1.

Kon Kontiki.

MBMP Bone Morphogenetic Proteins.
MHC Myosin Heavy Chain.
Mkx Mohawk.
MPC Muscle Precursor Cell.
MRFs Myogenic Regulatory Factor.
MSCs Mesenchymal Stem Cell.
MTJ Myotendinous Junction.

NGF Nerve Growth Factor.
NMJ NeuroMuscular Junction.

Pa Pascal.
Pani Polyaniline.
PAX Paired box Protein.
PBS Phosphate Buffered Saline.
PCL Poly-ε-Caprolacton.
PCL-PEG Poly-ε-caprolactone with a patterning of Polyethylene Glycol hydrogel.
PDMS Polydimethylsiloxane.
PEG Polyethylene Glycol.
PFA Paraformaldehyd.
PLGA Poly-Lactic-co-Glycolic Acid.
PS Penicillin-Streptomycin.
PU polyurethanes.
PVDF Polyfluorene de vinylidene RNA: Ribonucleic acid.

Robo Roundabout.
RTq PCR Reverse transcription quantitative polymerase chain reaction.

Sa Arithmetical mean height.
SCs Derived satellite cells.
SCX Scleraxis.
SEM Scanning electron microscopy.
Shh Sonic Hedgehog.
Sk-MSCs Skeletal muscle-derived multipotent stem cells.
Sku: Kurtosis.
SLRPs Small Leucine-Rich Proteoglycans.
SOT Self-Organized Tendon constructs.
Sp Height parameters peaks.
Sq Root mean square height.

Ssk Skewness.
Sv Height parameters Valleys.
Sz aximum height.

TE Tissue engineering.
TEC Tissue engineering construct .
TGF-b Transforming Growth Factor Beta.
Tnmd Tenomodulin.
TSPC Tendon Stem/Progenitor Cells.

VEGF Vascular Endothelial Growth Factor.
VL Ventro-Later.
Vn Neuroreguling-like ligan.

Bibliography

Abarzua, P., Padilla, C., Ramos, A., Isaacs, M., Ramos-Grez, J., Olguín, H. and Valenzuela, L. (2017), 'Improving myoblast differentiation on electrospun poly(ε-caprolactone) scaffolds', *Journal of biomedical materials research. Part A* **105**.

Adam, R. M., Roth, J. A., Cheng, H.-L., Rice, D. C., Khoury, J., Bauer, S. B., Peters, C. A. and Freeman, M. R. (2003), 'Signaling through PI3K/Akt mediates stretch and PDGF-BB-dependent DNA synthesis in bladder smooth muscle cells', *J Urol* **169**(6), 2388–2393.

Agrawal, C. M. and Ray, R. B. (2001), 'Biodegradable polymeric scaffolds for musculoskeletal tissue engineering', *Journal of Biomedical Materials Research* **55**(2), 141–150.

Agrogiannis, G. D., Sifakis, S., Patsouris, E. S. and Konstantinidou, A. E. (2014), 'Insulin-like growth factors in embryonic and fetal growth and skeletal development (Review)', *Molecular Medicine Reports* **10**(2), 579–584.
URL: *https://www.ncbi.nlm.nih.gov/pmc/articles/PMC4094767/*

Ahadian, S., Ramón-Azcón, J., Ostrovidov, S., Camci-Unal, G., Hosseini, V., Kaji, H., Ino, K., Shiku, H., Khademhosseini, A. and Matsue, T. (2012), 'Interdigitated array of Pt electrodes for electrical stimulation and engineering of aligned muscle tissue', *Lab on a Chip* **12**(18), 3491–3503. Publisher: The Royal Society of Chemistry.
URL: *https://pubs.rsc.org/en/content/articlelanding/2012/lc/c2lc40479f*

Ahmed, W. W., Wolfram, T., Goldyn, A. M., Bruellhoff, K., Aragu, B., Kemkemer, R., Spatz, J. P., Saif, T. A. and Mo, M. (2010*a*), 'Biomaterials Myoblast morphology and organization on biochemically micro-patterned hydrogel coatings under cyclic mechanical strain', **31**, 250–258.

Ahmed, W. W., Wolfram, T., Goldyn, A. M., Bruellhoff, K., Aragu, B., Kemkemer, R., Spatz, J. P., Saif, T. A. and Mo, M. (2010*b*), 'Biomaterials Myoblast morphology and organization on biochemically micro-patterned hydrogel coatings under cyclic mechanical strain', **31**, 250–258.

Ahn, S. Y., Mun, C. H. and Lee, S. H. (2015), 'Microfluidic spinning of fibrous alginate carrier having highly enhanced drug loading capability and delayed release profile', *RSC Advances* **5**(20), 15172–15181.
URL: *http://xlink.rsc.org/?DOI=C4RA11438H*

Alberton, P., Popov, C., Prägert, M., Kohler, J., Shukunami, C., Schieker, M. and Docheva, D. (2011), 'Conversion of Human Bone Marrow-Derived Mesenchymal Stem Cells into Tendon Progenitor Cells by Ectopic Expression of Scleraxis', *Stem Cells and Development* **21**(6), 846–858. Publisher: Mary Ann Liebert, Inc., publishers.
URL: *https://www.liebertpub.com/doi/abs/10.1089/scd.2011.0150*

Alberts, B., Bray, D., Lewis, J., Raff, M., Roberts, K. and Watson, J. (2014), Genesis, modulation, and regeneration of skeletal muscle, *in* 'Molecular Biology of the Cell (Sixth Edition)', Garland.

Altomare, L., Gadegaard, N., Visai, L., Tanzi, M. C. and Farè, S. (2010), 'Biodegradable microgrooved polymeric surfaces obtained by photolithography for skeletal muscle cell orientation and myotube development', *Acta Biomaterialia* **6**(6), 1948–1957.
URL: *http://dx.doi.org/10.1016/j.actbio.2009.12.040*

Ansari, S., Chen, C., Xu, X., Annabi, N., Zadeh, H. H., Wu, B. M., Khademhosseini, A., Shi, S. and Moshaverinia, A. (2016), 'Muscle Tissue Engineering Using Gingival Mesenchymal Stem Cells Encapsulated in Alginate Hydrogels Containing Multiple Growth Factors', *Ann Biomed Eng* **44**(6), 1908–1920.

Aubin, H., Nichol, J. W., Hutson, C. B., Bae, H., Sieminski, A. L., Cropek, D. M., Akhyari, P. and Khademhosseini, A. (2010), 'Directed 3D cell alignment and elongation in microengineered hydrogels', *Biomaterials* **31**(27), 6941–6951.
URL: *http://dx.doi.org/10.1016/j.biomaterials.2010.05.056*

Aviss, K. J., Gough, J. E. and Downes, S. (2010*a*), 'Aligned electrospun polymer fibres for skeletal muscle regeneration', *European Cells and Materials* **19**, 193–204.

Aviss, K. J., Gough, J. E. and Downes, S. (2010*b*), 'Aligned electrospun polymer fibres for skeletal muscle regeneration', *European Cells and Materials* **19**, 193–204.

Bachmann, C.-P. (2016), Characterization of Excitation-contraction-coupling in muscles from patients with X-linked myotubular myopathy, PhD thesis, University of Basel.

Bajaj, P., Jr, R., Millet, L. and Wei, C. (2011*a*), 'Integrative Biology Patterning the di ff erentiation of C2C12 skeletal myoblasts w', **3**(9).

Bajaj, P., Jr, R., Millet, L. and Wei, C. (2011*b*), 'Integrative Biology Patterning the di ff erentiation of C2C12 skeletal myoblasts w', **3**(9).

Bajaj, P., Rivera, J. A., Marchwiany, D., Solovyeva, V. and Bashir, R. (2014), 'Graphene-Based Patterning and Differentiation of C2C12 Myoblasts', pp. 995–1000.

Bandyopadhyay, B., Shah, V., Soram, M., Viswanathan, C. and Ghosh, D. (2013), 'In Vitro and In Vivo Evaluation of L-lactide/ε-caprolactone copolymer Scaffold to support Myoblast Growth and Differentiation.', *Biotechnology progress* .

Baniasadi, H., Mashayekhan, S., Fadaoddini, S. and Haghirsharifzamini, Y. (2016), 'Design, fabrication and characterization of oxidized alginate-gelatin hydrogels for muscle tissue engineering applications', *Journal of Biomaterials Applications* **31**(1), 152–161.
URL: *https://doi.org/10.1177/0885328216634057*

Bansai, S., Morikura, T., Onoe, H. and Miyata, S. (2019), 'Effect of Cyclic Stretch on Tissue Maturation in Myoblast-Laden Hydrogel Fibers', *Micromachines* **10**(6), 399.
URL: *https://www.mdpi.com/2072-666X/10/6/399*

Bareja, A. and Billin, A. N. (2013), 'Satellite cell therapy – from mice to men', *Skeletal Muscle* **3**, 2.
URL: *https://www.ncbi.nlm.nih.gov/pmc/articles/PMC3579761/*

Bark, T. H., McNurlan, M. A., Lang, C. H. and Garlick, P. J. (1998), 'Increased protein synthesis after acute IGF-I or insulin infusion is localized to muscle in mice', *American Journal of Physiology-Endocrinology and Metabolism* **275**(1), E118–E123. Publisher: American Physiological Society.
URL: *https://journals.physiology.org/doi/full/10.1152/ajpendo.1998.275.1.e118*

Barton, E. R. (2006), 'The ABCs of IGF-I isoforms: impact on muscle hypertrophy and implications for repair', *Applied Physiology, Nutrition, and Metabolism = Physiologie Appliquee, Nutrition Et Metabolisme* **31**(6), 791–797.

Baudequin, T., Legallais, C. and Bedoui, F. (2018), 'In vitro bone cell response to tensile mechanical solicitations: Is there an optimal protocol?', *Biotechnology Journal* **14**(1), 1800358.
URL: *https://doi.org/10.1002/biot.201800358*

Beldjilali-Labro, M., Garcia Garcia, A., Farhat, F., Bedoui, F., Grosset, J.-F., Dufresne, M. and Legallais, C. (2018*a*), 'Biomaterials in Tendon and Skeletal Muscle Tissue Engineering: Current Trends and Challenges', *Materials (Basel, Switzerland)* **11**(7).

Beldjilali-Labro, M., Garcia Garcia, A., Farhat, F., Bedoui, F., Grosset, J.-F., Dufresne, M. and Legallais, C. (2018*b*), 'Biomaterials in Tendon and Skeletal Muscle Tissue Engineering: Current Trends and Challenges', *Materials (Basel)* **11**(7).

Bentzinger, C. F., Wang, Y. X. and Rudnicki, M. A. (2012), 'Building muscle: molecular regulation of myogenesis', *Cold Spring Harbor Perspectives in Biology* **4**(2).

Bian, W. and Bursac, N. (2009), 'Engineered skeletal muscle tissue networks with controllable architecture', *Biomaterials* **30**(7), 1401–1412.
URL: *http://dx.doi.org/10.1016/j.biomaterials.2008.11.015*

Bian, W., Juhas, M., Pfeiler, T. W. and Bursac, N. (2012), 'Local tissue geometry determines contractile force generation of engineered muscle networks', *Tissue Eng Part A* **18**(9-10), 957–967.

Birch, H. L. (2007), 'Tendon matrix composition and turnover in relation to functional requirements', *International Journal of Experimental Pathology* **88**(4), 241–248.
URL: *https://doi.org/10.1111/j.1365-2613.2007.00552.x*

Bitar, M., C. Knowles, J., Lewis, M. P. and Salih, V. (2005), 'Soluble phosphate glass fibres for repair of bone-ligament interface', *Journal of Materials Science: Materials in Medicine* **16**(12), 1131–1136.
URL: *https://doi.org/10.1007/s10856-005-4718-3*

Bojsen-Møller, J. and Magnusson, S. P. (2019), 'Mechanical properties, physiological behavior, and function of aponeurosis and tendon', *Journal of Applied Physiology* **126**(6), 1800–1807.
URL: *https://www.physiology.org/doi/abs/10.1152/japplphysiol.00671.2018*

Boonen, K. J. M., Langelaan, M. L. P., Polak, R. B., van der Schaft, D. W. J., Baaijens, F. P. T. and Post, M. J. (2010), 'Effects of a combined mechanical stimulation protocol: Value for skeletal muscle tissue engineering', *Journal of Biomechanics* **43**(8), 1514–1521.

Boontheekul, T., Hill, E. E., Kong, H.-J. and Mooney, D. J. (2007), 'Regulating myoblast phenotype through controlled gel stiffness and degradation', *Tissue Engineering* **13**(7), 1431–1442.

Bottagisio, M., Lopa, S., Granata, V., Talò, G., Bazzocchi, C., Moretti, M. and Lovati, A. B. (2017), 'Different combinations of growth factors for the tenogenic differentiation of bone marrow mesenchymal stem cells in monolayer culture and in fibrin-based three-dimensional constructs', *Differentiation; Research in Biological Diversity* **95**, 44–53.

Bottinelli, R. and Reggiani, C. (2000), 'Human skeletal muscle fibres: molecular and functional diversity', *Progress in Biophysics and Molecular Biology* **73**(2), 195–262.
URL: *http://www.sciencedirect.com/science/article/pii/S0079610700000067*

Brennan, T. J. and Olson, E. N. (1990), 'Myogenin resides in the nucleus and acquires high affinity for a conserved enhancer element on heterodimerization', *Genes and Development* **4**(4), 582–595. Publisher: Cold Spring Harbor Laboratory Press.
URL: *https://utsouthwestern.pure.elsevier.com/en/publications/myogenin-resides-in-the-nucleus-and-acquires-high-affinity-for-a-*

Brent, A. E. and Tabin, C. J. (2002), 'Developmental regulation of somite derivatives: muscle, cartilage and tendon', *Current Opinion in Genetics & Development* **12**(5), 548–557.

Brown, D. M., Parr, T. and Brameld, J. M. (2012), 'Myosin heavy chain mRNA isoforms are expressed in two distinct cohorts during C2C12 myogenesis', *Journal of Muscle Research and Cell Motility* **32**(6), 383–390.

Bustamante, M., Fernández-Verdejo, R., Jaimovich, E. and Buvinic, S. (2014), 'Electrical stimulation induces IL-6 in skeletal muscle through extracellular ATP by activating Ca(2+) signals and an IL-6 autocrine loop', *Am J Physiol Endocrinol Metab* **306**(8), E869–882.

Buvinic, S., Almarza, G., Bustamante, M., Casas, M., López, J., Riquelme, M., Sáez, J. C., Huidobro-Toro, J. P. and Jaimovich, E. (2009), 'ATP released by electrical stimuli elicits calcium transients and gene expression in skeletal muscle', *J Biol Chem* **284**(50), 34490–34505.

Campion, D. R., Richardson, R. L., Kraeling, R. R. and Reagan, J. O. (1978), 'Regulation of skeletal muscle development by the central nervous system in the fetal pig', *Growth* **42**(2), 189–204.

Candiani, G., Riboldi, S. A., Sadr, N., Lorenzoni, S., Neuenschwander, P., Montevecchi, F. M. and Mantero, S. (2010), 'Cyclic Mechanical Stimulation Favors Myosin Heavy Chain Accumulation in Engineered Skeletal Muscle Constructs', *Journal of Applied Biomaterials and Biomechanics* **8**(2), 68–75. Publisher: SAGE Publications.
URL: *https://journals.sagepub.com/doi/abs/10.1177/228080001000800202*

Capdevila, J., Tabin, C. and Johnson, R. L. (1998), 'Control of dorsoventral somite patterning by Wnt-1 and beta-catenin', *Developmental Biology* **193**(2), 182–194.

Cardwell, R. D., Kluge, J. A., Thayer, P. S., Guelcher, S. A., Dahlgren, L. A., Kaplan, D. L. and Goldstein, A. S. (2015), 'Static and cyclic mechanical loading of mesenchymal stem cells on elastomeric, electrospun polyurethane meshes', *Journal of Biomechanical Engineering* **137**(7).

Catoira, M. C., Fusaro, L., Di Francesco, D., Ramella, M. and Boccafoschi, F. (2019), 'Overview of natural hydrogels for regenerative medicine applications', *Journal of Materials Science: Materials in Medicine* **30**(10), 115.
URL: *https://doi.org/10.1007/s10856-019-6318-7*

Cha, S. H., Lee, H. J. and Koh, W. G. (2017), 'Study of myoblast differentiation using multi-dimensional scaffolds consisting of nano and micropatterns', *Biomaterials Research* **21**(1), 1–9.
URL: *http://dx.doi.org/10.1186/s40824-016-0087-x*

Chakravarthy, M. V., Booth, F. W. and Spangenburg, E. E. (2001), 'The Molecular Responses of Skeletal Muscle Satellite Cells to Continuous Expression of IGF-1: Implications for the Rescue of Induced Muscular Atrophy in Aged Rats', *International Journal of Sport Nutrition and Exercise Metabolism* **11**(s1), S44–S48. Publisher: Human Kinetics, Inc. Section: International Journal of Sport Nutrition and Exercise Metabolism.
URL: *https://journals.humankinetics.com/view/journals/ijsnem/11/s1/article-pS44.xml*

Chal, J. and Pourquié, O. (2017), 'Making muscle: skeletal myogenesis in vivo and in vitro', *Development* **144**(12), 2104–2122. Publisher: Oxford University Press for The Company of Biologists Limited Section: REVIEW.
URL: *https://dev.biologists.org/content/144/12/2104*

Charest, J. L., García, A. J. and King, W. P. (2007), 'Myoblast alignment and differentiation on cell culture substrates with microscale topography and model chemistries', *Biomaterials* **28**(13), 2202–2210.

Charvet, B., Ruggiero, F. and Le Guellec, D. (2012), 'The development of the myotendinous junction. A review', *Muscles, Ligaments and Tendons Journal* **2**(2), 53–63.

Chattopadhyay, A., Galvez, M. G., Bachmann, M., Legrand, A., McGoldrick, R., Lovell, A., Jacobs, M., Crowe, C., Umansky, E. and Chang, J. (2016), 'Tendon Regeneration with Tendon Hydrogel-Based Cell Delivery: A Comparison of Fibroblasts and Adipose-Derived Stem Cells', *Plastic and Reconstructive Surgery* **138**(3), 617–626.

Chemello, F., Bean, C., Cancellara, P., Laveder, P., Reggiani, C. and Lanfranchi, G. (2011), 'Microgenomic Analysis in Skeletal Muscle: Expression Signatures of Individual Fast and Slow Myofibers', *PLoS ONE* **6**(2).
URL: *https://www.ncbi.nlm.nih.gov/pmc/articles/PMC3043066/*

Chen, C. H., Cao, Y., Wu, Y. F., Bais, A. J., Gao, J. S. and Tang, J. B. (2008), 'Tendon healing in vivo: gene expression and production of multiple growth factors in early tendon healing period', *The Journal of Hand Surgery* **33**(10), 1834–1842.

Chen, J. W. and Galloway, J. L. (2014), 'The development of zebrafish tendon and ligament progenitors', *Development* **141**(10), 2035–2045. Publisher: Oxford University Press for The Company of Biologists Limited Section: STEM CELLS AND REGENERATION.
URL: *https://dev.biologists.org/content/141/10/2035*

Cheng, Y.-W., Shiwarski, D. J., Ball, R. L., Whitehead, K. A. and Feinberg, A. W. (2020), 'Engineering Aligned Skeletal Muscle Tissue Using Decellularized Plant-Derived Scaffolds', *ACS Biomaterials Science & Engineering* **6**(5), 3046–3054. Publisher: American Chemical Society.
URL: *https://doi.org/10.1021/acsbiomaterials.0c00058*

Choi, J. S., Lee, S. J., Christ, G. J., Atala, A. and Yoo, J. J. (2008*a*), 'The influence of electrospun aligned poly(??-caprolactone)/collagen nanofiber meshes on the formation of self-aligned skeletal muscle myotubes', *Biomaterials* **29**(19), 2899–2906.

Choi, J. S., Lee, S. J., Christ, G. J., Atala, A. and Yoo, J. J. (2008*b*), 'The influence of electrospun aligned poly(ε-caprolactone)/collagen nanofiber meshes on the formation of self-aligned skeletal muscle myotubes', *Biomaterials* **29**(19), 2899–2906.

Choi, Y.-J., Kim, T. G., Jeong, J., Yi, H.-G., Park, J. W., Hwang, W. and Cho, D.-W. (2016), '3D Cell Printing of Functional Skeletal Muscle Constructs Using Skeletal Muscle-Derived Bioink', *Adv Healthc Mater* **5**(20), 2636–2645.

Clark, P., Dunn, G. A., Knibbs, A. and Peckham, M. (2002), 'Alignment of myoblasts on ultrafine gratings inhibits fusion in vitro', *The International Journal of Biochemistry & Cell Biology* **34**(7), 816–825.
URL: *http://www.sciencedirect.com/science/article/pii/S1357272501001807*

Collins, C. A. and Partridge, T. A. (2005), 'Self-Renewal of the Adult Skeletal Muscle Satellite Cell', *Cell Cycle* **4**(10), 1338–1341.
URL: *https://www.tandfonline.com/doi/full/10.4161/cc.4.10.2114*

Collinsworth, A. M. Y. M., Zhang, S., Kraus, W. E., Truskey, G. A., Carolina, N., Amy, M., Zhang, S., William, E. and Truskey, G. A. (2002), 'Apparent elastic modulus and hysteresis of skeletal muscle cells throughout differentiation', **0281**, 1219–1227.

Costantini, M., Idaszek, J., Szöke, K., Jaroszewicz, J., Dentini, M., Barbetta, A., Brinchmann, J. E. and Święszkowski, W. (2016), '3D bioprinting of BM-MSCs-loaded ECM biomimetic hydrogels for in vitro neocartilage formation', *Biofabrication* **8**(3), 035002. Publisher: IOP Publishing.
URL: *https://doi.org/10.1088/1758-5090/8/3/035002*

Costantini, M., Testa, S., Fornetti, E., Barbetta, A., Trombetta, M., Cannata, S. M., Gargioli, C. and Rainer, A. (2017), 'Engineering Muscle Networks in 3D Gelatin Methacryloyl Hydrogels: Influence of Mechanical Stiffness and Geometrical Confinement', *Frontiers in Bioengineering and Biotechnology* **5**(April), 1–8.
URL: *http://journal.frontiersin.org/article/10.3389/fbioe.2017.00022/full*

Courtney, T., Sacks, M. S., Stankus, J., Guan, J. and Wagner, W. R. (2006), 'Design and analysis of tissue engineering scaffolds that mimic soft tissue mechanical anisotropy', *Biomaterials* **27**(19), 3631–3638.

Csapo, R., Gumpenberger, M. and Wessner, B. (2020), 'Skeletal Muscle Extracellular Matrix – What Do We Know About Its Composition, Regulation, and Physiological Roles? A Narrative Review', *Frontiers in Physiology* **11**. Publisher: Frontiers.
URL: *https://www.frontiersin.org/articles/10.3389/fphys.2020.00253/full*

Cui, J., Wang, H., Shi, Q., Sun, T., Huang, Q. and Fukuda, T. (2019), 'Multicellular Co-Culture in Three-Dimensional Gelatin Methacryloyl Hydrogels for Liver Tissue Engineering', *Molecules* **24**(9).
URL: *https://www.ncbi.nlm.nih.gov/pmc/articles/PMC6539120/*

Cvetkovic, C., Raman, R., Chan, V., Williams, B. J., Tolish, M., Bajaj, P., Sakar, M. S., Asada, H. H., Saif, M. T. A. and Bashir, R. (2014), 'Three-dimensionally printed biological machines powered by skeletal muscle', *PNAS* **111**(28), 10125–10130. Publisher: National Academy of Sciences Section: Biological Sciences.
URL: *https://www.pnas.org/content/111/28/10125*

Cárdenas, C., Müller, M., Jaimovich, E., Pérez, F., Buchuk, D., Quest, A. F. G. and Carrasco, M. A. (2004), 'Depolarization of skeletal muscle cells induces phosphorylation of cAMP response element binding protein via calcium and protein kinase Calpha', *J Biol Chem* **279**(37), 39122–39131.

Dalby, M. J., Childs, S., Riehle, M. O., Johnstone, H. J. H., Affrossman, S. and Curtis, A. S. G. (2003), 'Fibroblast reaction to island topography: changes in cytoskeleton and morphology with time', *Biomaterials* **24**(6), 927–935.
URL: *https://www.sciencedirect.com/science/article/pii/S0142961202004271*

Danielson, K. G., Baribault, H., Holmes, D. F., Graham, H., Kadler, K. E. and Iozzo, R. V. (1997), 'Targeted disruption of decorin leads to abnormal collagen fibril morphology and skin fragility', *Journal of Cell Biology* **136**(3), 729–743.
URL: *https://doi.org/10.1083/jcb.136.3.729*

Dargelos, E., Dedieu, S., Moyen, C., Poussard, S., Veschambre, P., Brustis, J.-J. and Cottin, P. (2002), 'Characterization of the calcium-dependent proteolytic system in a mouse muscle cell line', *Mol Cell Biochem* **231**(1-2), 147–154.

Davidenko, N., Schuster, C. F., Bax, D. V., Raynal, N., Farndale, R. W., Best, S. M. and Cameron, R. E. (2015), 'Control of crosslinking for tailoring collagen-based scaffolds stability and mechanics', *Acta Biomater* **25**, 131–142.

Delgado Caceres, M., Pfeifer, C. G. and Docheva, D. (2018), 'Understanding Tendons: Lessons from Transgenic Mouse Models', *Stem Cells and Development* **27**(17), 1161–1174.

Dennis, R. G. and Kosnik, P. E. (2000), 'Excitability and isometric contractile properties of mammalian skeletal muscle constructs engineered in vitro', *In Vitro Cellular & Developmental Biology. Animal* **36**(5), 327–335.

Derwin, K. A., Soslowsky, L. J., Kimura, J. H. and Plaas, A. H. (2001), 'Proteoglycans and glycosaminoglycan fine structure in the mouse tail tendon fascicle', *Journal of Orthopaedic Research* **19**(2), 269–277.
URL: *https://doi.org/10.1016/s0736-0266(00)00032-2*

Dex, S., Alberton, P., Willkomm, L., Söllradl, T., Bago, S., Milz, S., Shakibaei, M., Ignatius, A., Bloch, W., Clausen-Schaumann, H., Shukunami, C., Schieker, M. and Docheva, D. (2017), 'Tenomodulin is Required for Tendon Endurance Running and Collagen I Fibril Adaptation to Mechanical Load', *EBioMedicine* **20**, 240–254.
URL: *http://www.sciencedirect.com/science/article/pii/S2352396417301949*

Dietze, D., Koenen, M., Röhrig, K., Horikoshi, H., Hauner, H. and Eckel, J. (2002), 'Impairment of insulin signaling in human skeletal muscle cells by co-culture with human adipocytes', *Diabetes* **51**(8), 2369–2376.

Discher, D. E., Janmey, P. and Wang, Y.-L. (2005), 'Tissue cells feel and respond to the stiffness of their substrate', *Science (New York, N.Y.)* **310**(5751), 1139–1143.

Discher, D. E., Mooney, D. J. and Zandstra, P. W. (2009), 'Growth factors, matrices, and forces combine and control stem cells', *Science (New York, N.Y.)* **324**(5935), 1673–1677.

Drexler, J. W. and Powell, H. M. (2011), 'Regulation of electrospun scaffold stiffness via coaxial core diameter', *Acta Biomater* **7**(3), 1133–1139.

Du, J., Yuan, Y., Si, T., Lian, J. and Zhao, H. (2012), 'Customized optimization of metabolic pathways by combinatorial transcriptional engineering', *Nucleic Acids Research* **40**(18), e142–e142.
URL: *https://doi.org/10.1093/nar/gks549*

Edom-Vovard, F., Schuler, B., Bonnin, M.-A., Teillet, M.-A. and Duprez, D. (2002), 'Fgf4 Positively Regulates scleraxis and Tenascin Expression in Chick Limb Tendons', *Developmental Biology* **247**(2), 351–366.
URL: *https://linkinghub.elsevier.com/retrieve/pii/S0012160602907074*

Eftimie, Brenner, H. R. and Buonanno, A. (1991), 'Myogenin and MyoD join a family of skeletal muscle genes regulated by electrical activity. | PNAS'.
URL: *https://www.pnas.org/content/88/4/1349.short*

Egerman, M. A. and Glass, D. J. (2014), 'Signaling pathways controlling skeletal muscle mass', *Critical Reviews in Biochemistry and Molecular Biology* **49**(1), 59–68. Publisher: Taylor & Francis _eprint: https://doi.org/10.3109/10409238.2013.857291.
URL: *https://doi.org/10.3109/10409238.2013.857291*

Ekwueme, E. C., Shah, J. V., Mohiuddin, M., Ghebes, C. A., Crispim, J. F., Saris, D. B. F., Fernandes, H. A. M. and Freeman, J. W. (2016), 'Cross-Talk Between Human Tenocytes and Bone Marrow Stromal Cells Potentiates Extracellular Matrix Remodeling In Vitro', *Journal of Cellular Biochemistry* **117**(3), 684–693.

Elamparithi, A., Punnoose, A. M., Kuruvilla, S., Ravi, M., Rao, S. and Paul, S. F. (2016), 'Electrospun polycaprolactone matrices with tensile properties suitable for soft tissue engineering', *Artificial Cells, Nanomedicine and Biotechnology* **44**(3), 878–884.

Eltit, J. M., García, A. A., Hidalgo, J., Liberona, J. L., Chiong, M., Lavandero, S., Maldonado, E. and Jaimovich, E. (2006), 'Membrane electrical activity elicits inositol 1,4,5-trisphosphate-dependent slow Ca2+ signals through a Gbetagamma/phosphatidylinositol 3-kinase gamma pathway in skeletal myotubes', *J Biol Chem* **281**(17), 12143–12154.

Em, W., Mm, H. and P, R. (2003), 'Autocrine growth factor signaling by insulin-like growth factor-II mediates MyoD-stimulated myocyte maturation.', *The Journal of Biological Chemistry* **278**(42), 41109–41113.
URL: *https://europepmc.org/article/med/12941952*

Engler, A. J., Griffin, M. A., Sen, S., Bönnemann, C. G., Sweeney, H. L. and Discher, D. E. (2004), 'Myotubes differentiate optimally on substrates with tissue-like stiffness', *Journal of Cell Biology* **166**(6), 877–887.
URL: *https://doi.org/10.1083/jcb.200405004*

Engler, A. J., Griffin, M. A., Sen, S., Bönnemann, C. G., Sweeney, H. L. and Discher, D. E. (2004), 'Myotubes differentiate optimally on substrates with tissue-like stiffness: pathological implications for soft or stiff microenvironments', *The Journal of Cell Biology* **166**(6), 877–887.

Engler, A. J., Sen, S., Sweeney, H. L. and Discher, D. E. (2006), 'Matrix elasticity directs stem cell lineage specification', *Cell* **126**(4), 677–689.
URL: *https://doi.org/10.1016/j.cell.2006.06.044*

Felsenthal, N. and Zelzer, E. (2017), 'Mechanical regulation of musculoskeletal system development', *Development (Cambridge, England)* **144**(23), 4271–4283.
URL: *https://www.ncbi.nlm.nih.gov/pmc/articles/PMC6514418/*

Fishman, J. M., Lowdell, M. W., Urbani, L., Ansari, T., Burns, A. J., Turmaine, M., North, J., Sibbons, P., Seifalian, A. M., Wood, K. J., Birchall, M. A. and Coppi, P. D. (2013), 'Immunomodulatory effect of a decellularized skeletal muscle scaffold in a discordant xenotransplantation model', *PNAS* **110**(35), 14360–14365. Publisher: National Academy of Sciences Section: Biological Sciences.
URL: *https://www.pnas.org/content/110/35/14360*

Ford, M. C., Bertram, J. P., Hynes, S. R., Michaud, M., Li, Q., Young, M., Segal, S. S., Madri, J. A. and Lavik, E. B. (2006), 'A macroporous hydrogel for the coculture of neural progenitor and endothelial cells to form functional vascular networks invivo', *Proceedings of the National Academy of Sciences* **103**(8), 2512–2517. Publisher: National Academy of Sciences Section: Research Articles.
URL: *https://www.pnas.org/content/103/8/2512*

Friday, B. B., Horsley, V. and Pavlath, G. K. (2000), 'Calcineurin activity is required for the initiation of skeletal muscle differentiation', *J Cell Biol* **149**(3), 657–666.

Frontera, W. R. and Ochala, J. (2015), 'Skeletal muscle: a brief review of structure and function', *Calcified Tissue International* **96**(3), 183–195.

Fujita, H., Shimizu, K., Yamamoto, Y., Ito, A., Kamihira, M. and Nagamori, E. (2010), 'Fabrication of scaffold-free contractile skeletal muscle tissue using magnetite-incorporated myogenic c2c12 cells', *Journal of Tissue Engineering and Regenerative Medicine* pp. n/a–n/a.
URL: *https://doi.org/10.1002/term.253*

Gamba, P. G., Conconi, M. T., Lo Piccolo, R., Zara, G., Spinazzi, R. and Parnigotto, P. P. (2002), 'Experimental abdominal wall defect repaired with acellular matrix', *Pediatr Surg Int* **18**(5-6), 327–331.

Garcia Garcia, A., Hébraud, A., Duval, J.-L., Wittmer, C. R., Gaut, L., Duprez, D., Egles, C., Bedoui, F., Schlatter, G. and Legallais, C. (2018), 'Poly(ε-caprolactone)/Hydroxyapatite 3D Honeycomb Scaffolds for a Cellular Microenvironment Adapted to Maxillofacial Bone Reconstruction', *ACS Biomaterials Science & Engineering* **4**(9), 3317–3326. Publisher: American Chemical Society.
URL: *https://doi.org/10.1021/acsbiomaterials.8b00521*

Gard, D. L. and Lazarides, E. (1980), 'The synthesis and distribution of desmin and vimentin during myogenesis in vitro', *Cell* **19**(1), 263–275.
URL: *http://www.sciencedirect.com/science/article/pii/0092867480904080*

Garvin, J., Qi, J., Maloney, M. and Banes, A. J. (2003), 'Novel system for engineering bioartificial tendons and application of mechanical load', *Tissue Engineering* **9**(5), 967–979.

Gaut, L. and Duprez, D. (2016), 'Tendon development and diseases', *WIREs Developmental Biology* **5**(1), 5–23. _eprint: https://onlinelibrary.wiley.com/doi/pdf/10.1002/wdev.201.
URL: *https://onlinelibrary.wiley.com/doi/abs/10.1002/wdev.201*

Gautel, M. and Djinović-Carugo, K. (2016), 'The sarcomeric cytoskeleton: from molecules to motion', *The Journal of Experimental Biology* **219**(Pt 2), 135–145.

Gawor, M. and Prószyński, T. J. (2018), 'The molecular cross talk of the dystrophin-glycoprotein complex', *Annals of the New York Academy of Sciences* **1412**(1), 62–72.

Gentleman, E., Lay, A. N., Dickerson, D. A., Nauman, E. A., Livesay, G. A. and Dee, K. C. (2003), 'Mechanical characterization of collagen fibers and scaffolds for tissue engineering', *Biomaterials* **24**(21), 3805–3813.

Gibas, I., and and, H. J. (2010), 'Review: Synthetic polymer hydrogels for biomedical applications', *Chemistry & Chemical Technology* **4**(4), 297–304.
URL: *https://doi.org/10.23939/chcht04.04.297*

Gilbert, S. F. (2000), *Developmental Biology*, Sinauer Associates.
URL: *https://www.xarg.org/ref/a/0878932437/*

Greising, S. M., Gransee, H. M., Mantilla, C. B. and Sieck, G. C. (2012), 'Systems biology of skeletal muscle: fiber type as an organizing principle', *Wiley Interdisciplinary Reviews. Systems Biology and Medicine* **4**(5), 457–473.

Griffin, M. A. (2004), 'Adhesion-contractile balance in myocyte differentiation', *Journal of Cell Science* **117**(24), 5855–5863.
URL: *https://doi.org/10.1242/jcs.01496*

Grounds, M. D., Sorokin, L. and White, J. (2005), 'Strength at the extracellular matrix-muscle interface', *Scandinavian Journal of Medicine and Science in Sports* **15**(6), 381–391.

Guerquin, M.-J., Charvet, B., Nourissat, G., Havis, E., Ronsin, O., Bonnin, M.-A., Ruggiu, M., Olivera-Martinez, I., Robert, N., Lu, Y., Kadler, K. E., Baumberger, T., Doursounian, L., Berenbaum, F. and Duprez, D. (2013), 'Transcription factor EGR1 directs tendon differentiation and promotes tendon repair', *The Journal of Clinical Investigation* **123**(8), 3564–3576.

Guex, A. G., Birrer, D. L., Fortunato, G., Tevaearai, H. T. and Giraud, M. N. (2013), 'Anisotropically oriented electrospun matrices with an imprinted periodic micropattern: A new scaffold for engineered muscle constructs', *Biomedical Materials (Bristol)* **8**(2).

Gunatillake, P. A. and Adhikari, R. (2003), 'Biodegradable synthetic polymers for tissue engineering', *European Cells & Materials* **5**, 1–16; discussion 16.

Handschin, C., Mortezavi, A., Plock, J. and Eberli, D. (2015), 'External physical and biochemical stimulation to enhance skeletal muscle bioengineering', *Advanced drug delivery reviews* **0**, 168–175.
URL: *https://www.ncbi.nlm.nih.gov/pmc/articles/PMC4444527/*

Hanke, N., Kubis, H.-P., Scheibe, R. J., Berthold-Losleben, M., Hüsing, O., Meissner, J. D. and Gros, G. (2010), 'Passive mechanical forces upregulate the fast myosin heavy chain IId/x via integrin and p38 MAP kinase activation in a primary muscle cell culture', *Am J Physiol Cell Physiol* **298**(4), C910–920.

Hara, M., Tabata, K., Suzuki, T., Do, M.-K. Q., Mizunoya, W., Nakamura, M., Nishimura, S., Tabata, S., Ikeuchi, Y., Sunagawa, K., Anderson, J. E., Allen, R. E. and Tatsumi, R. (2012), 'Calcium influx through a possible coupling of cation channels impacts skeletal muscle satellite cell activation in response to mechanical stretch', *Am J Physiol Cell Physiol* **302**(12), C1741–1750.

Hart, D. A., Kydd, A. and Reno, C. (1999), 'Gender and pregnancy affect neuropeptide responses of the rabbit achilles tendon', *Clinical Orthopaedics and Related Research* **365**, 237–246.
URL: *https://doi.org/10.1097/00003086-199908000-00029*

Hashimoto, H., Tamaki, T., Hirata, M., Uchiyama, Y., Sato, M. and Mochida, J. (2016), 'Reconstitution of the complete rupture in musculotendinous junction using skeletal muscle-derived multipotent stem cell sheet-pellets as a "bio-bond"', *PeerJ* **4**, e2231–e2231.
URL: *https://peerj.com/articles/2231*

Hashimoto, S. and Sato, F. (2012*a*), 'Effect of Pulsatile Electric Field on Cultured Muscle Cells in Vitro', **10**(1), 1–6.

Hashimoto, S. and Sato, F. (2012*b*), 'Effect of Pulsatile Electric Field on Cultured Muscle Cells in Vitro', **10**(1), 1–6.

Havis, E., Bonnin, M.-A., Lima, J. E. d., Charvet, B., Milet, C. and Duprez, D. (2016), 'TGFβ and FGF promote tendon progenitor fate and act downstream of muscle contraction to regulate tendon differentiation during chick limb development', *Development* **143**(20), 3839–3851. Publisher: Oxford University Press for The Company of Biologists Limited Section: RESEARCH ARTICLE.
URL: *https://dev.biologists.org/content/143/20/3839*

Havis, E., Bonnin, M.-A., Olivera-Martinez, I., Nazaret, N., Ruggiu, M., Weibel, J., Durand, C., Guerquin, M.-J., Bonod-Bidaud, C., Ruggiero, F., Schweitzer, R. and Duprez, D. (2014), 'Transcriptomic analysis of mouse limb tendon cells during development', *Development* **141**(19), 3683–3696. Publisher: Oxford University Press for The Company of Biologists Limited Section: RESEARCH ARTICLE.
URL: *https://dev.biologists.org/content/141/19/3683*

Heher, P., Maleiner, B., Prüller, J., Teuschl, A. H., Kollmitzer, J., Monforte, X., Wolbank, S., Redl, H., Rünzler, D. and Fuchs, C. (2015), 'A novel bioreactor for the generation of highly aligned 3D skeletal muscle-like constructs through orientation of fibrin via application of static strain', *Acta Biomater* **24**, 251–265.

Heinemeier, K. M., Schjerling, P., Heinemeier, J., Magnusson, S. P. and Kjaer, M. (2013), 'Lack of tissue renewal in human adult Achilles tendon is revealed by nuclear bomb 14C', *The FASEB Journal* **27**(5), 2074–2079. _eprint: https://faseb.onlinelibrary.wiley.com/doi/pdf/10.1096/fj.12-225599.
URL: *https://faseb.onlinelibrary.wiley.com/doi/abs/10.1096/fj.12-225599*

Hennink, W. E. and van Nostrum, C. F. (2002), 'Novel crosslinking methods to design hydrogels', *Advanced Drug Delivery Reviews* **54**(1), 13–36.
URL: *https://www.sciencedirect.com/science/article/pii/S0169409X0100240X*

Hernández-Hernández, J. M., García-González, E. G., Brun, C. E. and Rudnicki, M. A. (2017), 'The Myogenic Regulatory Factors, Determinants of Muscle Development, Cell Identity and Regeneration', *Seminars in cell & developmental biology* **72**, 10–18.
URL: *https://www.ncbi.nlm.nih.gov/pmc/articles/PMC5723221/*

Hinds, S., Tyhovych, N., Sistrunk, C. and Terracio, L. (2013), 'Improved Tissue Culture Conditions for Engineered Skeletal Muscle Sheets'. ISSN: 2356-6140 Library Catalog: www.hindawi.com Pages: e370151 Publisher: Hindawi Volume: 2013.
URL: *https://www.hindawi.com/journals/tswj/2013/370151/*

Hnia, K., Ramspacher, C., Vermot, J. and Laporte, J. (2015), 'Desmin in muscle and associated diseases: beyond the structural function', *Cell and Tissue Research* **360**(3), 591–608.

Holmberg, J. and Durbeej, M. (2013), 'Laminin-211 in skeletal muscle function', *Cell Adhesion & Migration* **7**(1), 111–121.
URL: *https://www.ncbi.nlm.nih.gov/pmc/articles/PMC3544775/*

Hosseini, V., Ahadian, S., Ostrovidov, S., Camci-Unal, G., Chen, S., Kaji, H., Ramalingam, M. and Khademhosseini, A. (2012), 'Engineered contractile skeletal muscle tissue on a microgrooved methacrylated gelatin substrate.', *Tissue engineering. Part A* **18**(23-24), 2453–65.
URL: *https://doi.org/10.1089/ten.TEA.2012.0181*

Hu, T., Li, Q., Dong, H., Xiao, W., Li, L. and Cao, X. (2016), 'Patterning electrospun nanofibers via agarose hydrogel stamps to spatially coordinate cell orientation in microfluidic device', *Small* **13**(3), 1602610.
URL: *https://doi.org/10.1002/smll.201602610*

Huang, X. and El-Sayed, M. (2010), 'Gold nanoparticles: Optical properties and implementations in cancer diagnosis and photothermal therapy', *Journal of Advanced Research* **1**, 13–28.

Huard, J., Li, Y. and Fu, F. H. (2002), 'Muscle injuries and repair: current trends in research', *The Journal of Bone and Joint Surgery. American Volume* **84**(5), 822–832.

Hughes, D., Baehr, L., Sharples, A. and Bodine, S. (2020), 'The role of UBR5 on Mitogen-activated protein kinase (MAPK) signalling and muscle mass regulation in mice', *The FASEB Journal* **34**, 1–1.

Hunt, N. C., Shelton, R. M. and Grover, L. (2009), 'An alginate hydrogel matrix for the localised delivery of a fibroblast/keratinocyte co-culture', *Biotechnology Journal* **4**(5), 730–737. _eprint: https://onlinelibrary.wiley.com/doi/pdf/10.1002/biot.200800292.
URL: *https://onlinelibrary.wiley.com/doi/abs/10.1002/biot.200800292*

Ignatius, A. A. and Claes, L. E. (1996), 'In vitro biocompatibility of bioresorbable polymers: poly(L, DL-lactide) and poly(L-lactide-co-glycolide)', *Biomaterials* **17**(8), 831–839.

Ikeda, K., Takayama, T., Suzuki, N., Shimada, K., Otsuka, K. and Ito, K. (2006), 'Effects of low-intensity pulsed ultrasound on the differentiation of c2c12 cells', *Life Sciences* **79**(20), 1936–1943.
URL: *https://doi.org/10.1016/j.lfs.2006.06.029*

Ito, A., Yamamoto, Y., Sato, M., Ikeda, K., Yamamoto, M., Fujita, H., Nagamori, E., Kawabe, Y. and Kamihira, M. (2014), 'Induction of functional tissue-engineered skeletal muscle constructs by defined electrical stimulation', *Scientific Reports* **4**(1), 1–7.
URL: *https://www.nature.com/articles/srep04781*

Ito, Y., Toriuchi, N., Yoshitaka, T., Ueno-Kudoh, H., Sato, T., Yokoyama, S., Nishida, K., Akimoto, T., Takahashi, M., Miyaki, S. and Asahara, H. (2010), 'The Mohawk homeobox gene is a critical regulator of tendon differentiation', *Proceedings of the National Academy of Sciences* **107**(23), 10538–10542.
URL: *http://www.pnas.org/cgi/doi/10.1073/pnas.1000525107*

Jakobsen, J. R., Mackey, A. L., Knudsen, A. B., Koch, M., Kjaer, M. and Krogsgaard, M. R. (2017), 'Composition and adaptation of human myotendinous junction and neighboring muscle fibers to heavy resistance training', *Scandinavian Journal of Medicine & Science in Sports* **27**(12), 1547–1559.

Janakiraman, V., Kienitz, B. L. and Baskaran, H. (2007), 'Lithography Technique for Topographical Micropatterning of Collagen-Glycosaminoglycan Membranes for Tissue Engineering Applications', *J Med Device* **1**(3), 233–237.

Janssen, I., Heymsfield, S. B., Wang, Z. M. and Ross, R. (2000), 'Skeletal muscle mass and distribution in 468 men and women aged 18-88 yr', *Journal of Applied Physiology (Bethesda, Md.: 1985)* **89**(1), 81–88.

Jiang, L., Wang, L., Wang, N., Gong, S., Wang, L., Li, Q., Shen, C. and Turng, L.-S. (2018), 'Fabrication of polycaprolactone electrospun fibers with different hierarchical structures mimicking collagen fibrils for tissue engineering scaffolds', *Applied Surface Science* **427**, 311–325.
URL: *http://www.sciencedirect.com/science/article/pii/S0169433217323188*

Jiang, T., Munguia-Lopez, J. G., Flores-Torres, S., Grant, J., Vijayakumar, S., Leon-Rodriguez, A. D. and Kinsella, J. M. (2017), 'Directing the Self-assembly of Tumour Spheroids by Bioprinting Cellular Heterogeneous Models within Alginate/Gelatin Hydrogels', *Scientific Reports* **7**(1), 4575.

Jiao, A., Moerk, C. T., Penland, N., Perla, M., Kim, J., Smith, A. S. T., Murry, C. E. and Kim, D.-H. (2018), 'Regulation of skeletal myotube formation and alignment by nanotopographically controlled cell-secreted extracellular matrix: REGULATION OF MYOTUBE FORMATION BY MATRIX NANOTOPOGRAPHY', *Journal of Biomedical Materials Research Part A* **106**(6), 1543–1551.
URL: *http://doi.wiley.com/10.1002/jbm.a.36351*

Jones, J. I. and Clemmons, D. R. (1995), 'Insulin-like growth factors and their binding proteins: biological actions', *Endocrine Reviews* **16**(1), 3–34.

(Joyce) Chen, C. n., Thompson, L. D. V. and Snow, L. A. (2017), Chapter 1 - Muscle Structure and Function, *in* J. D. Placzek and D. A. Boyce, eds, 'Orthopaedic Physical Therapy Secrets (Third Edition)', Elsevier, pp. 1–9.
URL: *http://www.sciencedirect.com/science/article/pii/B9780323286831000011*

Juhas, M. and Bursac, N. (2013), 'Engineering skeletal muscle repair', *Current Opinion in Biotechnology* **24**(5), 880–886.
URL: *http://www.sciencedirect.com/science/article/pii/S0958166913001110*

Jun, I., Jeong, S. and Shin, H. (2009), 'The stimulation of myoblast differentiation by electrically conductive sub-micron fibers', *Biomaterials* **30**(11), 2038–2047.

Junkin, M., Leung, S. L., Whitman, S., Gregorio, C. C. and Wong, P. K. (2011), 'Cellular self-organization by autocatalytic alignment feedback', *Journal of Cell Science* **124**(24), 4213–4220.
URL: *https://www.ncbi.nlm.nih.gov/pmc/articles/PMC3258106/*

Kalman, B., Monge, C., Bigot, A., Mouly, V., Picart, C. and Boudou, T. (2015), 'Engineering human 3D micromuscles with co-culture of fibroblasts and myoblasts', *Computer Methods in Biomechanics and Biomedical Engineering* **18 Suppl 1**, 1960–1961.

Kannus, P. (2000), 'Structure of the tendon connective tissue', *Scandinavian Journal of Medicine & Science in Sports* **10**(6), 312–320.

Kasemkijwattana, C., Menetrey, J., Bosch, P., Somogyi, G., Moreland, M. S., Fu, F. H., Buranapanitkit, B., Watkins, S. S. and Huard, J. (2000), 'Use of growth factors to improve muscle healing after strain injury', *Clinical Orthopaedics and Related Research* **370**, 272–285.
URL: *https://doi.org/10.1097/00003086-200001000-00028*

Kasper, A. M., Turner, D. C., Martin, N. R. and Sharples, A. P. (2018), 'Mimicking exercise in three-dimensional bioengineered skeletal muscle to investigate cellular and molecular mechanisms of physiological adaptation', *Journal of Cellular Physiology* **233**(3), 1985–1998.

Kasprzycka, P., Archacka, K., Kowalski, K., Mierzejewski, B., Zimowska, M., Grabowska, I., Piotrowski, M., Rafałko, M., Ryżko, A., Irhashava, A., Senderowski, K., Gołąbek, M., Stremińska, W., Jańczyk-Ilach, K., Koblowska, M., Iwanicka-Nowicka, R., Fogtman, A., Janowski, M., Walczak, P., Ciemerych, M. A. and Brzoska, E. (2019), 'The factors present in regenerating muscles impact bone marrow-derived mesenchymal stromal/stem cell fusion with myoblasts', *Stem Cell Research & Therapy* **10**(1), 343.

Ker, R. F., Alexander, R. M. and Bennett, M. B. (1988), 'Why are mammalian tendons so thick?', *Journal of Zoology* **216**(2), 309–324.
URL: *http://doi.wiley.com/10.1111/j.1469-7998.1988.tb02432.x*

Kheradmandi, M., Vasheghani-Farahani, E., Ghiaseddin, A. and Ganji, F. (2016), 'Skeletal muscle regeneration via engineered tissue culture over electrospun nanofibrous chitosan/PVA scaffold', *J Biomed Mater Res A* **104**(7), 1720–1727.

Khodabukus, A. and Baar, K. (2012), 'Defined electrical stimulation emphasizing excitability for the development and testing of engineered skeletal muscle', *Tissue Eng Part C Methods* **18**(5), 349–357.

Kim, H., Kim, M.-C. and Asada, H. H. (2019), 'Extracellular matrix remodelling induced by alternating electrical and mechanical stimulations increases the contraction of engineered skeletal muscle tissues', *Scientific Reports* **9**(1), 2732. Number: 1 Publisher: Nature Publishing Group.
URL: *https://www.nature.com/articles/s41598-019-39522-6*

Kim, M., Choi, Y. S., Yang, S. H., Hong, H.-N., Cho, S.-W., Cha, S. M., Pak, J. H., Kim, C. W., Kwon, S. W. and Park, C. J. (2006), 'Muscle regeneration by adipose tissue-derived adult stem cells attached to injectable PLGA spheres', *Biochem Biophys Res Commun* **348**(2), 386–392.

Kim, M. S., Jun, I., Shin, Y. M., Jang, W., Kim, S. I. and Shin, H. (2010), 'The development of genipin-crosslinked poly(caprolactone) (PCL)/gelatin nanofibers for tissue engineering applications', *Macromol Biosci* **10**(1), 91–100.

Kin, S., Hagiwara, A., Nakase, Y., Kuriu, Y., Nakashima, S., Yoshikawa, T., Sakakura, C., Otsuji, E., Nakamura, T. and Yamagishi, H. (2007), 'Regeneration of skeletal muscle using in situ tissue engineering on an acellular collagen sponge scaffold in a rabbit model', *ASAIO J* **53**(4), 506–513.

Kirkendall, D. T. and Garrett, W. E. (2007), 'Function and biomechanics of tendons', *Scandinavian Journal of Medicine & Science in Sports* **7**(2), 62–66.
URL: *https://doi.org/10.1111/j.1600-0838.1997.tb00120.x*

Kjaer, M. (2004), 'Role of extracellular matrix in adaptation of tendon and skeletal muscle to mechanical loading', *Physiol Rev* **84**(2), 649–698.

Klok, H.-A. (2005), 'Biological–synthetic hybrid block copolymers: Combining the best from two worlds', *Journal of Polymer Science Part A: Polymer Chemistry* **43**(1), 1–17. _eprint: https://onlinelibrary.wiley.com/doi/pdf/10.1002/pola.20527.
URL: *https://www.onlinelibrary.wiley.com/doi/abs/10.1002/pola.20527*

Ku, S. H. and Park, C. B. (2013), 'Myoblast differentiation on graphene oxide', *Biomaterials* **34**(8), 2017–2023.

Kuang, S., Gillespie, M. A. and Rudnicki, M. A. (2008), 'Niche Regulation of Muscle Satellite Cell Self-Renewal and Differentiation', *Cell Stem Cell* **2**(1), 22–31.

Kuang, S., Kuroda, K., Le Grand, F. and Rudnicki, M. A. (2007), 'Asymmetric Self-Renewal and Commitment of Satellite Stem Cells in Muscle', *Cell* **129**(5), 999–1010.
URL: *https://www.ncbi.nlm.nih.gov/pmc/articles/PMC2718740/*

Kuc, I. M. and Scott, P. G. (1997), 'Increased diameters of collagen fibrils precipitatedin vitroin the presence of decorin from various connective tissues', *Connective Tissue Research* **36**(4), 287–296.
URL: *https://doi.org/10.3109/03008209709160228*

Kuo, C. K., Marturano, J. E. and Tuan, R. S. (2010), 'Novel strategies in tendon and ligament tissue engineering: Advanced biomaterials and regeneration motifs', *Sports medicine, arthroscopy, rehabilitation, therapy & technology: SMARTT* **2**, 20.

Kuo, I. Y. and Ehrlich, B. E. (2015), 'Signaling in Muscle Contraction', *Cold Spring Harbor Perspectives in Biology* **7**(2).
URL: *https://www.ncbi.nlm.nih.gov/pmc/articles/PMC4315934/*

Kääriäinen, M., Järvinen, T., Järvinen, M., Rantanen, J. and Kalimo, H. (2000), 'Relation between myofibers and connective tissue during muscle injury repair', *Scandinavian Journal of Medicine & Science in Sports* **10**(6), 332–337.

Lacitignola, L., Crovace, A., Rossi, G. and Francioso, E. (2008), 'Cell therapy for tendinitis, experimental and clinical report', *Veterinary Research Communications* **32 Suppl 1**, S33–38.

LaCroix, A. S., Duenwald-Kuehl, S. E., Lakes, R. S. and Vanderby, R. (2013), 'Relationship between tendon stiffness and failure: a metaanalysis', *Journal of Applied Physiology* **115**(1), 43–51.
URL: *https://doi.org/10.1152/japplphysiol.01449.2012*

Ladd, M. R., Jin, S., Stitzel, J. D., Atala, A. and Yoo, J. J. (2011), 'Biomaterials Co-electrospun dual scaffolding system with potential for muscle e tendon junction tissue engineering', *Biomaterials* **32**(6), 1549–1559.
URL: *http://dx.doi.org/10.1016/j.biomaterials.2010.10.038*

Lam, M. T., Huang, Y. C., Birla, R. K. and Takayama, S. (2009), 'Microfeature guided skeletal muscle tissue engineering for highly organized 3-dimensional free-standing constructs', *Biomaterials* **30**(6), 1150–1155.

Lam, M. T., Sim, S., Zhu, X. and Takayama, S. (2006*a*), 'The effect of continuous wavy micropatterns on silicone substrates on the alignment of skeletal muscle myoblasts and myotubes', *Biomaterials* **27**(24), 4340–4347.

Lam, M. T., Sim, S., Zhu, X. and Takayama, S. (2006*b*), 'The effect of continuous wavy micropatterns on silicone substrates on the alignment of skeletal muscle myoblasts and myotubes', *Biomaterials* **27**(24), 4340–4347.

Langelaan, M. L. P., Boonen, K. J. M., Rosaria-Chak, K. Y., Schaft, D. W. J. v. d., Post, M. J. and Baaijens, F. P. T. (2011*a*), 'Advanced maturation by electrical stimulation: Differences in response between C2C12 and primary muscle progenitor cells', *Journal of Tissue Engineering and Regenerative Medicine* **5**(7), 529–539. _eprint: https://onlinelibrary.wiley.com/doi/pdf/10.1002/term.345.
URL: *https://onlinelibrary.wiley.com/doi/abs/10.1002/term.345*

Langelaan, M. L. P., Boonen, K. J. M., Rosaria-Chak, K. Y., Schaft, D. W. J. v. d., Post, M. J. and Baaijens, F. P. T. (2011*b*), 'Advanced maturation by electrical stimulation: Differences in response between C2C12 and primary muscle progenitor cells', *Journal of Tissue Engineering and Regenerative Medicine* **5**(7), 529–539. _eprint: https://onlinelibrary.wiley.com/doi/pdf/10.1002/term.345.
URL: *https://onlinelibrary.wiley.com/doi/abs/10.1002/term.345*

Larkin, L. M., Calve, S., Kostrominova, T. Y. and Arruda, E. M. (2006), 'Structure and functional evaluation of tendon-skeletal muscle constructs engineered in vitro', *Tissue Engineering* **12**(11), 3149–3158.

Lee, J. H., Lee, S. J., Khang, G. and Lee, H. B. (1999), 'Interaction of fibroblasts on polycarbonate membrane surfaces with different micropore sizes and hydrophilicity', *J Biomater Sci Polym Ed* **10**(3), 283–294.

Lejard, V., Blais, F., Guerquin, M.-J., Bonnet, A., Bonnin, M.-A., Havis, E., Malbouyres, M., Bidaud, C. B., Maro, G., Gilardi-Hebenstreit, P., Rossert, J., Ruggiero, F. and Duprez, D. (2011), 'EGR1 and EGR2 Involvement in Vertebrate Tendon Differentiation', *Journal of Biological Chemistry* **286**(7), 5855–5867. Publisher: American Society for Biochemistry and Molecular Biology.
URL: *http://www.jbc.org/content/286/7/5855*

Lemke, S. B. and Schnorrer, F. (2017), 'Mechanical forces during muscle development', *Mechanisms of Development* **144**(Pt A), 92–101.

Leon-Valdivieso, C. Y., Garcia-Garcia, A., Legallais, C. and Bedoui, F. (2020), 'Electrospinning of biomedically relevant multi-region scaffolds: From honeycomb to randomly-oriented microstructure', *Polymer* **202**, 122606.
URL: *http://www.sciencedirect.com/science/article/pii/S0032386120304377*

Lepper, C. and Fan, C.-M. (2010), 'Inducible lineage tracing of Pax7-descendant cells reveals embryonic origin of adult satellite cells', *Genesis (New York, N.Y.: 2000)* **48**(7), 424–436.

Leung, A. F., Hwang, J. C. and Cheung, Y. M. (1983), 'Determination of myofibrillar diameter by light diffractometry', *Pflügers Archiv* **396**(3), 238–242.
URL: *https://doi.org/10.1007/BF00587861*

Li, W.-J., Mauck, R. L., Cooper, J. A., Yuan, X. and Tuan, R. S. (2007), 'Engineering controllable anisotropy in electrospun biodegradable nanofibrous scaffolds for musculoskeletal tissue engineering', *J Biomech* **40**(8), 1686–1693.

Liao, H., Zhou, G.-q. and Ph, D. (2009), 'Development and Progress of Engineering of Skeletal Muscle Tissue', *Tissue Engineering Part B* **15**(3), 319–331.

Liao, I.-C., Liu, J. B., Bursac, N. and Leong, K. W. (2008), 'Effect of Electromechanical Stimulation on the Maturation of Myotubes on Aligned Electrospun Fibers', *Cell Mol Bioeng* **1**(2-3), 133–145.
URL: *https://www.ncbi.nlm.nih.gov/pmc/articles/PMC2747747/*

Lieber, R. L. (2002), *Skeletal Muscle Structure, Function, and Plasticity*, Lippincott Williams & Wilkins. Google-Books-ID: T0fbq_b89cAC.

Lima, K. M. M. e., Costa Júnior, J. F. S., Pereira, W. C. d. A. and de Oliveira, L. F. (2018), 'Assessment of the mechanical properties of the muscle-tendon unit by supersonic shear wave imaging elastography: a review', *Ultrasonography* **37**(1), 3–15.
URL: *https://www.ncbi.nlm.nih.gov/pmc/articles/PMC5769952/*

Lin, C.-H., Yang, J.-R., Chiang, N.-J., Ma, H. and Tsay, R.-Y. (2014), 'Evaluation of decellularized extracellular matrix of skeletal muscle for tissue engineering', *The International Journal of Artificial Organs* **37**(7), 546–555.
URL: *http://www.artificial-organs.com/article/evaluation-of-decellularized-extracellular-matrix-of-skeletal-muscle-for-tissue-engineering*

Liu, H., Zhang, C., Zhu, S., Lu, P., Zhu, T., Gong, X., Zhang, Z., Hu, J., Yin, Z., Heng, B. C., Chen, X. and Ouyang, H. W. (2015), 'Mohawk promotes the tenogenesis of mesenchymal stem cells through activation of the TGFβ signaling pathway', *Stem Cells (Dayton, Ohio)* **33**(2), 443–455.

Liu, Z. C. and Geisbrecht, E. R. (2011), 'Moleskin is essential for the formation of the myotendinous junction in Drosophila', *Developmental biology* **359**(2), 176–189.
URL: *https://www.ncbi.nlm.nih.gov/pmc/articles/PMC4066395/*

Low, S. Y. and Taylor, P. M. (1998), 'Integrin and cytoskeletal involvement in signalling cell volume changes to glutamine transport in rat skeletal muscle', *J Physiol* **512 (Pt 2)**, 481–485.

MacDonald, R. A., Voge, C. M., Kariolis, M. and Stegemann, J. P. (2008), 'Carbon nanotubes increase the electrical conductivity of fibroblast-seeded collagen hydrogels', *Acta Biomater* **4**(6), 1583–1592.

MacLean, S., Khan, W. S., Malik, A. A., Snow, M. and Anand, S. (2012), 'Tendon regeneration and repair with stem cells', *Stem Cells International* **2012**, 316281.

Maeda, T., Sakabe, T., Sunaga, A., Sakai, K., Rivera, A. L., Keene, D. R., Sasaki, T., Stavnezer, E., Iannotti, J., Schweitzer, R., Ilic, D., Baskaran, H. and Sakai, T. (2011), 'Conversion of Mechanical Force into TGF-β-Mediated Biochemical Signals', *Current Biology* **21**(11), 933–941.
URL: *http://www.sciencedirect.com/science/article/pii/S0960982211004234*

Maganaris, C. N. and Paul, J. P. (1999), 'In vivo human tendon mechanical properties', *The Journal of Physiology* **521**(Pt 1), 307–313.
URL: *https://www.ncbi.nlm.nih.gov/pmc/articles/PMC2269645/*

Mallick, K. K. and Cox, S. C. (2013), 'Biomaterial scaffolds for tissue engineering', *Frontiers in Bioscience (Elite Edition)* **5**, 341–360.

Martin, J., Mehr, D., Pardubsky, P. and Buckwalter, J. (2003), 'The role of tenascin-c in adaptation of tendons to compressive loading', *Biorheology* **40**, 321–329.

Martin, N. R. W., Passey, S. L., Player, D. J., Khodabukus, A., Ferguson, R. A., Sharples, A. P., Mudera, V., Baar, K. and Lewis, M. P. (2013), 'Factors affecting the structure and maturation of human tissue engineered skeletal muscle', *Biomaterials* **34**(23), 5759–5765.

Martins, P. M., Ribeiro, S., Ribeiro, C., Sencadas, V., Gomes, a. C., Gama, F. M. and Lanceros-Mendez, S. (2013), 'Effect of poling state and morphology of piezoelectric poly(vinylidene fluoride) membranes for skeletal muscle tissue engineering', *RSC Advances* **3**(September), 17938–17944.
URL: *http://dx.doi.org/10.1039/C3RA43499K*

Mauro, A. (2002), 'PKCalpha-mediated ERK, JNK and p38 activation regulates the myogenic program in human rhabdomyosarcoma cells', *Journal of Cell Science* **115**(18), 3587–3599.
URL: *https://doi.org/10.1242/jcs.00037*

McCormick, R. (1999), 'Extracellular modifications to muscle collagen: implications for meat quality', *Poultry Science* **78**(5), 785–791.
URL: *https://doi.org/10.1093/ps/78.5.785*

McKeon-Fischer, K. D., Flagg, D. H. and Freeman, J. W. (2011*a*), 'Coaxial electrospun poly(ε-caprolactone), multiwalled carbon nanotubes, and polyacrylic acid/polyvinyl alcohol scaffold for skeletal muscle tissue engineering', *Journal of Biomedical Materials Research Part A* **99A**(3), 493–499.
URL: *https://doi.org/10.1002/jbm.a.33116*

McKeon-Fischer, K. D., Flagg, D. H. and Freeman, J. W. (2011*b*), 'Poly(acrylic acid)/poly(vinyl alcohol) compositions coaxially electrospun with poly(ε-caprolactone) and multi-walled carbon nanotubes to create nanoactuating scaffolds', *Polymer* **21**(52), 4736–4743.
URL: *https://www.infona.pl//resource/bwmeta1.element.elsevier-f762f312-3e20-3d03-b8dd-2b4347d5075d*

McKeon-Fischer, K. D. and Freeman, J. W. (2011), 'Characterization of electrospun poly(L-lactide) and gold nanoparticle composite scaffolds for skeletal muscle tissue engineering', *J Tissue Eng Regen Med* **5**(7), 560–568.

McKeon-Fischer, K. D., Rossmeisl, J. H., Whittington, A. R. and Freeman, J. W. (2014), 'In vivo skeletal muscle biocompatibility of composite, coaxial electrospun, and microfibrous scaffolds', *Tissue Eng Part A* **20**(13-14), 1961–1970.

McKinsey, T. A., Zhang, C. L. and Olson, E. N. (2001), 'Control of muscle development by dueling HATs and HDACs', *Current Opinion in Genetics & Development* **11**(5), 497–504.

McKinsey, T. A., Zhang, C. L. and Olson, E. N. (2002), 'Signaling chromatin to make muscle', *Current Opinion in Cell Biology* **14**(6), 763–772.

Medler, S. (2019), 'Mixing it up: the biological significance of hybrid skeletal muscle fibers', *Journal of Experimental Biology* **222**(23). Publisher: The Company of Biologists Ltd Section: Review.
URL: *https://jeb.biologists.org/content/222/23/jeb200832*

Merceron, T. K., Burt, M., Seol, Y.-J., Kang, H.-W., Lee, S. J., Yoo, J. J. and Atala, A. (2015*a*), 'A 3d bioprinted complex structure for engineering the muscle–tendon unit', *Biofabrication* **7**(3), 035003.
URL: *https://doi.org/10.1088/1758-5090/7/3/035003*

Merceron, T. K., Burt, M., Seol, Y.-J., Kang, H.-W., Lee, S. J., Yoo, J. J. and Atala, A. (2015*b*), 'A 3D bioprinted complex structure for engineering the muscle–tendon unit', *Biofabrication* **7**(3), 035003–035003.
URL: *https://doi.org/10.1088/1758-5090/7/3/035003*

Michailovici, I., Harrington, H. A., Azogui, H. H., Yahalom-Ronen, Y., Plotnikov, A., Ching, S., Stumpf, M. P. H., Klein, O. D., Seger, R. and Tzahor, E. (2014), 'Nuclear to cytoplasmic shuttling of ERK promotes differentiation of muscle stem/progenitor cells', *Development* **141**(13), 2611–2620.
URL: *https://doi.org/10.1242/dev.107078*

Middleton, J. C. and Tipton, A. J. (2000), 'Synthetic biodegradable polymers as orthopedic devices', *Biomaterials* **21**(23), 2335–2346.
URL: *https://www.sciencedirect.com/science/article/pii/S0142961200001010*

Mienaltowski, M. J. and Birk, D. E. (2014), 'Structure, physiology, and biochemistry of collagens', *Advances in Experimental Medicine and Biology* **802**, 5–29.

Mikos, A. G., Herring, S. W., Ochareon, P., Elisseeff, J., Lu, H. H., Kandel, R., Schoen, F. J., Toner, M., Mooney, D., Atala, A., Van Dyke, M. E., Kaplan, D. and Vunjak-Novakovic, G. (2006), 'Engineering complex tissues', *Tissue Engineering* **12**(12), 3307–3339.

Millay, D. P., O'Rourke, J. R., Sutherland, L. B., Bezprozvannaya, S., Shelton, J. M., Bassel-Duby, R. and Olson, E. N. (2013), 'Myomaker is a membrane activator of myoblast fusion and muscle formation', *Nature* **499**(7458), 301–305.

Miosge, N., Klenczar, C., Herken, R., Willem, M. and Mayer, U. (1999), 'Organization of the myotendinous junction is dependent on the presence of alpha7beta1 integrin', *Laboratory Investigation; a Journal of Technical Methods and Pathology* **79**(12), 1591–1599.

Moffat, K. L., Kwei, A. S.-P., Spalazzi, J. P., Doty, S. B., Levine, W. N. and Lu, H. H. (2009), 'Novel nanofiber-based scaffold for rotator cuff repair and augmentation', *Tissue Engineering. Part A* **15**(1), 115–126.

Moon du, G., Christ, G., Stitzel, J. D., Atala, A. and Yoo, J. J. (2008), 'Cyclic mechanical preconditioning improves engineered muscle contraction', *Tissue Eng Part A* **14**(4), 473–482.
URL: *http://doi.org/10.1089/tea.2007.0104*

Motohashi, N. and Asakura, A. (2014), 'Muscle satellite cell heterogeneity and self-renewal', *Frontiers in Cell and Developmental Biology* **2**.
URL: *https://www.ncbi.nlm.nih.gov/pmc/articles/PMC4206996/*

Munger, J. S. and Sheppard, D. (2011), 'Cross talk among TGF-β signaling pathways, integrins, and the extracellular matrix', *Cold Spring Harbor Perspectives in Biology* **3**(11), a005017.

Myers, B. S., Woolley, C. T., Slotter, T. L., Garrett, W. E. and Best, T. M. (1998), 'The Influence of Strain Rate on the Passive and Stimulated Engineering Stress–Large Strain Behavior of the Rabbit Tibialis Anterior Muscle', *Journal of Biomechanical Engineering* **120**(1), 126–132. Publisher: American Society of Mechanical Engineers Digital Collection.
URL: *https://asmedigitalcollection.asme.org/biomechanical/article/120/1/126/398203/The-Influence-of-Strain-Rate-on-the-Passive-and*

Müller, S. A., Dürselen, L., Heisterbach, P., Evans, C. and Majewski, M. (2016), 'Effect of a Simple Collagen Type I Sponge for Achilles Tendon Repair in a Rat Model', *The American Journal of Sports Medicine* **44**(8), 1998–2004.

Naghashzargar, E., Farè, S., Catto, V., Bertoldi, S., Semnani, D., Karbasi, S. and Tanzi, M. C. (2015), 'Nano/micro hybrid scaffold of PCL or P3HB nanofibers combined with silk fibroin for tendon and ligament tissue engineering', *Journal of Applied Biomaterials & Functional Materials* **13**(2), 0–0.
URL: *http://journals.sagepub.com/doi/10.5301/jabfm.5000216*

Nassari, S., Duprez, D. and Fournier-Thibault, C. (2017), 'Non-myogenic Contribution to Muscle Development and Homeostasis: The Role of Connective Tissues', *Frontiers in Cell and Developmental Biology* **5**. Publisher: Frontiers.
URL: *https://www.frontiersin.org/articles/10.3389/fcell.2017.00022/full*

Ogneva, I. V., Lebedev, D. V. and Shenkman, B. S. (2010), 'Transversal Stiffness and Young's Modulus of Single Fibers from Rat Soleus Muscle Probed by Atomic Force Microscopy', *Biophysical Journal* **98**(3), 418–424.
URL: *https://www.ncbi.nlm.nih.gov/pmc/articles/PMC2814213/*

Okano, T., Satoh, S., Oka, T. and Matsuda, T. (1997), 'Tissue engineering of skeletal muscle. Highly dense, highly oriented hybrid muscular tissues biomimicking native tissues', *ASAIO J* **43**(5), M749–753.

Olson, E. N. (1992), 'Interplay between proliferation and differentiation within the myogenic lineage', *Developmental Biology* **154**(2), 261–272.
URL: *https://linkinghub.elsevier.com/retrieve/pii/001216069290066P*

Omidian, H., Rocca, J. G. and Park, K. (2006), 'Elastic, superporous hydrogel hybrids of polyacrylamide and sodium alginate', *Macromol Biosci* **6**(9), 703–710.

Ordan, E. and Volk, T. (2015), 'A non-signaling role of Robo2 in tendons is essential for Slit processing and muscle patterning', *Development (Cambridge, England)* **142**(20), 3512–3518.

Ostrovidov, S., Ahadian, S., Ramon-Azcon, J., Hosseini, V., Fujie, T., Parthiban, S. P., Shiku, H., Matsue, T., Kaji, H., Ramalingam, M., Bae, H. and Khademhosseini, A. (2017), 'Three-dimensional co-culture of C2C12/PC12 cells improves skeletal muscle tissue formation and function', *Journal of Tissue Engineering and Regenerative Medicine* **11**(2), 582–595.

Ostrovidov, S., Shi, X., Zhang, L., Liang, X., Kim, S. B., Fujie, T., Ramalingam, M., Chen, M., Nakajima, K., Al-Hazmi, F., Bae, H., Memic, A. and Khademhosseini, A. (2014), 'Myotube formation on gelatin nanofibers - Multi-walled carbon nanotubes hybrid scaffolds', *Biomaterials* **35**(24), 6268–6277.
URL: *http://dx.doi.org/10.1016/j.biomaterials.2014.04.021*

Pardo-Yissar, V., Gabai, R., Shipway, A. N., Bourenko, T. and Willner, I. (2001), 'Gold Nanoparticle/Hydrogel Composites with Solvent-Switchable Electronic Properties', *Advanced Materials* **13**(17), 1320–1323. _eprint: https://onlinelibrary.wiley.com/doi/pdf/10.1002/1521-4095%28200109%2913%3A17%3C1320%3A%3AAID-ADMA1320%3E3.0.CO%3B2-8.
URL: *https://doi.org/10.1002/1521-4095(200109)13:17<1320::AID-ADMA1320>3.0.CO;2-8*

Park, J.-W. and Shumaker-Parry, J. S. (2014), 'Structural Study of Citrate Layers on Gold Nanoparticles: Role of Intermolecular Interactions in Stabilizing Nanoparticles', *Journal of the American Chemical Society* **136**(5), 1907–1921. Publisher: American Chemical Society.
URL: *https://doi.org/10.1021/ja4097384*

Park, S. H., Choi, Y.-J., Moon, S. W., Lee, B. H., Shim, J.-H., Cho, D.-W. and Wang, J. H. (2018), 'Three-Dimensional Bio-Printed Scaffold Sleeves With Mesenchymal Stem Cells for Enhancement of Tendon-to-Bone Healing in Anterior Cruciate Ligament Reconstruction Using Soft-Tissue Tendon Graft', *Arthroscopy: The Journal of Arthroscopic & Related Surgery: Official Publication of the Arthroscopy Association of North America and the International Arthroscopy Association* **34**(1), 166–179.

Patz, T. M., Doraiswamy, A., Narayan, R. J., Modi, R. and Chrisey, D. B. (2005), 'Two-dimensional differential adherence and alignment of C2C12 myoblasts', *Materials Science and Engineering: B* **123**(3), 242–247.
URL: *http://www.sciencedirect.com/science/article/pii/S0921510705004423*

Pavesi, A., Adriani, G., Rasponi, M., Zervantonakis, I. K., Fiore, G. B. and Kamm, R. D. (2015), 'Controlled electromechanical cell stimulation on-a-chip', *Sci Rep* **5**, 11800.

Pennisi, C. P., Olesen, C. G., de Zee, M., Rasmussen, J. and Zachar, V. (2011), 'Uniaxial Cyclic Strain Drives Assembly and Differentiation of Skeletal Myocytes', *Tissue Engineering Part A* **17**(19-20), 2543–2550.
URL: *http://www.liebertonline.com/doi/abs/10.1089/ten.tea.2011.0089*

Perez-Ruiz, A., Gnocchi, V. F. and Zammit, P. S. (2007), 'Control of Myf5 activation in adult skeletal myonuclei requires ERK signalling', *Cell Signal* **19**(8), 1671–1680.

Pollock, C. M. and Shadwick, R. E. (1994), 'Relationship between body mass and biomechanical properties of limb tendons in adult mammals', *American Journal of Physiology-Regulatory, Integrative and Comparative Physiology* **266**(3), R1016–R1021. Publisher: American Physiological Society.
URL: *https://journals.physiology.org/doi/abs/10.1152/ajpregu.1994.266.3.R1016*

Pollot, B. E., Rathbone, C. R., Wenke, J. C. and Guda, T. (2018), 'Natural polymeric hydrogel evaluation for skeletal muscle tissue engineering', *Journal of Biomedical Materials Research Part B: Applied Biomaterials* **106**(2), 672–679. _eprint: https://onlinelibrary.wiley.com/doi/pdf/10.1002/jbm.b.33859.
URL: *https://onlinelibrary.wiley.com/doi/abs/10.1002/jbm.b.33859*

Porzionato, A., Sfriso, M. M., Pontini, A., Macchi, V., Petrelli, L., Pavan, P. G., Natali, A. N., Bassetto, F., Vindigni, V. and De Caro, R. (2015), 'Decellularized human skeletal muscle as biologic scaffold for reconstructive surgery', *International Journal of Molecular Sciences* **16**(7), 14808–14831.

Powell, C. a., Smiley, B. L., Mills, J. and Vandenburgh, H. H. (2002), 'Mechanical stimulation improves tissue-engineered human skeletal muscle.', *American journal of physiology. Cell physiology* **283**(5), C1557–C1565.

Puttini, S., Lekka, M., Dorchies, O. M., Saugy, D., Incitti, T., Ruegg, U. T., Bozzoni, I., Kulik, A. J. and Mermod, N. (2009), 'Gene-mediated restoration of normal myofiber elasticity in dystrophic muscles', *Molecular Therapy* **17**(1), 19–25.
URL: *https://doi.org/10.1038/mt.2008.239*

Qazi, T. H., Mooney, D. J., Pumberger, M., Geißler, S. and Duda, G. N. (2015), 'Biomaterials based strategies for skeletal muscle tissue engineering: Existing technologies and future trends', *Biomaterials* **53**, 502–521.
URL: *http://dx.doi.org/10.1016/j.biomaterials.2015.02.110*

Qin, Y.-X. and Hu, M. (2014), 'Mechanotransduction in musculoskeletal tissue regeneration: effects of fluid flow, loading, and cellular-molecular pathways', *BioMed Research International* **2014**, 863421.

Rahnert, J. A. and Burkholder, T. J. (2011), 'ERK phosphorylation correlates with intensity of electrical stimulation in mouse tibialis anterior', *The FASEB Journal* **25**(S1), 1051.19–1051.19.
URL: *https://faseb.onlinelibrary.wiley.com/doi/abs/10.1096/fasebj.25.1supplement.1051.19*

Ramón-Azcón, J., Ahadian, S., Estili, M., Liang, X., Ostrovidov, S., Kaji, H., Shiku, H., Ramalingam, M., Nakajima, K., Sakka, Y., Khademhosseini, A. and Matsue, T. (2013), 'Dielectrophoretically aligned carbon nanotubes to control electrical and mechanical properties of hydrogels to fabricate contractile muscle myofibers', *Adv Mater* **25**(29), 4028–4034.

Rangarajan, S., Madden, L. and Bursac, N. (2014*a*), 'Use of flow, electrical, and mechanical stimulation to promote engineering of striated muscles', *Ann Biomed Eng* **42**(7), 1391–1405.

Rangarajan, S., Madden, L. and Bursac, N. (2014*b*), 'Use of flow, electrical, and mechanical stimulation to promote engineering of striated muscles', *Annals of Biomedical Engineering* **42**(7), 1391–1405.

Rantanen, J., Hurme, T., Lukka, R., Heino, J. and Kalimo, H. (1995), 'Satellite cell proliferation and the expression of myogenin and desmin in regenerating skeletal muscle: evidence for two different populations of satellite cells', *Laboratory Investigation; a Journal of Technical Methods and Pathology* **72**(3), 341–347.

Relaix, F. and Zammit, P. S. (2012), 'Satellite cells are essential for skeletal muscle regeneration: the cell on the edge returns centre stage', *Development (Cambridge, England)* **139**(16), 2845–2856.

Ren, K., Crouzier, T., Roy, C. and Picart, C. (2008), 'Polyelectrolyte Multilayer Films of Controlled Stiffness Modulate Myoblast Cell Differentiation', *Advanced Functional Materials* **18**(9), 1378–1389. _eprint: https://onlinelibrary.wiley.com/doi/pdf/10.1002/adfm.200701297.
URL: *https://onlinelibrary.wiley.com/doi/abs/10.1002/adfm.200701297*

Riboldi, S. A., Sampaolesi, M., Neuenschwander, P., Cossu, G. and Mantero, S. (2005), 'Electrospun degradable polyesterurethane membranes : potential scaffolds for skeletal muscle tissue engineering', **26**, 4606–4615.

Ricotti, L., Fujie, T., Vazão, H., Ciofani, G., Marotta, R., Brescia, R., Filippeschi, C., Corradini, I., Matteoli, M., Mattoli, V., Ferreira, L. and Menciassi, A. (2013), 'Boron nitride nanotube-mediated stimulation of cell co-culture on micro-engineered hydrogels', *PLoS ONE* **8**(8), e71707.
URL: *https://doi.org/10.1371/journal.pone.0071707*

Ricotti, L., Polini, A., Genchi, G. G., Ciofani, G., Iandolo, D., Vazão, H., Mattoli, V., Ferreira, L., Menciassi, A. and Pisignano, D. (2012), 'Proliferation and skeletal myotube formation capability of C2C12 and H9c2 cells on isotropic and anisotropic electrospun nanofibrous PHB scaffolds', *Biomedical Materials (Bristol, England)* **7**(3), 035010.

Ricotti, L., Taccola, S., Pensabene, V., Mattoli, V., Fujie, T., Takeoka, S., Menciassi, A. and Dario, P. (2010), 'Adhesion and proliferation of skeletal muscle cells on single layer poly(lactic acid) ultra-thin films', *Biomed Microdevices* **12**(5), 809–819.

Rigby, B. J., Hirai, N., Spikes, J. D. and Eyring, H. (1959), 'The Mechanical Properties of Rat Tail Tendon', *The Journal of General Physiology* **43**(2), 265–283.

Rimington, R. P., Capel, A. J., Christie, S. D. R. and Lewis, M. P. (2017), 'Biocompatible 3D printed polymers via fused deposition modelling direct C2C12 cellular phenotype in vitro', *Lab Chip* **17**(17), 2982–2993. Publisher: The Royal Society of Chemistry.
URL: *https://pubs.rsc.org/en/content/articlelanding/2017/lc/c7lc00577f*

Roman, W. and Gomes, E. R. (2018), 'Nuclear positioning in skeletal muscle', *Seminars in Cell & Developmental Biology* **82**, 51–56.

Rommel, C., Bodine, S. C., Clarke, B. A., Rossman, R., Nunez, L., Stitt, T. N., Yancopoulos, G. D. and Glass, D. J. (2001), 'Mediation of IGF-1-induced skeletal myotube hypertrophy by PI(3)K/Akt/mTOR and PI(3)K/Akt/GSK3 pathways', *Nature Cell Biology* **3**(11), 1009–1013. Number: 11 Publisher: Nature Publishing Group.
URL: *https://www.nature.com/articles/ncb1101-1009*

Rowley, J. A. and Mooney, D. J. (2002), 'Alginate type and RGD density control myoblast phenotype', *J Biomed Mater Res* **60**(2), 217–223.

Salahshoor, H. and Rahbar, N. (2014), 'Multi-scale mechanical and transport properties of a hydrogel', *J Mech Behav Biomed Mater* **37**, 299–306.

Salgarella, A. R., Cafarelli, A., Ricotti, L., Capineri, L., Dario, P. and Menciassi, A. (2017), 'Optimal ultrasound exposure conditions for maximizing c2c12 muscle cell proliferation and differentiation', *Ultrasound in Medicine & Biology* **43**(7), 1452–1465.
URL: *https://doi.org/10.1016/j.ultrasmedbio.2017.03.003*

Salimath, A. S. and García, A. J. (2016), 'Biofunctional hydrogels for skeletal muscle constructs', *J Tissue Eng Regen Med* **10**(11), 967–976.

Sanger, J. W., Chowrashi, P., Shaner, N. C., Spalthoff, S., Wang, J., Freeman, N. L. and Sanger, J. M. (2002), 'Myofibrillogenesis in skeletal muscle cells', *Clinical Orthopaedics and Related Research* **403**, S153–S162.
URL: *https://doi.org/10.1097/00003086-200210001-00018*

Sanzari, I., Callisti, M., Grazia, A. D., Evans, D. J., Polcar, T. and Prodromakis, T. (2017), 'Parylene C topographic micropattern as a template for patterning PDMS and Polyacrylamide hydrogel', *Sci Rep* **7**(1), 5764.

Sartorelli, V. and Caretti, G. (2005), 'Mechanisms underlying the transcriptional regulation of skeletal myogenesis', *Current Opinion in Genetics & Development* **15**(5), 528–535.
URL: *http://www.sciencedirect.com/science/article/pii/S0959437X05001267*

Sawadkar, P., Alexander, S., Tolk, M., Wong, J., McGrouther, D., Bozec, L. and Mudera, V. (2013), 'Development of a surgically optimized graft insertion suture technique to accommodate a tissue-engineered tendon in vivo', *BioResearch Open Access* **2**(5), 327–335.

Saxena, A. K., Marler, J., Benvenuto, M., Willital, G. H. and Vacanti, J. P. (1999), 'Skeletal Muscle Tissue Engineering Using Isolated Myoblasts on Synthetic Biodegradable Polymers: Preliminary Studies', *Tissue Engineering* **5**(6), 525–531. Publisher: Mary Ann Liebert, Inc., publishers.
URL: *https://www.liebertpub.com/doi/10.1089/ten.1999.5.525*

Saxena, A. K., Willital, G. H. and Vacanti, J. P. (2001), 'Vascularized three-dimensional skeletal muscle tissue-engineering', *Bio-Medical Materials and Engineering* **11**(4), 275–281. Publisher: IOS Press.
URL: *https://content.iospress.com/articles/bio-medical-materials-and-engineering/bme192*

Schnorrer, F., Kalchhauser, I. and Dickson, B. J. (2007), 'The Transmembrane Protein Kontiki Couples to Dgrip to Mediate Myotube Targeting in Drosophila', *Developmental Cell* **12**(5), 751–766.
URL: *http://www.sciencedirect.com/science/article/pii/S1534580707000962*

Schönherr, E., Witsch-Prehm, P., Harrach, B., Robenek, H., Rauterberg, J. and Kresse, H. (1995), 'Interaction of biglycan with type i collagen', *Journal of Biological Chemistry* **270**(6), 2776–2783.
URL: *https://doi.org/10.1074/jbc.270.6.2776*

Schweitzer, R., Chyung, J. H., Murtaugh, L. C., Brent, A. E., Rosen, V., Olson, E. N., Lassar, A. and Tabin, C. J. (2001), 'Analysis of the tendon cell fate using Scleraxis, a specific marker for tendons and ligaments', *Development* **128**(19), 3855–3866. Publisher: The Company of Biologists Ltd Section: Research Article.
URL: *https://dev.biologists.org/content/128/19/3855*

Seaborne, R. A., Hughes, D. C., Turner, D. C., Owens, D. J., Baehr, L. M., Gorski, P., Semenova, E. A., Borisov, O. V., Larin, A. K., Popov, D. V., Generozov, E. V., Sutherland, H., Ahmetov, I. I., Jarvis, J. C., Bodine, S. C. and Sharples, A. P. (2019), 'UBR5 is a novel E3 ubiquitin ligase involved in skeletal muscle hypertrophy and recovery from atrophy', *The Journal of Physiology* **597**(14), 3727–3749. _eprint: https://physoc.onlinelibrary.wiley.com/doi/pdf/10.1113/JP278073.
URL: *https://physoc.onlinelibrary.wiley.com/doi/abs/10.1113/JP278073*

Sensini, A., Gualandi, C., Zucchelli, A., Boyle, L. A., Kao, A. P., Reilly, G. C., Tozzi, G., Cristofolini, L. and Focarete, M. L. (2018), 'Tendon Fascicle-Inspired Nanofibrous Scaffold of Polylactic acid/Collagen with Enhanced 3D-Structure and Biomechanical Properties', *Scientific Reports* **8**(1), 17167. Number: 1 Publisher: Nature Publishing Group.
URL: *https://www.nature.com/articles/s41598-018-35536-8*

Serena, E., Flaibani, M., Carnio, S., Boldrin, L., Vitiello, L., De Coppi, P. and Elvassore, N. (2008), 'Electrophysiologic stimulation improves myogenic potential of muscle precursor cells grown in a 3D collagen scaffold', *Neurol Res* **30**(2), 207–214.

Shadrach, J. L. and Wagers, A. J. (2011), 'Stem cells for skeletal muscle repair.'.
URL: *http://rstb.royalsocietypublishing.org/content/366/1575/2297*

Shadrin, I. Y., Khodabukus, A. and Bursac, N. (2016), 'Striated muscle function, regeneration, and repair', *Cellular and molecular life sciences: CMLS* **73**(22), 4175–4202.

Sharma, P. and Maffulli, N. (2006), 'Biology of tendon injury: healing, modeling and remodeling', *Journal of Musculoskeletal and Neuronal Interactions* **6**(2), 181–190.

Shavlakadze, T., Chai, J., Maley, K., Cozens, G., Grounds, G., Winn, N., Rosenthal, N. and Grounds, M. D. (2010), 'A growth stimulus is needed for IGF-1 to induce skeletal muscle hypertrophy in vivo', *Journal of Cell Science* **123**(6), 960–971. Publisher: The Company of Biologists Ltd Section: Research Article.
URL: *https://jcs.biologists.org/content/123/6/960*

Sher, R. B., Cox, G. A. and Ackert-Bicknell, C. (2012), Chapter 2.5 - Development and Disease of Mouse Muscular and Skeletal Systems, *in* H. J. Hedrich, ed., 'The Laboratory Mouse (Second Edition)', Academic Press, Boston, pp. 209–239.
URL: *http://www.sciencedirect.com/science/article/pii/B9780123820082000106*

Shibata, Y., Takeshita, H., Sasakawa, N. and Sawa, H. (2010), 'Double bromodomain protein BET-1 and MYST HATs establish and maintain stable cell fates in C. elegans', *Development* **137**(7), 1045–1053. Publisher: Oxford University Press for The Company of Biologists Limited Section: DEVELOPMENT AND STEM CELLS.
URL: *https://dev.biologists.org/content/137/7/1045*

Shim, J.-H., Kim, J. Y., Park, M., Park, J. and Cho, D.-W. (2011), 'Development of a hybrid scaffold with synthetic biomaterials and hydrogel using solid freeform fabrication technology', *Biofabrication* **3**(3), 034102.

Shimizu, K., Fujita, H. and Nagamori, E. (2009), 'Alignment of skeletal muscle myoblasts and myotubes using linear micropatterned surfaces ground with abrasives', *Biotechnology and Bioengineering* **103**(3), 631–638.

Shin, Y. C., Lee, J. H., Jin, L., Kim, M. J., Kim, Y. J., Hyun, J. K., Jung, T. G., Hong, S. W. and Han, D. W. (2015), 'Stimulated myoblast differentiation on graphene oxide-impregnated PLGA-collagen hybrid fibre matrices matrices', *Journal of Nanobiotechnology* **13**(1), 1–11.

Shukunami, C., Takimoto, A., Nishizaki, Y., Yoshimoto, Y., Tanaka, S., Miura, S., Watanabe, H., Sakuma, T., Yamamoto, T., Kondoh, G. and Hiraki, Y. (2018), 'Scleraxis is a transcriptional activator that regulates the expression of Tenomodulin, a marker of mature tenocytes and ligamentocytes', *Scientific Reports* **8**(1), 3155. Number: 1 Publisher: Nature Publishing Group.
URL: *https://www.nature.com/articles/s41598-018-21194-3*

Silver, F. H., Freeman, J. W. and Seehra, G. P. (2003), 'Collagen self-assembly and the development of tendon mechanical properties', *Journal of Biomechanics* **36**(10), 1529–1553.
URL: *http://www.sciencedirect.com/science/article/pii/S0021929003001350*

Sirivisoot, S. and Harrison, B. S. (2011), 'Skeletal myotube formation enhanced by electrospun polyurethane carbon nanotube scaffolds', *Int J Nanomedicine* **6**, 2483–2497.

Sosa, H., Popp, D., Ouyang, G. and Huxley, H. (1994), 'Ultrastructure of skeletal muscle fibers studied by a plunge quick freezing method: myofilament lengths', *Biophysical Journal* **67**(1), 283–292.
URL: *https://linkinghub.elsevier.com/retrieve/pii/S0006349594804795*

Sreerekha, P. R., Menon, D., Nair, S. V. and Chennazhi, K. P. (2013), 'Fabrication of fibrin based electrospun multiscale composite scaffold for tissue engineering applications', *J Biomed Nanotechnol* **9**(5), 790–800.

Stern-Straeter, J., Bach, A. D., Stangenberg, L., Foerster, V. T., Horch, R. E., Stark, G. B. and Beier, J. P. (2005), 'Impact of electrical stimulation on three-dimensional myoblast cultures - a real-time RT-PCR study', *Journal of Cellular and Molecular Medicine* **9**(4), 883–892. _eprint: https://onlinelibrary.wiley.com/doi/pdf/10.1111/j.1582-4934.2005.tb00386.x.
URL: *https://onlinelibrary.wiley.com/doi/abs/10.1111/j.1582-4934.2005.tb00386.x*

Subramanian, A., Kanzaki, L. F., Galloway, J. L. and Schilling, T. F. (2018), 'Mechanical force regulates tendon extracellular matrix organization and tenocyte morphogenesis through TGFbeta signaling', *eLife* **7**, e38069. Publisher: eLife Sciences Publications, Ltd.
URL: *https://doi.org/10.7554/eLife.38069*

Subramanian, A. and Schilling, T. F. (2015), 'Tendon development and musculoskeletal assembly: emerging roles for the extracellular matrix', *Development (Cambridge, England)* **142**(24), 4191–4204.

Suh, G. C., Bettadapur, A., Santoso, J. W. and McCain, M. L. (2017), 'Fabrication of Micromolded Gelatin Hydrogels for Long-Term Culture of Aligned Skeletal Myotubes', *Methods Mol Biol* **1668**, 147–163.

Suzuki, J., Yamazaki, Y., Li, G., Kaziro, Y., Koide, H. and Guang, L. (2000), 'Involvement of Ras and Ral in chemotactic migration of skeletal myoblasts', *Mol Cell Biol* **20**(13), 4658–4665.

Swasdison, S. and Mayne, R. (1991), 'In vitro attachment of skeletal muscle fibers to a collagen gel duplicates the structure of the myotendinous junction', *Experimental Cell Research* **193**(1), 227–231.

Sweeney, H. L. and Hammers, D. W. (2018), 'Muscle Contraction', *Cold Spring Harbor Perspectives in Biology* **10**(2).
URL: *https://www.ncbi.nlm.nih.gov/pmc/articles/PMC5793755/*

Sørensen, V., Zhen, Y., Zakrzewska, M., Haugsten, E. M., Wälchli, S., Nilsen, T., Olsnes, S. and Wiedlocha, A. (2008), 'Phosphorylation of fibroblast growth factor (FGF) receptor 1 at Ser777 by p38 mitogen-activated protein kinase regulates translocation of exogenous FGF1 to the cytosol and nucleus', *Mol Cell Biol* **28**(12), 4129–4141.

Takeda, N., Tamura, K., Mineguchi, R., Ishikawa, Y., Haraguchi, Y., Shimizu, T. and Hara, Y. (2016), 'In situ cross-linked electrospun fiber scaffold of collagen for fabricating cell-dense muscle tissue', *Journal of Artificial Organs* **19**(2), 141–148.

Tanaka, T., Hattori-Aramaki, N., Sunohara, A., Okabe, K., Sakamoto, Y., Ochiai, H., Hayashi, R. and Kishi, K. (2014), 'Alignment of Skeletal Muscle Cells Cultured in Collagen Gel by Mechanical and Electrical Stimulation'.
URL: *https://www.hindawi.com/journals/ijte/2014/621529/*

Tang, M., Gandhi, N. S., Burrage, K. and Gu, Y. (2019), 'Interaction of gold nanosurfaces/nanoparticles with collagen-like peptides', *Physical Chemistry Chemical Physics* **21**(7), 3701–3711. Publisher: The Royal Society of Chemistry.
URL: *https://pubs.rsc.org/en/content/articlelanding/2019/cp/c8cp05191g*

Tatsumi, R., Hattori, A., Ikeuchi, Y., Anderson, J. E. and Allen, R. E. (2002), 'Release of hepatocyte growth factor from mechanically stretched skeletal muscle satellite cells and role of pH and nitric oxide', *Mol Biol Cell* **13**(8), 2909–2918.

Teo, W.-E., He, W. and Ramakrishna, S. (2006), 'Electrospun scaffold tailored for tissue-specific extracellular matrix', *Biotechnology Journal* **1**(9), 918–929. _eprint: https://onlinelibrary.wiley.com/doi/pdf/10.1002/biot.200600044.
URL: *https://onlinelibrary.wiley.com/doi/abs/10.1002/biot.200600044*

Theodossiou, S. K. and Schiele, N. R. (2019), 'Models of tendon development and injury', *BMC Biomedical Engineering* **1**(1), 32.
URL: *https://doi.org/10.1186/s42490-019-0029-5*

Tidball, J. G. and Chan, M. (1989), 'Adhesive strength of single muscle cells to basement membrane at myotendinous junctions', *Journal of Applied Physiology* **67**(3), 1063–1069. Publisher: American Physiological Society.
URL: *https://journals.physiology.org/doi/abs/10.1152/jappl.1989.67.3.1063*

Tidball, J. G. and Lin, C. (1989), 'Structural changes at the myogenic cell surface during the formation of myotendinous junctions.', *Cell and tissue research* **257**(1), 77–84.

Trovato, F. M., Imbesi, R., Conway, N. and Castrogiovanni, P. (2016), 'Morphological and Functional Aspects of Human Skeletal Muscle', *Journal of Functional Morphology and Kinesiology* **1**(3), 289–302. Number: 3 Publisher: Multidisciplinary Digital Publishing Institute.
URL: *https://www.mdpi.com/2411-5142/1/3/289*

Turner, C. E. (2000), 'Paxillin and focal adhesion signalling', *Nature Cell Biology* **2**(12), E231–236.

Uquillas, J. A., Kishore, V. and Akkus, O. (2011), 'Effects of phosphate-buffered saline concentration and incubation time on the mechanical and structural properties of electrochemically aligned collagen threads', *Biomedical Materials (Bristol, England)* **6**(3), 035008.

Utley, R. T. and Côté, J. (2003), 'The MYST family of histone acetyltransferases', *Current Topics in Microbiology and Immunology* **274**, 203–236.

Valdivia, M., Vega-Macaya, F. and Olguín, P. (2017), 'Mechanical Control of Myotendinous Junction Formation and Tendon Differentiation during Development', *Frontiers in Cell and Developmental Biology* **5**.
URL: *https://www.ncbi.nlm.nih.gov/pmc/articles/PMC5362613/*

Valentin, J. E., Turner, N. J., Gilbert, T. W. and Badylak, S. F. (2010), 'Functional skeletal muscle formation with a biologic scaffold', *Biomaterials* **31**(29), 7475–7484.
URL: *https://doi.org/10.1016/j.biomaterials.2010.06.039*

Vandenburgh, H. H., Karlisch, P. and Farr, L. (1988), 'Maintenance of highly contractile tissue-cultured avian skeletal myotubes in collagen gel', *In Vitro Cell Dev Biol* **24**(3), 166–174.

VanDusen, K. W. and Larkin, L. M. (2015), 17 - Muscle–tendon interface, *in* S. P. Nukavarapu, J. W. Freeman and C. T. Laurencin, eds, 'Regenerative Engineering of Musculoskeletal Tissues and Interfaces', Woodhead Publishing, pp. 409–429.
URL: *http://www.sciencedirect.com/science/article/pii/B9781782423010000173*

Vogel, K. G. and Koob, T. J. (1989), Structural specialization in tendons under compression, *in* 'International Review of Cytology', Elsevier, pp. 267–293.
URL: *https://doi.org/10.1016/s0074-7696(08)60632-4*

Wakelam, M. J. (1985), 'The fusion of myoblasts.', *Biochemical Journal* **228**(1), 1.
URL: *https://www.ncbi.nlm.nih.gov/pmc/articles/PMC1144947/*

Walker, N., Kahamba, T., Woudberg, N., Goetsch, K. and Niesler, C. (2015), 'Dose-dependent modulation of myogenesis by HGF: implications for c-Met expression and downstream signalling pathways', *Growth Factors* **33**(3), 229–241.

Wang, H., Xu, Q., Xiao, F., Jiang, Y. and Wu, Z. (2008), 'Involvement of the p38 mitogen-activated protein kinase α, β, and γisoforms in myogenic differentiation', *Molecular Biology of the Cell* **19**(4), 1519–1528.
URL: *https://doi.org/10.1091/mbc.e07-08-0817*

Wang, L., Wu, Y., Guo, B. and Ma, P. X. (2015), 'Nanofiber Yarn/Hydrogel Core-Shell Scaffolds Mimicking Native Skeletal Muscle Tissue for Guiding 3D Myoblast Alignment, Elongation, and Differentiation', *ACS Nano* **9**(9), 9167–9179.

Wang, P.-Y., Yu, H.-T. and Tsai, W.-B. (2010), 'Modulation of alignment and differentiation of skeletal myoblasts by submicron ridges/grooves surface structure', *Biotechnology and Bioengineering* **106**(2), 285–294.

Weintraub, H., Dwarki, V. J., Verma, I., Davis, R., Hollenberg, S., Snider, L., Lassar, A. and Tapscott, S. J. (1991), 'Muscle-specific transcriptional activation by MyoD.', *Genes & Development* **5**(8), 1377–1386.
URL: *https://doi.org/10.1101/gad.5.8.1377*

Weitkunat, M., Brasse, M., Bausch, A. R. and Schnorrer, F. (2017), 'Mechanical tension and spontaneous muscle twitching precede the formation of cross-striated muscle in vivo', *Development (Cambridge, England)* **144**(7), 1261–1272.

Weitkunat, M., Kaya-Çopur, A., Grill, S. W. and Schnorrer, F. (2014), 'Tension and force-resistant attachment are essential for myofibrillogenesis in Drosophila flight muscle', *Current biology: CB* **24**(7), 705–716.

Witherick, J. and Brady, S. (2018), 'Update on muscle disease', *Journal of Neurology* **265**(7), 1717–1725.

Xu, B., Magli, A., Anugrah, Y., Koester, S. J., Perlingeiro, R. C. R. and Shen, W. (2018), 'Nanotopography-responsive myotube alignment and orientation as a sensitive phenotypic biomarker for Duchenne Muscular Dystrophy', *Biomaterials* **183**, 54–66.

Xu, J., Xie, Y., Zhang, H., Ye, Z. and Zhang, W. (2014), 'Fabrication of PLGA/MWNTs composite electrospun fibrous scaffolds for improved myogenic differentiation of C2C12 cells', *Colloids Surf B Biointerfaces* **123**, 907–915.

Xu, Y., Wu, J., Wang, H., Li, H., Di, N., Song, L., Li, S., Li, D., Xiang, Y., Liu, W., Mo, X. and Zhou, Q. (2013), 'Fabrication of electrospun poly(L-lactide-co-ε-caprolactone)/collagen nanoyarn network as a novel, three-dimensional, macroporous, aligned scaffold for tendon tissue engineering', *Tissue Engineering. Part C, Methods* **19**(12), 925–936.

Yang, C., Han, B., Cao, C., Yang, D., Qu, X. and Wang, X. (2018), 'An injectable double-network hydrogel for the co-culture of vascular endothelial cells and bone marrow mesenchymal stem cells for simultaneously enhancing vascularization and osteogenesis', *Journal of Materials Chemistry B* **6**(47), 7811–7821. Publisher: The Royal Society of Chemistry.
URL: *https://pubs.rsc.org/en/content/articlelanding/2018/tb/c8tb02244e*

Yang, H. S., Ieronimakis, N., Tsui, J. H., Kim, H. N., Suh, K.-Y., Reyes, M. and Kim, D.-H. (2014), 'Nanopatterned muscle cell patches for enhanced myogenesis and dystrophin expression in a mouse model of muscular dystrophy', *Biomaterials* **35**(5), 1478–1486.

Yang, K., Jung, H., Lee, H.-R., Lee, J. S., Kim, S. R., Song, K. Y., Cheong, E., Bang, J., Im, S. G. and Cho, S.-W. (2014), 'Multiscale, Hierarchically Patterned Topography for Directing Human Neural Stem Cells into Functional Neurons', *ACS Nano* **8**(8), 7809–7822. Publisher: American Chemical Society.
URL: *https://doi.org/10.1021/nn501182f*

Yin, Z., Guo, J., Wu, T.-y., Chen, X., Xu, L.-l., Lin, S.-e., Sun, Y.-x., Chan, K.-M., Ouyang, H. and Li, G. (2016), 'Stepwise Differentiation of Mesenchymal Stem Cells Augments Tendon-Like Tissue Formation and Defect Repair In Vivo', *STEM CELLS Translational Medicine* **5**(8), 1106–1116. _eprint: https://stemcellsjournals.onlinelibrary.wiley.com/doi/pdf/10.5966/sctm.2015-0215.
URL: *https://stemcellsjournals.onlinelibrary.wiley.com/doi/abs/10.5966/sctm.2015-0215*

Yn, F., Yp, L., Cl, L. and Zj, Z. (2018), 'Assessing the elastic properties of skeletal muscle and tendon using shearwave ultrasound elastography and MyotonPRO.', *Scientific Reports* **8**(1), 17064–17064.
URL: *https://europepmc.org/article/med/30459432*

Yokoyama, S. and Asahara, H. (2011), 'The myogenic transcriptional network', *Cellular and molecular life sciences: CMLS* **68**(11), 1843–1849.

Yoon, J. H. and Halper, J. (2005), 'Tendon proteoglycans: biochemistry and function.', *Journal of musculoskeletal & neuronal interactions* .

Yusuf, F. and Brand-Saberi, B. (2006), 'The eventful somite: patterning, fate determination and cell division in the somite', *Anatomy and Embryology* **211 Suppl 1**, 21–30.

Zhang, H., Lin, C.-Y. and Hollister, S. J. (2009), 'The interaction between bone marrow stromal cells and RGD-modified three-dimensional porous polycaprolactone scaffolds', *Biomaterials* **30**(25), 4063–4069.
URL: *http://www.sciencedirect.com/science/article/pii/S0142961209004098*

Zhang, S. J., Truskey, G. A. and Kraus, W. E. (2007), 'Effect of cyclic stretch on beta1D-integrin expression and activation of FAK and RhoA', *Am J Physiol Cell Physiol* **292**(6), C2057–2069.

Zhao, C., Wang, S., Wang, G., Su, M., Song, L., Chen, J., Fan, S. and Lin, X. (2018), 'Preparation of decellularized biphasic hierarchical myotendinous junction extracellular matrix for muscle regeneration', *Acta Biomaterialia* **68**, 15–28.

Zhao, W., Li, J., Jin, K., Liu, W., Qiu, X. and Li, C. (2016), 'Fabrication of functional PLGA-based electrospun scaffolds and their applications in biomedical engineering', *Materials Science and Engineering: C* **59**, 1181–1194.
URL: *https://doi.org/10.1016/j.msec.2015.11.026*

Zheng, Z., Ran, J., Chen, W., Hu, Y., Zhu, T., Chen, X., Yin, Z., Heng, B. C., Feng, G., Le, H., Tang, C., Huang, J., Chen, Y., Zhou, Y., Dominique, P., Shen, W. and Ouyang, H.-W. (2017), 'Alignment of collagen fiber in knitted silk scaffold for functional massive rotator cuff repair', *Acta Biomaterialia* **51**, 317–329.

Zhong, J., Zhang, H., Yan, J. and Gong, X. (2015), 'Effect of nanofiber orientation of electrospun nanofibrous scaffolds on cell growth and elastin expression of muscle cells', *Colloids and Surfaces B: Biointerfaces* **136**, 772–778.
URL: *http://www.sciencedirect.com/science/article/pii/S0927776515302484*

Zuk, P. A., Benhaim, P. and Hedrick, M. H. (2004), 40 - Stem Cells from Adipose Tissue, *in* R. Lanza, J. Gearhart, B. Hogan, D. Melton, R. Pedersen, J. Thomson and M. West, eds, 'Handbook of Stem Cells', Academic Press, Burlington, pp. 425–447.
URL: *http://www.sciencedirect.com/science/article/pii/B9780124366435501309*

Zöllner, A. M., Abilez, O. J., Böl, M. and Kuhl, E. (2012), 'Stretching skeletal muscle: chronic muscle lengthening through sarcomerogenesis', *PLoS One* **7**(10), e45661.